ABSTRACT

INGRAM, JOSHUA A. Investigation of Lab Scale Tests for Predicting After-flame and Garment Shrinkage in Protective Garments in PyroMan™ Tests. (Under the direction of Dr. Roger Barker).

Instrumented fire manikin tests provide invaluable evaluation of systems-level thermal protective performance of fire protective clothing. Performing these tests, however, requires large facilities and extensive training. Small-scale materials-level tests that can predict the thermal protective performance of garments in systems-level testing would be of considerable practical value. Several small-scale tests exist that evaluate two key characteristics of thermal protective performance: after-flame and thermal shrinkage. Some of these bench-scale tests form the basis of most NFPA performance requirements for fire protective clothing [1-2]. Despite this widespread reliance on these small-scale tests, the relationship between the after-flame and thermal shrinkage measured in small-scale tests and the after-flame, garment shrinkage, and thermal protective performance in fire manikin testing has yet to be studied. This research sought to identify which bench-scale tests of after-flame and thermal shrinkage, if any, are able to accurately predict after-flame and garment shrinkage behaviors in fire manikin testing. This research also investigated how the after-flame and shrinkage evaluated in both small-scale tests and fire manikin tests relate to the thermal protection offered by fire manikin testing.

Standard bench-scale tests of after-flame, including the Vertical Flame Test (ASTM D6413) called for in NFPA performance requirements, did not accurately predict observed after-flame in PyroMan™ testing of both FR coveralls and FR rainwear materials. Although some bench-scale flammability tests correlated with observed after-flame in PyroMan™ testing, their relationships are complicated. After-flame observed in bench-scale flammability tests failed to exhibit a significant relationship with the thermal protective performance in PyroMan™ testing.

Furthermore, the after-flame in PyroMan™ testing failed to establish a strong relationship with the thermal protective performance of FR coveralls and failed to establish a significant relationship with the thermal protective performance of FR rainwear materials, suggesting a complex relationship between after-flame phenomena and thermal protection offered by FR clothing.

Bench-scale tests of thermal shrinkage did not accurately predict garment shrinkage behavior in PyroMan™ testing. However, many of these tests, including the 500°F oven test called for by NFPA performance standards, correlate well with garment shrinkage measured in PyroMan™ testing. The cylindrical TPP test proved to provide the most accurate predictions of thermal protective performance for FR coveralls, while the spaced configuration of the standard TPP test provided the best correlations between thermal shrinkage and thermal protective performance in PyroMan™ testing.

The results of this research raise questions about the necessity of including certain bench-scale performance requirements in standards such as NFPA 2112. This research highlights the need for the development of a new bench-scale test for evaluation of after-flame and thermal shrinkage that will more accurately predict performance in systems-level tests.

Investigation of Lab Scale Tests for Predicting After-flame and Garment Shrinkage in Protective Garments in PyroMan™ Tests.

by
Joshua A Ingram

A thesis submitted to the Graduate Faculty of
North Carolina State University
in partial fulfillment of the
requirements for the degree of
Master of Science

Textile Engineering

Raleigh, North Carolina
2019

APPROVED BY:

_____	_____
Dr. Roger Barker Committee Chair	Dr. A. Blanton Godfrey
_____	
Dr. Bryan Ormond	

DEDICATION

To my loving parents, Paul and Pam Ingram.

BIOGRAPHY

Joshua Ingram was born and raised in Greensboro North Carolina. He attended North Carolina State University where he completed his Bachelor of Science degree in Materials Science and Engineering in May 2017. In Fall 2017, he entered the master's program for Textile Engineering at North Carolina State University. He worked as a Research Assistant in the Textile Protection and Comfort Center, where he worked on investigating the relationship between bench-scale test methods of flammability and thermal shrinkage and the after-flame and thermal shrinkage observed in the PyroMan™ fire manikin test.

ACKNOWLEDGMENTS

First, I would like to acknowledge my advisor, Dr. Barker, for his guidance throughout this process. His guidance, encouragement, and expertise has been an enormous help. I would also like to thank the other members of my committee: Dr. Godfrey and Dr. Ormond.

Next, I would like to thank the remaining members of my group project, Shawn Deaton and John Morton-Aslanis for their mentorship during my time working on this project. I would also like to thank W.L. Gore and Associates for sponsoring this research. Without their support, this project would not have been possible. Most importantly, I would like to thank my family who have been an enormous support throughout my entire life and have shaped me into who I am today.

TABLE OF CONTENTS

LIST OF TABLES

LIST OF FIGURES

CHAPTER 1: Research Overview

1.1 Introduction

Instrumented fire manikin tests provide invaluable evaluation of systems-level thermal protective performance of fire protective clothing. Nevertheless, few studies have focused on predicting after-flame and thermal shrinkage behavior observed in fire manikin testing. Correlations between bench-scale test methods and the after-flame/ thermal shrinkage observed in fire manikin tests have yet to be established in scientifically qualified experimental studies. This is a significant gap, since the availability of well-qualified lab-scale tests for predicting the performance of materials in fire manikin tests would be of considerable practical value. These tests would accelerate research and development by identifying promising prototype materials and constructions prior to fire manikin testing.

Standardized bench-scale tests of fabric flammability and thermal shrinkage are the primary means of evaluating the suitability of materials for use in fire and heat resistant protective clothing. These tests form the basis of most NFPA performance requirements for fire resistant protective clothing [1-2]. Two test methods stand out: The Vertical Flame Test (ASTM D6413) and the 500ºF Oven Shrinkage Test [1-3]. In spite of the widespread reliance on these methods, apart from screening thermoplastic materials, and identifying materials of normal flammability, little scientific basis exits for qualifying the utility of these methods for differentiating materials thermal performance in full-scale fires, or for protecting against burn injury in fire exposures.

Instrumented fire manikin technology, PyroMan™, permits assessment of the thermal protective performance of materials and garments in realistic simulations of flash fire exposures. Fire manikin provides an ideal testing platform to address these fundamental questions: How do

bench-scale tests of after-flame and thermal shrinkage correlate with after-flame and garment shrinkage observed in realistic simulation of flash fire exposures? If they do not correlate, how can we devise bench-scale tests methods to predict materials response in fire manikin tests?

This research studied the relationships between standard small-scale tests of flammability and thermal shrinkage and the after-flame, shrinkage and thermal protective performance evaluated in fire manikin tests. This chapter will provide a broad overview of the research, while more detailed analysis of the results of these studies will be presented in separate chapters.

1.2 Background

1.2.1 Predicting After-flame in PyroMan™ Fire Manikin Tests

Many different factors influence the burning behavior of garments in fire manikin testing. Flame dynamics, the geometry of the manikin, garment design, flame propagation, and modes of flame impingement, among other factors, can all have an impact on the burning behavior of garments, and each adds to the complexity involved in predicting the after-flame in fire manikin testing. The influence that each of these factors have on the burning behavior of garments is poorly understood.

1.2.2 Measuring After-flame in Bench-Scale Flammability Tests

The conditions that exist in full-sale flame manikin tests are very different than the conditions that exist in bench-scale flammability test methods. Despite a wide range of differences, numerous standardized test methods are available for evaluating the flammability of flame protective clothing fabrics. A review of these methods identified three standardized test methods that are widely used for evaluating FR materials: the ASTM D6413 vertical flame test (referenced in NFPA standards), ASTM F1358 folded edge flame test, and the CGSB-4.2, No. 27.10 Canadian flammability test (shown in Figures 1.1, 1.2, and 1.3) [3-5]. Each bench-scale

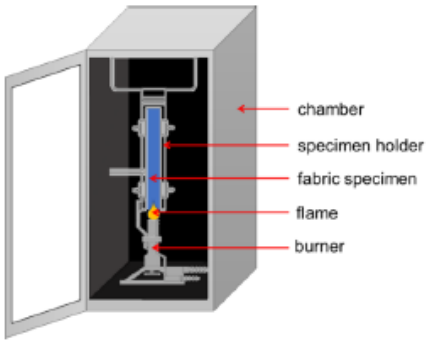

Figure 1.1 Schematic illustration of fabric vertical flame test set-up

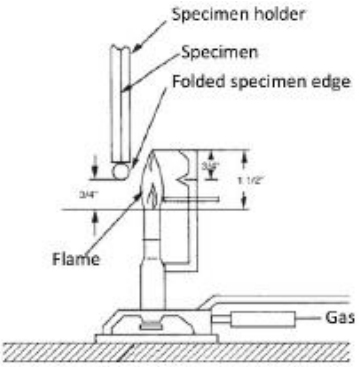

Figure 1.2 Schematic illustration of folded edge ignition-vertical flame test set-up (redrawn from [4]).

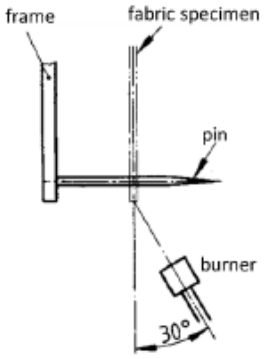

Figure 1.3 Schematic illustration of vertical flame test with an angled burner (redrawn from [5]).

test employs a small flame as the ignition source to evaluate the ability of fabrics to ignite, propagate flames beyond the initial ignition point, and the after-flame. One of the main parameters that is different among the bench-scale flammability tests is the mode of flame

contact (edge, surface, folded surface). Additionally, the tests represent different sample orientations with respect to the flame, which can range from vertical to 30 degree to perpendicular flame ignition. Other tests, such as the cone calorimeter (ASTM E1354), measure the rate of heat released in the combustion of the test specimen [6-7].

1.2.3 Correlation of Bench-Scale After-flame with After-flame in PyroMan™ Tests

A review of pertinent literature confirmed that the relationship between bench-scale measures of after-flame and the after-flame observed in fire manikin tests has not been qualified in a systematic research study. Nevertheless, garment after-flame is assumed to contribute to predicted body burn in PyroMan™ tests. This is certainly true if the after-flame phenomenon is evidence of uncontrolled material combustion and sustained burning. Therefore, an important research goal is to determine if small-scale after-flame tests are predictive of general combustion and sustained burning in PyroMan™ exposures.

1.2.4 Predicting Thermal Shrinkage in PyroMan™ Fire Manikin Tests

Like with after-flame, many different factors may impact the shrinkage behavior of garments in the PyroMan™ test. Flame intensity, exposure duration, garment fit, ventilation, and environmental conditions in the test chamber each may have an impact on the shrinkage behaviors observed in PyroMan™ testing, adding to the complexity of predicting garment shrinkage.

Multiple studies have shown that thermally induced shrinkage can increase the predicted burn injury in instrumented manikin tests. This is largely due to the reduction or elimination of the insulating air gap layer between the garment and the manikin surface [8]. Garment shrinkage can therefore contribute to burn injury in multiple ways: the reduction of the insulating air gap layer and heat transfer directly from the hot garment to the skin.

1.2.5 Measuring Thermal Shrinkage in Bench-Scale Tests

A review of standardized test methods for evaluating thermal shrinkage found the 500°F (260°C) hot air circulating oven test, as outlined in ASTM F2894, as the only standardized bench-scale thermal shrinkage test [9]. This test method is called for in NFPA performance standards [1-2].

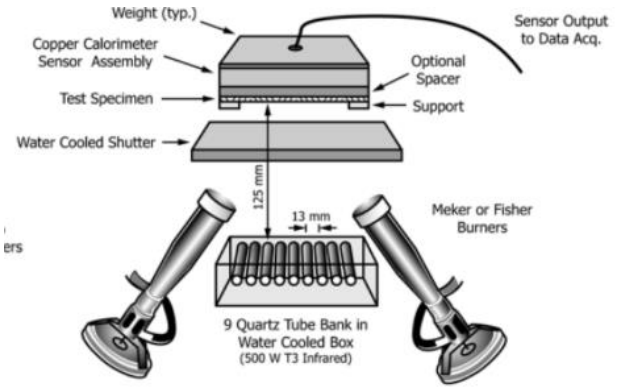

Figure 1.4 Schematic illustration of TPP burner and sensor assembly (Redrawn from [10]).

1.2.4.1 Measuring Thermal Shrinkage in Thermal Protective Performance (TPP) Tests

The thermal protective performance (TPP) test is an ideal bench-scale test for evaluating the protective performance of FR materials. TPP tests (Figure 1.4) expose fabric specimens to flame intensities similar to those experienced in flash-fire manikin testing. While not part of the standard TPP test method (ASTM F2700), multiple studies have used the TPP test and its variants to measure the thermally induced shrinkage of protective textiles [10]. Wang and Li used an image processing technique to characterize the change in surface area of TPP samples after repeated 3-second exposures [11]. In a different study, Li et al measured the surface appearance of burned TPP samples using a handheld laser scanner and was able to quantify the material shrinkage of the samples using 3D software [12].

In addition to the ASTM F2700 TPP test, variations of the TPP test have been developed which further investigate the influence of material shrinkage on the thermal protective performance. The dynamic TPP (DTPP) test, developed in a study performed at North Carolina State University, utilizes a specialized frame that introduces dynamic forces on the fabric specimen during TPP exposure [13]. Crown et al developed a cylindrical sensor apparatus for the TPP test to measure the effect of shrinkage on the thermal protective performance [14]. These studies do not provide a method for evaluating the thermal shrinkage but do acknowledge the impact that thermal shrinkage has on the thermal protective performance of the test materials.

1.2.6 Measuring Garment Shrinkage in PyroMan™ Fire Manikin Tests

While measuring the garment shrinkage is not incorporated into the ASTM F1930 standard manikin test method, researchers have employed multiple methods to obtain a numerical measurement of garment shrinkage [15]. Garment shrinkage has been measured largely through two distinct methods: physical marks on the garments and 3-D scanning technology. Li et al sealed stamps on the backside of test garments at locations of the garment that matched the heat sensor locations on the manikin to investigate how different body postures impact the thermal shrinkage and thermal protective performance of FR garments. These circular stamps were marked to measure the thermal shrinkage in the warp, fill, and ±45 degrees to the warp direction of woven test fabrics [16].

The second method of measuring the thermal shrinkage of garments used in flame manikin testing is 3-D scanning. Song used 3-D body scanning technology to measure the reduction in the insulative air gap layer that results from garment shrinkage [8]. In more recent studies, Wang and Li employed a portable 3-D scanner mounted in the manikin test chamber to obtain 3-D images of the nude manikin and the clothed manikin immediately prior to and

following flash fire exposure. The shrinkage was measured by superimposing the scans of the clothed manikin onto the scans of the nude manikin. The length and girth of the garment was measured by the surface area change, while the change in insulative air gap was calculated by the volume change and air gap thickness change [17].

1.2.7 Correlation of Bench-Scale Thermal Shrinkage with Garment Shrinkage in PyroMan™ Tests

Unlike after-flame phenomena, many studies have shown the importance of the thermal stability and shrinkage of FR materials and thermal protection measured in fire manikin tests. Most of these studies have focused on correlating TPP tests with predicted body burn in fire manikin exposures [8, 16, 19, 20-22]. Several studies conducted at NC State have shown the relationship between clothing air layers and the role of garment shrinkage on distributed body burn measured on PyroMan™ [8, 19]. TPP tests, measured in both sample contact or sample spaced test configurations, have been found to provide localized prediction of PyroMan™ burn. TPP tests correlate with manikin burn predictions when they are precisely matched with the spatial configuration (spaced or contact) found between the manikin thermal sensor and test garment. These findings were consistent with Crown and Dale's study that demonstrated the importance of thermal shrinkage, as measured using a cylindrical TPP test arrangement [14].

In a recent study, Wang and Li used a portable 3D body scanner to measure shrinkage in Nomex® IIIA test garments as a function of exposure time in fire manikin tests [20, 22]. They assessed the effects of thermal shrinkage as reductions in the fabric surface area in the TPP test, and by thermally induced changes in the garment/manikin interface air volume in the fire manikin test.

Previous research studies provide a strong basis for using TPP testing variants to evaluate materials thermal shrinkage in order to predict shrinkage in PyroMan™ tests. At the same time, scientifically-based studies demonstrating a similar utility for the 500ºF oven test were not found. On the contrary, recent corporate studies appear to show that the 500ºF oven shrinkage test does not correlate with thermal shrinkage and burn protection measured on PyroMan™ for some materials [24]. Adams presented data indicating that thermal shrinkage measured in the 500ºF oven test does not correlate with predicted PyroMan™ body burn [25]. These limited data are not viewed as a definitive assessment of the value of the 500ºF oven test as a predictor of PyroMan™ performance. However, these reports do suggest questions that need to be addressed in a systematically designed research study.

1.3 Experimental Methods

1.3.1 Evaluating After-flame and Heat Released in PyroMan™ Tests

After-flame time was measured in the PyroMan™ test using video analysis. Video images were recorded using cameras filming from both the front and back sides of the PyroMan™ manikin. After-flame was recorded as the time from end of flame exposure from the propane torches to when flames from the burning test garment could no longer be observed. Video recordings were analyzed, frame by frame, to precisely assess when visible after-flame ends. After-flame time was calculated by dividing the total number of frames by the camera's frame speed. This objectively measured video analysis procedure ensures after-flame measurements of a PyroMan™ test are more accurate than after-flame measurements in small-scale flammability tests.

Peak heat release rate (PHRR) and total heat release (THR) were also determined in the PyroMan™ tests. This enabled comparison with the heat release parameters reported in cone

calorimeter tests. During the test interval, manikin PHRR was determined as the average heat flux recorded by manikin thermal sensors (at a sampling rate of 0.1s) and was calculated as the maximum average heat flux measurement over the same interval. THR was recorded as the average heat flux measured multiplied by the elapsed time of the test. It should be noted that these measurements consider only the PHRR and THR on the manikin back side of the test garment, while heat release calculated in the cone calorimeter test measures full combustion of the sample.

1.3.2 Evaluating Garment Shrinkage in PyroMan™ Tests

This study developed multiple methods to evaluate garment thermal shrinkage in PyroMan™ tests. The first method used a variant of the procedure described by Li: circular markers of known size (12.7 cm diameter for coveralls and 7.6 cm diameter for rainwear) were drawn at selected locations of the manikin test garment (Figures 1.5a and 1.5b) [16]. The circular section was marked in the warp and filling directions to enable shrinkage measurement (Figure 1.5c). Markers were drawn at 38 locations on FR coveralls and 18 locations on FR rainwear, avoiding seams, reflective striping and pockets. The percent thermal shrinkage was estimated by measuring changes in the circular marker dimensions (warp and filling direction) following garment exposure in PyroMan™ tests.

The other method used in evaluating the garment shrinkage in fire manikin testing was 3-D scanning. This study used the Structure Sensor 3D scanner by Occipital, a portable 3-D scanner that attaches to an iPad, along with itSeez3D software to capture three-dimensional scans of the dressed manikin before and after flash fire exposure [26-27]. To ensure accuracy, each test garment was scanned three times before and after the exposure. Each of the scans were exported into Autodesk Fusion 360 modeling software, where any part of the scans not covered by the

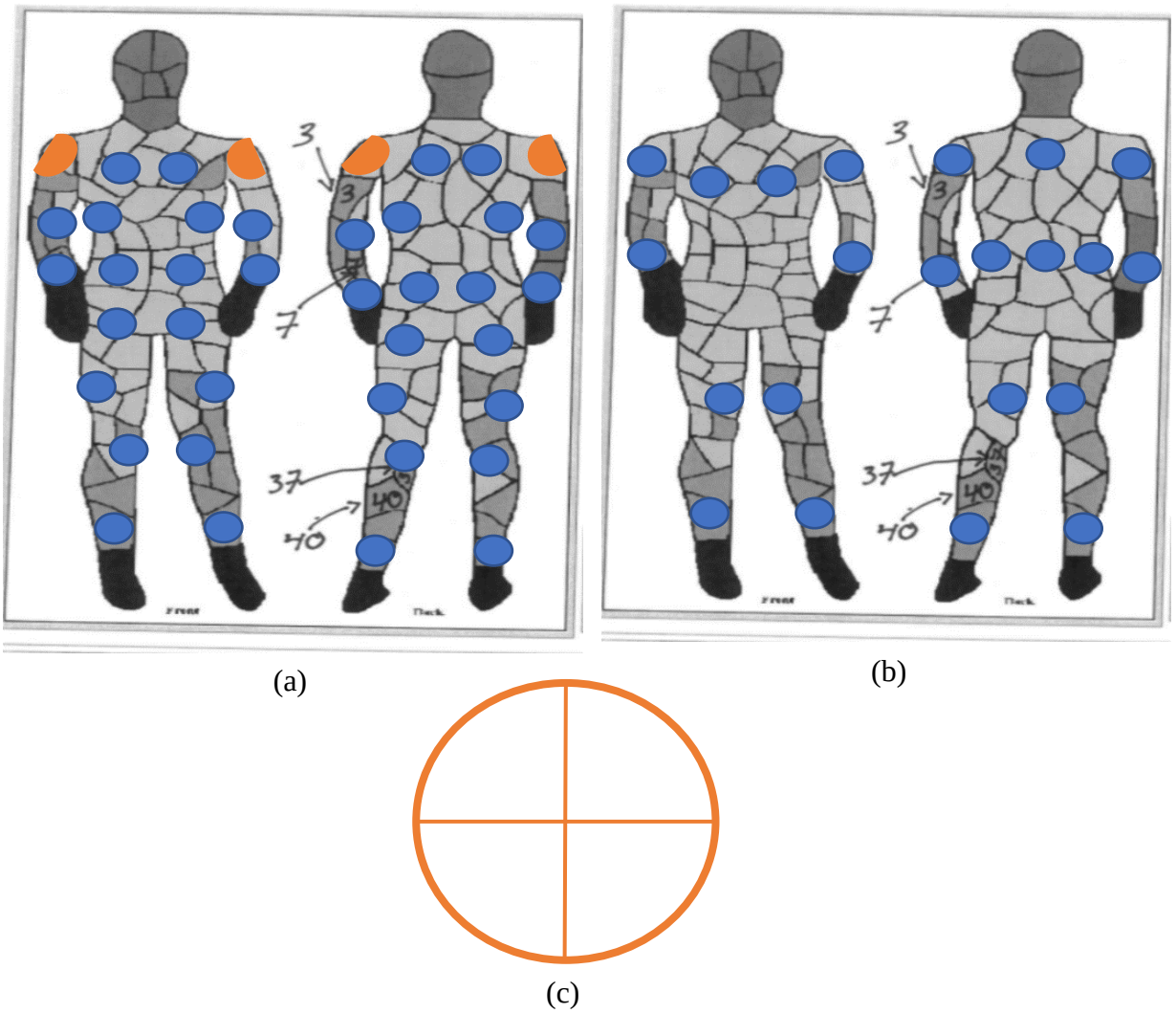

Figure 1.5 (a) Approximate locations of markers on FR coverall garments used in fire manikin testing; (b) approximate locations of markers on FR rainwear garments used in fire manikin testing; (c) drawing of the marker used in measuring dimensional shrinkage in fire manikin testing

garment was removed (Figure 1.6), the scans were set to the correct scale, and the scan file was converted from a mesh to a solid body [28]. The correct scale for the scan was set based on the height of the manikin in the initial scan (not including the stabilizing block underneath the foot) and the total height of the manikin as specified in the ASTM F1930 standard [15]. The Autodesk Fusion 360 software then measures the surface area and volume of the manikin. These

measurements are recorded and used to calculate the areal and volumetric shrinkage exhibited by each garment.

1.4 Test Materials

A variety of different fire protective fabric materials were selected for this study. Table 1.1 provides a summarized description of the test materials. Test materials fall into two broad categories: one group was selected to represent a range of flammability and thermal shrinkage characteristics found in single-layer woven FR industrial workwear or military uniform fabrics. The other group represented FR rainwear laminates.

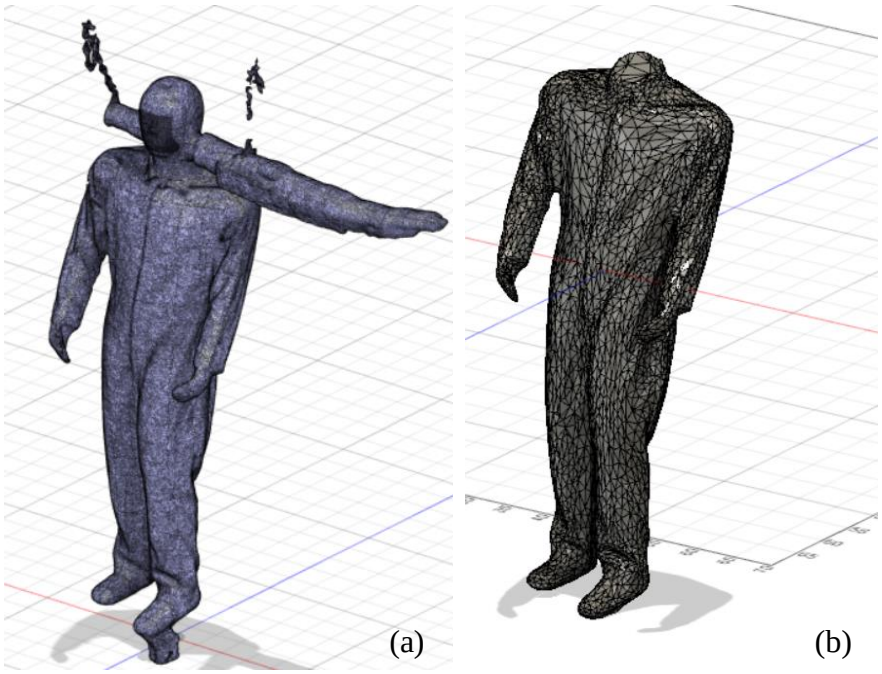

Figure 1.6 (a) Unedited 3-D scan inserted in Autodesk Fusion 360 Software; (b) 3-D scan in Autodesk Fusion 360 Software after removal of areas not covered by garment, scaling, and file conversion for surface area and volume measurements.

1.4.1 Aramids

Three different meta-aramid fabrics: 4.5osy (Material A), 6.0osy (Material B), and 7.5osy (Material C). Temperatures above the glass transition temperature (T_g) of meta-aramid fibers are

observed in flash fires causing fabrics made with meta-aramid fibers to shrink [29]. To improve high temperature thermal stability, meta-aramid fibers are blended with other more heat-resistant fibers, including para-aramid fibers. Meta-aramid fibers have a T_g of 275°C, while para-aramid fibers have a T_g of 327°C. Meta-aramid fibers swell in high-heat exposures, which seals openings in the fabric reducing heat transfer to the skin [29].

1.4.2 Polybenzimidazole (PBI)

A 7osy twill-weave fabric of 70%/30% "PBI-dominant" para-aramid blend/para-aramid filament (Material I). PBI has a high T_g (400°C) and thermal decomposition temperature (1175°C), indicating thermal stability (shrinkage resistance) in flash fire conditions [30].

1.4.3 Modacrylic Blends

Two twill-weave variants composed of blends of 45% modacrylic/35% Lyocell/ 20% aramid in a 7osy (Materials G) and 8.5 osy (Materials H) basis weight. Both fabrics are NFPA 2112 certified, indicating that they exhibit less than 2 seconds of after-flame time on the vertical flame test and less than 10% shrinkage in the 500°F oven test. Because modacrylic fibers are composed of an acrylic and modacrylic co-polymer composition, they undergo a two-stage degradation at temperatures of 236°C and 503°C. The acrylic component protects by char formation, while the modacrylic flame retardant component suppresses burning via vapor-phase free radical (halogen) reactions [29].

1.4.4 FR Cotton

The FR cotton fabric used in this study is a 7osy twill construction incorporating an 88/12% blend of cotton and nylon fibers (Materials J). This test fabric uses a FR finish containing tetrakis(hydroxymethylol) phosphonium salts to achieve flame resistance. It is NFPA 2112 certified, meaning that it has less than 2 seconds after-flame time in the vertical flame test,

and less than 10% shrinkage in the 500°F oven test. Once the FR finish is consumed during a flame exposure, the cotton will quickly degrade, rapidly increasing after-flame and heat transfer [31].

Table 1.1 Summarized Description of Test Materials

ID	**Material**	**Fiber Content**	**Construction**	**Fabric Weight** (osy)	(1)**Nominal After-flame** (sec)	(2)**Nominal Shrinkage** (%)
A	Aramid	93% meta-aramid/ 5% para-aramid/ 2% antistat	Plain Weave	4.5	< 2	< 10%
B	Aramid	93% meta-aramid/ 5% para-aramid/ 2% antistat	Plain Weave	6.0	< 2	< 10%
C	Aramid	93% meta-aramid/ 5% para-aramid/ 2% antistat	Plain Weave	7.5	< 2	< 10%
D	FR Laminate	100% nylon	Plain Weave	4.0	< 2	high
E	FR Laminate	100% nylon 6,6	Rip-stop	5.3	< 2	high
F	FR Laminate	100% polyester	Twill Weave	6.5	< 2	high
G	Modacrylic	45% modacrylic/ 35% Lyocell/ 20% aramid	Twill Weave	7.0	< 2	< 10%
H	Modacrylic	45% modacrylic/ 35% Lyocell/ 20% aramid	Twill Weave	8.5	< 2	< 10%
I	PBI	70% PBI/ 30% para-aramid	Twill Weave	7.0	< 2	< 10%
J	FR Cotton	88% FR cotton/ 12% nylon	Twill Weave	7.0	< 2	< 10%
K	FR Rainwear	100% meta-aramid	FR PVC/ on meta-aramid nonwoven	11.3	< 2	
L	FR Rainwear	100% meta-aramid	FR PVC on meta-aramid nonwoven	9.5	< 2	
M	FR Rainwear	100% polyester	Twill Weave	8.3	< 2	high
N	FR Rainwear	93% meta-aramid/ 5% para-aramid/ 2% antistat	FR neoprene on plain weave meta-aramid	13.5	< 2	
O	FR Rainwear	100% FR cotton	FR polyurethane on FR cotton knit	10.0	< 2	

1.4.5 FR Laminate

Proprietary technology FR laminate materials incorporate a char-forming FR component. Three different substrate constructions and weights were studied: Material D used a 100% nylon plain weave substrate in a 4osy construction, Material E used a twill rip-stop weave made of 100% nylon 6,6, and Material F featured a 100% polyester twill weave 100% polyester substrate fabric. These laminate constructions form stable char contributing to increased structural integrity in flame exposures [32]. They have less than 2 seconds after-flame time in the vertical flame test but exhibit high levels of thermal shrinkage in the 500°F oven test [32]. Because these laminate materials are used in rainwear ensembles, these three FR laminates were included in both the FR coverall and FR rainwear categories of garment test materials.

1.4.6 FR Rainwear

This study included materials used in FR rainwear garments (rain jacket and bibs/overalls). Rainwear material M is a proprietary char-forming laminate technology incorporated in a 8.3osy construction. Other FR rainwear test materials consisted of a FR poly(vinyl) chloride (PVC) barrier laminated on a nonwoven meta-aramid fabric in a 11.3osy construction (material K), and in 9.5osy laminate (material L). The low T_g and low flash point of PVC material means that they will burn and propagate flame more readily than other FR rainwear materials. Additionally, phthalates are often used as PVC plasticizers and may be present in these materials. The presence of phthalate plasticizers could affect how the material burns and propagates flames [33]. Another of the rainwear test materials (material N) used a FR neoprene coating on meta-aramid fabric in a 13.5osy construction. The halogens in the polychloroprene coating produce radical reactions when exposed to a flame, the source of the FR properties in this material. Finally, rainwear garment material O is a laminate composed of a FR

polyurethane coating on 10osy 100% knit FR cotton. Each of the rainwear test materials is compliant with the ASTM F2733 standard, meaning that they exhibit less than 2 seconds of after-flame in the ASTM D6413 vertical flame test.

1.5 Experimental Approach

1.5.1 Bench-Scale Test Methods of After-flame

Table 1.2 shows the battery of bench-scale flammability tests used to evaluate after-flame and combustion characteristics of the test materials described in Table 1.1.

Table 1.2 Battery of Bench-Scale Test Methods for Predicting PyroMan™ After-flame

Test Method	Rationale
ASTM D6413- Vertical Flame	Test used in NFPA standards, orientation produces severe flame exposure
CGSB- 4.2, 27.10- Configuration A (perpendicular application)	Surface exposure is more practical, orientation produces severe flame exposure
CGSB-4.2, 27.10- Configuration B (30-degree angle edge application)	More stringent than surface ignition
ASTM F1358 Folded Edge	Curved test surface
ASTM E1354 Cone Calorimeter	PHRR or THR may correlate with PyroMan™ after-flame

1.5.2 Bench-Scale Test Methods of Thermal Shrinkage

Table 1.3 shows the battery of bench-scale shrinkage tests used to evaluate the thermal shrinkage of the test materials described in Table 1.1.

Table 1.3 Battery of Bench-Scale Test Methods for Predicting PyroMan™ Garment Shrinkage

Test Method	Rationale
ASTM F2894 (500°F Oven)	Test used in NFPA standards
TPP Test	Convective-radiant heat flux level comparable to PyroMan™
Cylindrical TPP Test	Convective -radiant heat flux level comparable to PyroMan™; Thermal shrinkage experienced in the sample can eliminate air gap, increasing rate of heat transfer

1.5.3 PyroMan™ Test

PyroMan™ tests were conducted following the ASTM F1930 standard test method [15]. Standard procedures were used to calculate predicted body burn injury [15] while novel procedures were developed to measure after-flame time, PHRR, and THR. The testing series were conducted at the standard calibrated average incident heat exposure intensity of 84 kW/m^2 for three- and four-seconds exposure times. No undergarments were used in these tests. Test materials were used to construct FR coveralls and rainwear garments for testing on PyroMan™. Triplicate tests were made for each of garment types. Table 1.4 shows the PyroMan™ measurement parameters.

Table 1.4 PyroMan™ Test Measurements (3, 4-second exposures)

Report	Measurements
% Body burn	Recorded temperature data
Duration of after-flame	Video recordings (front and rear)
Garment Shrinkage	Markers on backside of garments; 3-D Scanning

1.6 Results and Discussion

1.6.1 After-flame

Data tables summarizing the results of after-flame testing of the materials described in Table 1.1 are found in Chapter 2. An initial review of the data indicates that, while many of the test materials exhibit little after-flame in bench-scale tests, PyroMan™ tests of the same materials exhibit significant after-flame. There are exceptions to this pattern, particularly in the edge ignition (Configuration B) of the Canadian flame test.

Multiple statistically-based methods were used to determine whether small-scale flammability tests could be used to predict after-flame behavior in PyroMan™ tests. A t-test analysis compared after-flame times measured in bench-scale tests with after-flame in coveralls (made from these same materials) tested on PyroMan™. This statistical analysis shows whether

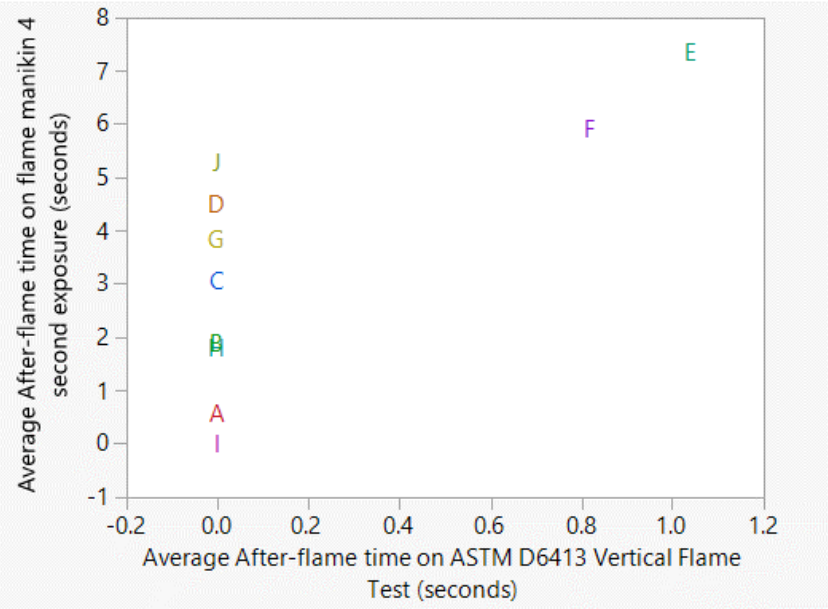

Figure 1.7 Vertical Flame test after-flame vs after-flame in 4-second PyroMan exposure (FR coverall fabrics).

the bench-scale test overestimates, underestimates or accurately predicts manikin after-flame. The model's hypothesis is as follows: If the bench-scale test after-flame time is neither significantly longer nor shorter than the manikin after-flame time, the bench test is judged to be an accurate predictor of manikin after-flame. T-test analysis demonstrates that bench-scale flammability tests do not accurately predict PyroMan™ after-flame. It shows that bench-scale tests tend to underestimate the extent of burning in PyroMan™ tests in both FR coveralls and FR rainwear. This is not a surprising result considering the significant differences in flame intensities, materials configurations and combustion dynamics between bench-scale flame exposures and the PyroMan™ flame environment.

Correlation analysis was used to identify relationships between bench-scale measures of after-flame and PyroMan™ after-flame. Tables showing the correlations between bench-scale after-flame and after-flame exhibited in PyroMan™ testing can be found in Chapter 2.

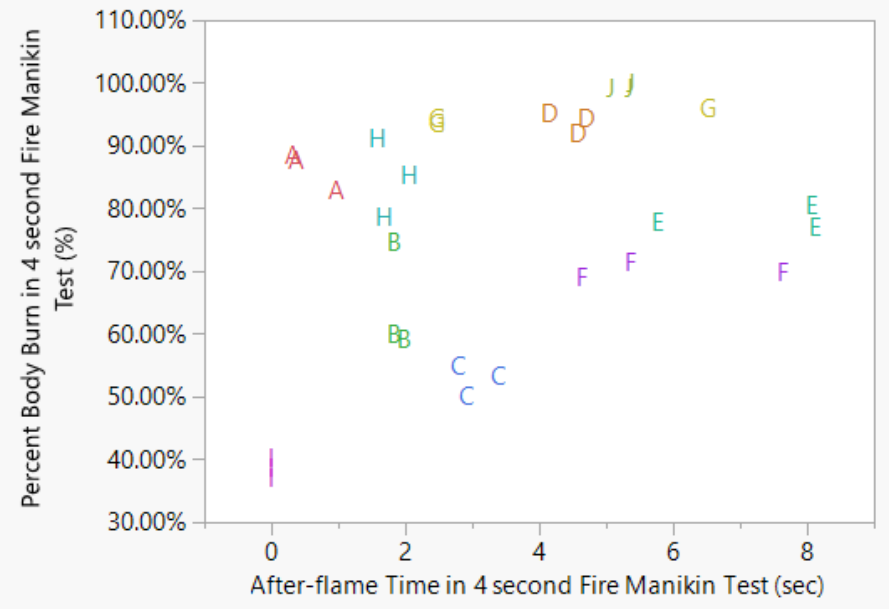

Figure 1.8 After-flame time in 4-second PyroMan tests v. Percent Body Burn in 4-second PyroMan tests (FR Coveralls)

The analysis shows that, for FR coveralls, significant correlations were found between bench-scale measures of after-flame and after-flame observed in 4-second PyroMan™ tests, but not for 3-second PyroMan™ tests. Although the relationships between the after-flame evaluated in the ASTM D6413 vertical flame test and Canadian flame tests and after-flame observed in 4-second PyroMan™ tests, the relationships are more complex than the correlation coefficients indicate. Figure 1.7 shows the relationship between the average after-flame measured in the ASTM D6413 vertical flame test and the average after-flame observed in 4-seconds PyroMan™ exposures for FR coveralls. With the exception of Materials E and F, no FR coverall material exhibited any after-flame in the vertical flame test despite the same materials exhibiting a range of after-flame times in PyroMan™ tests. Excluding Materials E and F from this relationship would result in no correlation whatsoever, revealing the complexity of the relationship.

For FR rainwear, the relationship between the THR in the cone calorimeter and the after-flame in 4-second PyroMan™ tests was statistically significant, indicating that the cone

calorimeter may be of used for predicting the after-flame of FR rainwear garments in 4-second PyroMan™ tests.

In addition to evaluating the relationships between bench-scale after-flame and after-flame in PyroMan™ tests, this research investigated the relationship between after-flame, measured in both bench-scale tests and manikin tests, and thermal protective performance (in terms of body burn injury) of garments in PyroMan™ tests. Tables that summarize the relationships between after-flame and percent body burn can be found in Chapter 2. Only one correlation was statistically significant: the relationship between the after-flame and percent body burn in 4-second PyroMan™ tests (Figure 1.8). However, the correlation coefficient indicates that the relationship is weak, confirming the complex relationship between after-flame and thermal protective performance (in terms of percent body burn).

1.6.2 Garment Shrinkage

Tables providing some of the summarized thermal shrinkage data measured in bench-scale tests and in PyroMan™ tests (500°F Oven, 3-second exposures in Cylindrical TPP, TPP, and PyroMan™) are shown in Chapter 3. Summarized data for the dimensional shrinkage measured in 4-second exposures on the Cylindrical TPP, TPP, and PyroMan™ tests as well as tables for the areal shrinkage and PyroMan™ volumetric shrinkage data can be found in Appendix B. The data show a wide variety of shrinkage behaviors.

T-tests were also used to compare the shrinkage measured in bench-scale tests to the shrinkage measured in PyroMan™ tests. The results of this analysis reveal that the bench-scale shrinkage test methods generally overestimate the PyroMan™ garment shrinkage for both FR coveralls and FR rainwear.

Correlation analysis was utilized to identify relationships between the bench-scale shrinkage and PyroMan™ garment shrinkage (Tables shown in Chapter 3). These results show that many of the bench-scale methods are highly correlated with the garment shrinkage in PyroMan™ tests of both exposure durations for FR coveralls. Bench-scale test methods are highly correlated with the garment shrinkage in 3-second PyroMan™ tests for FR rainwear, but not with garment shrinkage in 4-second PyroMan™ tests. These strong correlations indicate that bench-scale shrinkage test methods are useful in predicting PyroMan™ performance, even if they are unable to accurately predict the exact values of garment shrinkage in PyroMan™ tests.

Analysis of the relationships between thermal shrinkage, measured in bench-scale tests and on PyroMan™ test garments, and the thermal protective performance (in terms of predicted body burn) measured in PyroMan™ tests reveals that the thermal shrinkage measured in the spaced configuration of the cylindrical TPP test is useful for predicting the thermal protective performance in 3-second PyroMan™ tests of garments of FR coverall materials (Table shown in Chapter 3). Correlation analysis of the relationships between thermal shrinkage and percent body burn for FR rainwear showed that the spaced configuration of 3 and 4-second TPP tests are useful for predicting the thermal protective performance in 3 and 4-second PyroMan™ tests, respectively (Table shown in Chapter 3). However, complex differences in the thermal responses for FR rainwear materials make identifying these correlations more challenging.

1.7 Conclusions

The results of this research show that after-flame measured in bench-scale tests does not correlate with after-flame time or garment-level thermal protective performance measured in fire manikin tests. These findings raise questions about the inherent value of after-flame performance requirements for FR materials, beyond broad screening tests for differentiating between FR and

non-FR clothing materials. They further question the use of the ASTM D6413 Vertical Flame Test Methods for determining the after-flame performance requirement in NFPA 2112 and ASTM F2733 [34]. This study has definitively shown that after-flame time measured using the ASTM D6413 method cannot be used to predict after-flame or thermal protective performance in full-scale fire manikin tests. Furthermore, the use of after-flame requirements as a basis for certifying compliance to these standards could eliminate some FR materials that perform poorly in the ASTM D6413 flammability test, while providing adequate thermal protection in full-scale fire manikin tests.

The findings of the shrinkage study show that thermal shrinkage measured using a cylindrical TPP method would be a more useful test for establishing thermal shrinkage requirements for FR coveralls than the 500°F oven test in the NFPA 2112 Standard for FR workwear clothing. The cylindrical TPP method should become a standardized test method. Incorporating a TPP-type thermal shrinkage requirement in the FR rainwear standards may be particularly useful, since this test can be used to rank FR rainwear materials based on garment shrinkage and thermal protective performance in fire manikin tests.

1.8 References

1. NFPA 2112 Standard on Flame-Resistant Clothing for Protection of Industrial Personnel Against Short-Duration Thermal Exposures from Fire, National Fire Protection Association, Quincy, MA, 2007.

2. NFPA 1971 Standard on Protective Ensembles for Structural Fire Fighting and Proximity Fire Fighting, National Fire Protection Association, Quincy, MA, 2013.

3. ASTM D6413/D6413M-15 Standard Test Method for Flame Resistance of Textiles (Vertical Test), ASTM International, West Conshohocken, PA, 2015.

4. ASTM F1358-16 Standard Test Method for Effects of Flame Impingement on Materials Used in Protective Clothing Not Designated Primarily for Flame Resistance, ASTM International, West Conshohocken, PA, 2016.

5. CAN/CGSB 4.2 NO. 27.10 Textile test methods-Flame resistance, Canadian General Standards Board, 2011.

6. V. Babrauskas, The Cone Calorimeter, in: SFPE Handb. Fire Prot. Eng., Springer, New York, NY, 2016: pp. 952–980. doi:10.1007/978-1-4939-2565-0_28.

7. ASTM E1354-17 Standard Test Method for Heat and Visible Smoke Release Rates for Materials and Products Using an Oxygen Consumption Calorimeter, ASTM International, West Conshohocken, PA, 2017.

8. G. Song, Clothing Air Gap Layers and Thermal Protective Performance in Single Layer Garment, J. Ind. Text. 36 (2007) 193–205. doi:10.1177/1528083707069506.

9. ASTM F2894-14 Standard Test Method for Evaluation of Materials, Protective Clothing and Equipment for Heat Resistance Using a Hot Air Circulating Oven, ASTM International, West Conshohocken, PA, 2014.

10. ASTM F2700-08 Standard Test Method for Unsteady-State Heat Transfer Evaluation of Flame Resistant Materials for Clothing with Continuous Heating, ASTM International, West Conshohocken, PA, 2008.

11. M. Wang, J. Li, Thermal protection retention of fire protective clothing after repeated flash fire exposure, J. Ind. Text. 46 (2016) 737–755. doi:10.1177/1528083715594977.

12. J. Li, M. Zhao, Y. Xie, Y. Wang, Thermal shrinkage of fabrics used for out layer of firefighter protective clothing under flash fire, Fire Mater. 39 (2015) 732–740. doi:10.1002/fam.2260.

13. Barker, R., Geshury, A., Behnke, W. “The Effect of Nomex®/Kevlar® Fiber Blend Ratio and Fabric Weight on Fabric Performance in Static and Dynamic TPP Tests,” Performance of Protective Clothing, Fifth Volume, ASTM STP 1237, James S. Johnson and S. Z. Mansdorf, Eds., American Society for Testing and Materials, Philadelphia, PA (1996).

14. E.M. Crown, J.D. Dale, E. Bitner, A comparative analysis of protocols for measuring heat transmission through flame resistant materials: capturing the effects of thermal shrinkage, Fire Mater. 26 (2002) 207–213. doi:10.1002/fam.797.

15. ASTM F1930-17, Standard Test Method for Evaluation of Flame Resistant Clothing for Protection Against Fire Simulations Using an Instrumented Manikin, ASTM International, West Conshohocken, PA, 2017.

16. X. Li, Y. Lu, L. Zhai, M. Wang, J. Li, Y. Wang, Analyzing Thermal Shrinkage of Fire-Protective Clothing Exposed to Flash Fire, Fire Technol. 51 (2015) 195–211. doi:10.1007/s10694-013-0375-0.

17. M. Wang, X. Li, J. Li, B. Xu, A new approach to quantify the thermal shrinkage of fire protective clothing after flash fire exposure, Text. Res. J. 86 (2016) 580–592. doi:10.1177/0040517515595028.

18. J. Li, M. Zhao, Y. Xie, Y. Wang, Thermal shrinkage of fabrics used for out layer of firefighter protective clothing under flash fire, Fire Mater. 39 (2015) 732–740. doi:10.1002/fam.2260.

19. Pawar, M., Barker, R., Shalev, I., Hamouda, H., Behnke, W., Bender, M., “Analyzing the Performance of Protective Garments in Manikin Fire Tests,” Proceedings of the Fifth Scandinavian Symposium on Protective Clothing, Elsinore, Denmark, May 1997.

20. Wang, X. Li, J. Li, Correlation of bench scale and manikin testing of fire protective clothing with thermal shrinkage effect considered, Fibers Polym. 16 (2015) 1370–1377. doi:10.1007/s12221-015-1370-5.

21. C. Lee, I.Y. Kim, A. Wood, Investigation and correlation of manikin and bench-scale fire testing of clothing systems, Fire Mater. 26 (2002) 269–278. doi:10.1002/fam.808.

22. G. Song, R.L. Barker, H. Hamouda, A.V. Kuznetsov, P. Chitrphiromsri, R.V. Grimes, Modeling the Thermal Protective Performance of Heat Resistant Garments in Flash Fire Exposures, Text. Res. J. 74 (2004)

23. Arifoglu, M., “Innovations in Heat and Flame Protection Using Gore Fabric Technology,” AATCC International Conference Proceedings, Wilmington, NC, March 2017.

24. Adams, D., “Fire Resistant Fabric Testing and Significance,” AATCC Flammability Symposium, Raleigh, NC 2016

25. Structure Sensor- 3D scanning, augmented reality, and more for mobile devices. Available: https://structure.io/.

26. itSeez3D. Available: https://itseez3d.com/.

27. Autodesk. Autodesk Fusion 360. Available: https://www.autodesk.com/.

28. K. Varga et al, "Thermal and sorption study of flame-resistant fibers," Lenzinger Berichte, vol. 89, pp. 50-59, 2011.

29. PBI Products, "PBI Max". Available: https://www.pbiproducts.com/.

30. S. Francis, "Understanding Fibers and Fabrics: The Engineering of Arc Rated/Flame Resistant Fabrics," *Westex by Milliken,* 2018.

31. Gore® Pyrad® fabric technology: durable flame retardant protection. Available: https://www.gore-workwear.co.uk/technologies/gore-pyrad-fabric-technology.

32. B. C. Nutt, J. P. Towey, D. Narasimhan and M. S. Zedalis, "Flexible Lightweight Arc Flash and Flash Fire Resistant Polyvinylchloride Fabric and Garments and Methods Therefor " US 2016.003917OA1, Feb, 2016.

33. ASTM F2733-17 Standard Specification for Flame-Resistant Rainwear for Protection Against Flame Hazards, ASTM International, West Conshohocken, PA, 2017.

CHAPTER 2: Investigation of Lab Scale Tests for Predicting After-flame in Protective Garments in PyroMan™ Tests

2.1 Introduction

Instrumented fire manikin tests provide invaluable evaluation of systems-level thermal protective performance of fire protective clothing. Nevertheless, few studies have focused on predicting after-flame behavior observed in fire manikin testing. Correlations between bench-scale test methods and the after-flame observed in fire manikin tests have yet to be established in scientifically qualified experimental studies. This is a significant gap, since the availability of well-qualified lab-scale tests for predicting the performance of materials in fire manikin tests would be of considerable practical value. These tests would accelerate research and development by identifying promising prototype materials and constructions prior to fire manikin testing.

Standardized bench-scale tests of fabric flammability are the primary means of evaluating the suitability of materials for use in fire and heat resistant protective clothing. These tests form the basis of most NFPA performance requirements for fire resistant protective clothing [1-2]. One test method stands out: The Vertical Flame Test (ASTM D6413) [3]. In spite of the widespread reliance on this method, apart from screening thermoplastic materials, and identifying materials of normal flammability, little scientific basis exits for qualifying the utility of these methods for differentiating materials thermal performance in full-scale fires, or for protecting against burn injury in fire exposures.

Instrumented fire manikin technology, PyroMan™, permits assessment of the thermal protective performance of materials and garments in realistic simulations of flash fire exposures. Fire manikin provides an ideal testing platform to address these fundamental questions: How do bench-scale tests of after-flame correlate with after-flame observed in realistic simulation of

flash fire exposures? If they do not correlate, how can bench-scale test methods be devised to predict materials response in fire manikin tests?

The objective of this study was to assess the applicability of using standard flammability tests, such as ASTM D6413, to predict PyroMan™ after-flame. This study also sought to qualify the impact of after-flame on the thermal protective performance or burn injury prediction provided by PyroMan™ tests.

2.2 Background

2.2.1 Predicting After-flame in PyroMan™ Fire Manikin Tests

Many different factors influence the burning behavior of garments in fire manikin testing. Some of the most important factors include flame intensity and duration, convective and radiant components of the heat, and the orientation of fabric with respect to the flames. The potential for flame propagation resulting from the burning of flammable gases adds to the difficulty of predicting the after-flame in manikin testing.

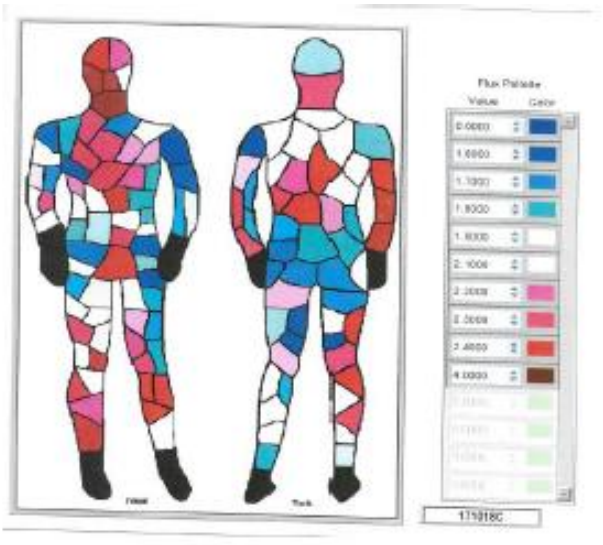

Figure 2.1 Distribution of Incident Heat Flux in PyroMan™ calibration burn.

While the average incident heat flux in fire manikin testing is 84 kW/m^2, the distribution of the incident heat flux can vary significantly and is dependent on the location on the manikin body (Figure 2.1). The complex geometry of the manikin form, fit of the garment, ventilation, available oxygen, and flame propagation all impact the burning behavior of garments and show that the extreme conditions experienced in fire manikin testing are physically complicated themselves.

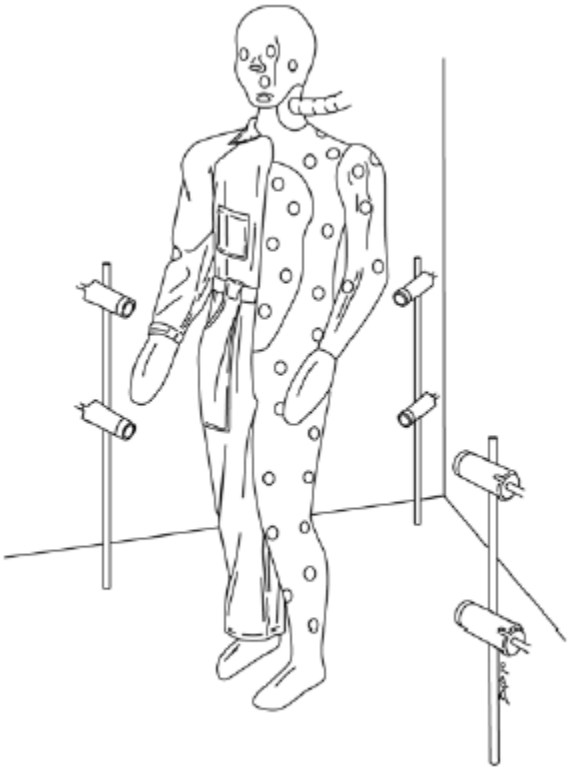

NOTE 1—Only six of eight burners are shown.

Figure 2.2 Burner layout of fire manikin test (redrawn from [15]).

In addition to the complexities of the flames and manikin themselves, the orientation of the manikin and test garment with respect to the flames may affect the after-flame and thermal shrinkage behavior of garment materials. While the ASTM F1930 outlines one layout for the burners used to deliver the flash fire exposure, there is no requirement or specified layout that is

required for laboratories to follow. While the ASTM F1930 requires at least 8 burners and offers two suggested layouts, there is no specific layout requirement for the burner layout. The first suggested layout involves a total of 8 industrial propane burners, with 2 in each quadrant of the test chamber (Figure 2.2) [15]. The PyroMan™ test system follows this suggested layout. Regardless of the position of the burners with respect to the manikin, the flames from the burners contact the manikin at a variety of angles, from nearly perpendicular contact to acute angles of contact. Contact with flames occurs largely at the outer surface of the material. However, contact with folded edges may also occur at sewn features such as pockets. Flames may also be able to travel into the garment at openings on the garment, such as the end of the legs and sleeves and at the collar. The ability of flames to infiltrate the garment is dependent on the garment design. Garment design with respect to variations in the fit and air layers over the manikin can also influence the ignition and shrinkage of materials as well as flame propagation. Gas pressure and velocity as well as the conditioning of the test chamber all contribute to the complexity of test environment. These variables and their effects with regard to predicting the after-flame and thermal shrinkage in manikin tests are poorly understood.

The self-sustained burning and after-flame behavior of fabrics occurs when the temperature of the fabric reach “ignition temperatures,” which triggers uncontrolled exothermic reactions and the presence of flame [34]. These ignition temperatures occur in fire manikin testing when the thermal energy from the flash fire exposure consumes the flame-retardant mechanism in the FR fabric. When this occurs, a catastrophic release of thermal energy is triggered in the direction of the manikin sensors. This release of energy has been observed in TPP tests of FR treated fabrics [35].

2.2.2 Measuring After-flame in Bench-Scale Flammability Tests

The conditions that exist in full-sale flame manikin tests are very different than the conditions that exist in bench-scale flammability test methods. One of the greatest differences is flame intensity. While fire manikin tests typically expose garments to a heat flux of 84 kW/m^2, the heat flux of the flame exposure in bench-scale flammability testing is not defined in standardized test methods. A study by Wang et al determined the average net heat flux of a Bunsen flame in the UL94 vertical burning test for polymers to be approximately 53.15 kW/m^2 [36]. However, it should be noted that the height of the Bunsen flame in this study was 20mm while multiple of the standard flammability tests for FR textile materials calls for a flame height of 38mm. Despite a wide range of differences, numerous standardized test methods are available for evaluating the flammability of flame protective clothing fabrics. Each bench-scale test employs a small flame as the ignition source to evaluate the ability of fabrics to ignite, propagate flames beyond the initial ignition point, and the after-flame. One of the main parameters that is different among the bench-scale flammability tests is the mode of flame contact (edge, surface, folded surface). Additionally, the tests represent different sample orientations with respect to the flame, which can range from vertical to 30 degree to perpendicular flame ignition. Some tests,

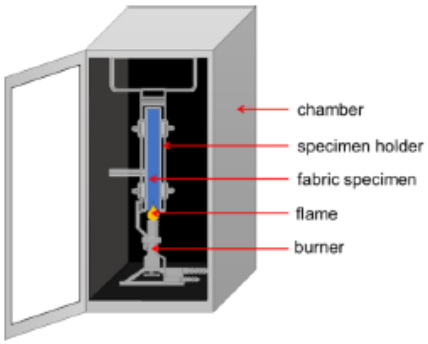

Figure 2.3 Schematic illustration of fabric vertical flame test set-up

such as the cone calorimeter (ASTM E1354), measure the rate of heat released in the combustion of the test specimen [6-7].

The vertical flame test method (Figure 2.3) (ASTM D6413), is the most widely used method for testing the flammability of materials used in fire resistant garments [3]. In the vertical flame test method, the bottom edge of a vertically oriented fabric specimen is exposed to a standardized flame until self-sustained burning is observed or for a 12-second maximum, whichever occurs first. The 12x3 inch test sample is restrained at the edges running along the length of the fabric in a metal sample holder. A study performed by An, Barker, and Stull tested fabric samples without restraining them to evaluate the effect of shrinkage [37]. Many standards outlining the vertical flame test method call for the measurement of the after-flame time, afterglow time, and char length. The char length, which is a measure of the tear resistance of the burned fabric sample, indicates the extent of decomposition experienced by the specimen as a result of combustion beyond the point of ignition. Multiple performance standards such as the NFPA 2112 Standard for Fire Resistant Protective Clothing call for the ASTM D6413 vertical flame test in assessment of FR garment materials. The NFPA 2112 standard, for example, requires compliant materials to have a char length of less than 4 inches and an after-flame time of less than 2 seconds [1,3]. The ASTM F2733 Standard Specification for Flame-Resistant Rainwear for Protection Against Flame Hazards is another performance standard that cites the ASTM D6413 vertical flame test. The ASTM F2733 standard requires compliant FR rainwear garment materials to have a char length of less than 4 inches and an after-flame time of less than 2 seconds [3, 33].

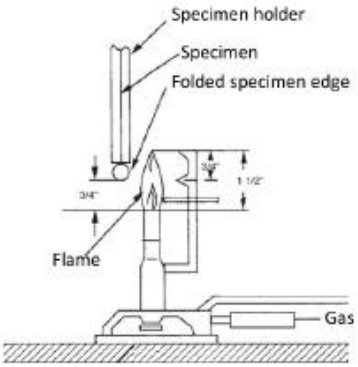

Figure 2.4 Schematic illustration of folded edge ignition-vertical flame test set-up (redrawn from [4]).

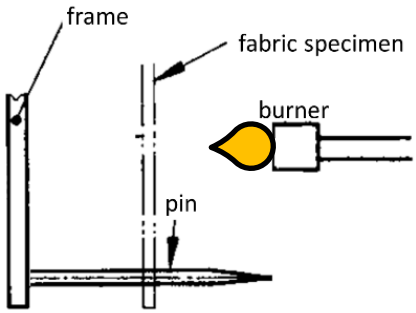

Figure 2.5 Schematic illustration of CGSB-4.2, No. 27.10-A Canadian flame test-surface ignition (redrawn from [5]).

The vertical orientation of the test sample with respect to the ignition source produces the most severe flame exposures encountered in bench-scale flammability tests. One weakness of the vertical flame test methods is that the flame exposure occurs at the cut edge of the specimen. This type of exposure is not often experienced in real-world scenarios or in the PyroMan™ instrumented fire manikin test of protective garment systems. A study conducted at North Carolina State University investigating the flammability of materials used in chemical protective suits developed a method for exposing the surface of the fabric test specimen to a standardized flame in a vertical testing configuration [37]. The method followed the typical procedure used in the vertical flame test with the modification that the specimens were folded so that the folded

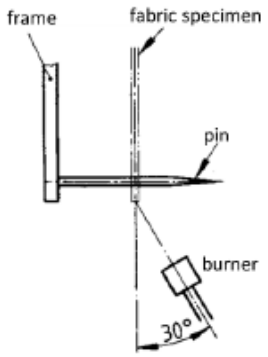

Figure 2.6 Schematic illustration of vertical flame test with an angled burner (redrawn from [5]).

edge contacts the flame (Figure 2.4) The fold is created by placing a ¼-inch diameter rod at the bend of the material. The specimen is then restrained in the sample holder and the rod is removed prior to the exposure. This folded edge vertical flame test method is standardized in ASTM F1358 [4].

The Canadian (CGSB) standardized flammability test, CGSB-4.2, No. 27.10 determines the burning behavior of flame-resistant fabrics held in a vertical orientation. The standard outlines two different configurations for flame exposure: surface ignition with a horizontally-oriented burner held perpendicular to the surface of the specimen (Figure 2.5) and edge ignition with the burner at a 30-degree angle to the vertical towards the bottom edge of the sample (Figure 2.6). Perhaps the greatest difference between the CGSB standard and the vertical flame and folded edge flame tests is the conditioning of the samples prior to testing. The char length (in cm) is also measured in the CGSB standard [5]. While the ASTM D6413 and ASTM F1358 standards call for the specimens to be held at 21°C/65% RH for 24 hours prior to testing, the CGSB standard requires for the samples to be dried in an oven at 105°C for an hour then cooled for at least 30 minutes in a desiccator prior to testing [3-5]. This conditioning requirement means that the specimens will be much drier during flammability testing than the specimens in the

ASTM D6413 and ASTM F1358 standards, resulting in samples burning more readily and potentially exhibiting longer after-flame times and longer char lengths than observed in the other bench-scale flammability tests. ISO 15025 is similar to CGSB-4.2, No. 2710. The ISO performance standard requires FR materials to have an after-flame time greater than 2.0 seconds in both Procedure A (horizontal flame application) and Procedure B (30-degree angle flame application) testing protocols [5, 38].

2.2.3 Correlating Bench-Scale Measures with After-flame in PyroMan™ Tests

A review of the pertinent literature confirmed that the relationship between bench-scale measures of after-flame and the after-flame observed in fire manikin tests has not been qualified in a systematic research study. Nevertheless, it is assumed that garment after-flame may contribute to predicted body burn in PyroMan™ tests. This is certainly true if the after-flame phenomenon is evidence of uncontrolled material combustion and sustained burning. Therefore, an important research goal is to determine if small-scale after-flame tests are predictive of general combustion and sustained burning in PyroMan™ exposures.

2.3 Experimental Methods and Procedures

The above described bench-scale flammability test methods were used to measure the after-flame characteristics of a selected set of heat resistant test materials. As discussed, these small-scale methods differ in the flame ignitions source, flame contact with the test specimen, specimen orientation, and the intensity and duration of the small flame ignition source. They also differ in the degree to which the testing procedure automates the measurement of the duration of observed after-flame. Other differences may affect the accuracy of measurement. The ASTM D6413 vertical flame test, for example, uses an automatic timer to start and stop the flame exposure. It calls for a stopwatch to be started immediately after the flame is removed. The

ASTM F1358 folded edge flame test also uses an automatic timer to start and stop the flame exposure. The apparatus used for the folded edge flame test in this study also used a timer that automatically started once the flame exposure ended. The operator then manually stopped the timer to measure the after-flame duration. These techniques differ from the CGSB-4.2, No. 27.10 flame test standard. The after-flame for this test method was measured by starting a stopwatch when the flame contacts the fabric specimen and stopping the stopwatch after the after-flame is completely dissipated. Because the operator must manually start the stopwatch when the flame contacts the specimen and manually remove the flame after the specified exposure duration, there is an increased opportunity for measurement error.

2.3.1 Measuring After-flame and Heat Released in PyroMan™ Tests

After-flame time was measured in the PyroMan™ test using video analysis. Video images were recorded using cameras filming from both the front and back sides of the PyroMan™ manikin. After-flame was recorded as the time from end of flame exposure from the propane torches to when flames from the burning test garment could no longer be observed. Video recordings were analyzed, frame by frame, to precisely assess when visible after-flame ends. After-flame time was calculated by dividing the total number of frames by the camera's frame speed. This objectively measured video analysis procedure ensures after-flame measurements of a PyroMan™ test are more accurate than after-flame measurements in small-scale flammability tests.

Peak heat release rate (PHRR) and total heat release (THR) were also determined in the PyroMan™ tests. This enabled comparison with the heat release parameters reported in cone calorimeter tests. During the test interval, manikin PHRR was determined as the average heat flux recorded by manikin thermal sensors (at a sampling rate of 0.1s) and was calculated as the

maximum average heat flux measurement over the same interval. THR was recorded as the average heat flux measured multiplied by the elapsed time of the test. It should be noted that these measurements consider only the PHRR and THR on the manikin back side of the test garment, while heat release calculated in the cone calorimeter test measures full combustion of the sample.

2.4 Test Materials

A variety of different fire protective fabric materials were selected for this study. Table 2.1 provides a summarized description of the test materials. Test materials fall into two broad categories: one group was selected to represent a range of flammability and thermal shrinkage characteristics found in single-layer woven FR industrial workwear or military uniform fabrics. The other group represented FR rainwear laminates.

2.4.1 Aramids

Three different meta-aramid fabrics: 4.5osy (Material A), 6.0osy (Material B), and 7.5osy (Material C). Temperatures above the glass transition temperature (T_g) of meta-aramid fibers are observed in flash fires causing fabrics made with meta-aramid fibers to shrink [28]. To improve high temperature thermal stability, meta-aramid fibers are blended with other more heat-resistant fibers, including para-aramid fibers. Meta-aramid fibers have a glass transition temperature (T_g) of 275°C, while para-aramid fibers have a T_g of 327°C. Meta-aramid fibers swell in high-heat exposures, which seals openings in the fabric reducing heat transfer to the skin [28].

2.4.2 Polybenzimidazole (PBI)

A 7osy twill-weave fabric of 70%/30% “PBI-dominant” para-aramid blend/para-aramid filament (Material I). PBI has a high T_g (400°C) and thermal decomposition temperature (1175°C), indicating thermal stability (shrinkage resistance) in flash fire conditions [29].

2.4.3 Modacrylic Blends

Two twill-weave variants composed of blends of 45% modacrylic/35% Lyocell/ 20% aramid in a 7osy (Materials G) and 8.5 osy (Materials H) basis weight. Both fabrics are NFPA 2112 certified, indicating that they exhibit less than 2 seconds of after-flame time on the vertical flame test and less than 10% shrinkage in the 500°F oven test [1]. Because modacrylic fibers are composed of an acrylic and modacrylic co-polymer composition, they undergo a two-stage degradation at temperatures of 236°C and 503°C. The acrylic component protects by char formation, while the modacrylic flame retardant component suppresses burning via vapor-phase free radical (halogen) reactions [28].

2.4.4 FR Cotton

The FR cotton fabric used in this study is a 7osy twill construction incorporating an 88/12% blend of cotton and nylon fibers (Materials J). This test fabric uses a FR finish containing tetrakis(hydroxymethylol) phosphonium salts to achieve flame resistance. It is NFPA 2112 certified, meaning that it has less than 2 seconds after-flame time in the vertical flame test, and less than 10% shrinkage in the 500°F oven test [1]. Once the FR finish is consumed during a flame exposure, the cotton will quickly degrade, rapidly increasing after-flame and heat transfer [30].

2.4.5 FR Laminate

Proprietary technology FR laminate materials incorporate a char-forming FR component. Three different substrate constructions and weights were studied: Material D used a 100% nylon plain weave substrate in a 4osy construction, Material E used a twill rip-stop weave made of 100% nylon 6,6, and Material F featured a 100% polyester twill weave 100% polyester substrate fabric. These laminate constructions form stable char contributing to increased structural

integrity in flame exposures [31]. They have less than 2 seconds after-flame time in the vertical flame test but exhibit high levels of thermal shrinkage in the 500°F oven test [31]. Because these laminate materials are used in rainwear ensembles, these three FR laminates were included in both the FR coverall and FR rainwear categories of garment test materials.

2.4.6 FR Rainwear

This study included materials used in FR rainwear garments (rain jacket and bibs/overalls). Rainwear material M is a proprietary char-forming laminate technology incorporated in a 8.3osy construction. Other FR rainwear test materials consisted of a FR poly(vinyl) chloride (PVC) barrier laminated on a nonwoven meta-aramid fabric in a 11.3osy construction (material K), and in 9.5osy laminate (material L). The low T_g and low flash point of PVC material means that they will burn and propagate flame more readily than other FR rainwear materials. Additionally, phthalates are often used as PVC plasticizers and may be present in these materials. The presence of phthalate plasticizers could affect how the material burns and propagates flames [32]. Another of the rainwear test materials (material N) used a FR neoprene coating on meta-aramid fabric in a 13.5osy construction. The halogens in the neoprene coating produce radical reactions when exposed to a flame, the source of the FR properties in this material. Finally, rainwear garment material O is a laminate composed of a FR polyurethane coating on 10osy 100% knit FR cotton. Each of the rainwear test materials is compliant with the ASTM F2733 standard, meaning that they exhibit less than 2 seconds of after-flame in the ASTM D6413 vertical flame test.

Table 2.1 Summarized Description of Test Materials

ID	**Material**	**Fiber Content**	**Construction**	**Fabric Weight** (osy)	(1)**Nominal After-flame** (sec)	(2)**Nominal Shrinkage** (%)
A	Aramid	93% meta-aramid/ 5% para-aramid/ 2% antistat	Plain Weave	4.5	< 2	< 10%
B	Aramid	93% meta-aramid/ 5% para-aramid/ 2% antistat	Plain Weave	6.0	< 2	< 10%
C	Aramid	93% meta-aramid/ 5% para-aramid/ 2% antistat	Plain Weave	7.5	< 2	< 10%
D	FR Laminate	100% nylon	Plain Weave	4.0	< 2	high
E	FR Laminate	100% nylon 6,6	Rip-stop	5.3	< 2	high
F	FR Laminate	100% polyester	Twill Weave	6.5	< 2	high
G	Modacrylic	45% modacrylic/ 35% Lyocell/ 20% aramid	Twill Weave	7.0	< 2	< 10%
H	Modacrylic	45% modacrylic/ 35% Lyocell/ 20% aramid	Twill Weave	8.5	< 2	< 10%
I	PBI	70% PBI/ 30% para-aramid	Twill Weave	7.0	< 2	< 10%
J	FR Cotton	88% FR cotton/ 12% nylon	Twill Weave	7.0	< 2	< 10%
K	FR Rainwear	100% meta-aramid	FR PVC/ on meta-aramid nonwoven	11.3	< 2	
L	FR Rainwear	100% meta-aramid	FR PVC on meta-aramid nonwoven	9.5	< 2	
M	FR Rainwear	100% polyester	Twill Weave	8.3	< 2	high
N	FR Rainwear	93% meta-aramid/ 5% para-aramid/ 2% antistat	FR neoprene on plain weave meta-aramid	13.5	< 2	
O	FR Rainwear	100% FR cotton	FR polyurethane on FR cotton knit	10.0	< 2	

2.5 Test Methods

Prior to use in testing, each test material was washed for one cycle with a water temperature of 140°F using the AATCC standard reference detergent. Each test specimen was dried at a temperature of 155°F.

Table 2.2 shows the battery of bench-scale flammability tests used to evaluate the after-flame and combustion characteristics of the test materials described in Table 2.1.

Table 2.2 Battery of Bench-Scale Test Methods for Predicting PyroMan™ After-flame

Test Method	Rationale
ASTM D6413- Vertical Flame	Test used in NFPA standards, orientation produces severe flame exposure
CGSB- 4.2, 27.10- Configuration A (perpendicular application)	Surface exposure is more practical, orientation produces severe flame exposure
CGSB-4.2, 27.10- Configuration B (30-degree angle edge application)	More stringent than surface ignition
ASTM F1358 Folded Edge	Curved test surface
ASTM E1354 Cone Calorimeter	PHRR or THR may correlate with PyroMan™ after-flame

Test materials were used to construct FR coveralls and rainwear garments for testing on PyroMan™. Triplicate tests were made for each of the garment types. Table 2.3 shows the PyroMan™ measurement parameters.

Table 2.3 PyroMan™ Test Measurements (3, 4-second exposures)

Report	Measurements
% Body burn	Recorded temperature data
Duration of after-flame	Video recordings (front and rear)
Garment Shrinkage	Markers on backside of garments; 3-D Scanning

2.5.1 Small-scale Flammability Test Methods

2.5.1.1 Vertical Flame Test

The ASTM D6413 vertical flame test was included in this study because of its wide usage, and because it is required by the NFPA 2112 and ASTM F2733 Standards for FR

workwear and FR rainwear. The vertical orientation of the test specimen produces the most severe flame exposures. A limitation of the vertical flame test is that the edge exposure does not represent the most realistic testing configuration for simulating flame contact with garments. Most real-world applications involve the ignition at the fabric surface rather than at the cut edge of the fabric.

2.5.1.2 Folded Edge Flame Test

The ASTM F1358 folded-edge flame test method evaluates the burning behavior of a curved fabric surface rather than a flat surface or edge. The vertical orientation in the folded edge sample produces the most severe flame exposures. The curved surface is more representative of most real-world flame exposures involving ignition of curved fabric surfaces rather than flame contact with flat surfaces or cut edges.

2.5.1.3 Canadian Flammability Test

The Canadian standard test method for flammability, CGSB-4.2, No. 27.10, was selected because it provides flame exposures at several different angles compared to the vertical flame and folded edge flame tests. This standard includes two different configurations, both of which have been included.

Configuration A (Perpendicular Surface Ignition): The vertical flame and folded edge flame tests, the vertical orientation of the specimens produces the most severe flame exposures. The flame exposure at the surface of the fabric may more accurately represent the real-world applications where fabrics are more likely to be exposed at the surface rather than at the cut edge. However, the flat surface exposure could produce less accurate results in comparison to the folded edge flame test, which exposes a curved fabric surface rather than a flat surface exposure.

Configuration B (30-degree Edge Ignition): The edge ignition configuration of the Canadian flammability test produces more stringent conditions than the surface configuration of this test. Again, the ignition of the cut edge of samples may not accurately represent how fabrics are exposed in real-world applications where the surface of fabrics typically come into contact with flames.

2.5.1.4 Cone Calorimeter

The cone calorimeter test (ASTM E1354) measures heat release rates based on oxygen consumption calorimetry. Although this test does not measure after-flame, it was considered on the assumption that the peak heat release rate (PHRR), or total heat release (THR), may correlate with after-flame time measured in bench-scale and/or in full-scale manikin testing. Cone calorimetry is widely used for materials combustion analytics and in polymer-level development and characterization of developmental FR materials in advance of PyroMan™ testing.

2.5.2 Full-Scale Flammability Test

2.5.2.1 PyroMan™ Test

The ASTM F1930 protocol was followed in conducting the PyroMan™ tests. Standard procedures were used to calculate predicted body burn injury [15] while novel procedures were developed to measure after-flame time, PHRR, and THR (discussed in section 2.2.5). The testing series were conducted at the standard calibrated average incident heat exposure intensity of 84 kW/m^2 for three- and four-seconds exposure times. No undergarments were used in these tests.

2.6 Results and Discussion

2.6.1 FR Coveralls

Table 2.4 shows the average after-flame times measured in bench-scale flammability tests and in PyroMan™ burns.

Table 2.4 Average After-flame Time (Seconds) Measured in Bench-Scale Flammability Tests and in PyroMan™ Burns (FR Coveralls).

ID	Material Class	Vertical Flame (D6413)	Folded Edge (F1358)	Canadian Edge Ignition (27.10-B)	Canadian Surface Ignition (27.10-A)	PyroMan™ 3-seconds exposure	PyroMan™ 4-seconds exposure
A	Aramid	0.00	0.79	0.00	0.00	0.71	0.56
B	Aramid	0.00	0.77	0.00	0.00	3.07	1.89
C	Aramid	0.00	0.82	0.15	0.00	3.23	3.04
D	FR Laminate	0.00	0.87	4.71	0.76	3.64	4.49
E	FR Laminate	1.04	1.93	18.45	0.56	2.53	7.33
F	FR Laminate	0.82	0.86	1.01	0.00	1.52	5.90
G	Modacrylic	0.00	0.82	0.00	0.30	0.62	3.84
H	Modacrylic	0.00	0.65	0.17	0.00	0.00	1.78
I	PBI	0.00	1.41	0.00	0.00	0.00	0.00
J	FR Cotton	0.00	0.74	0.00	0.46	3.28	5.26

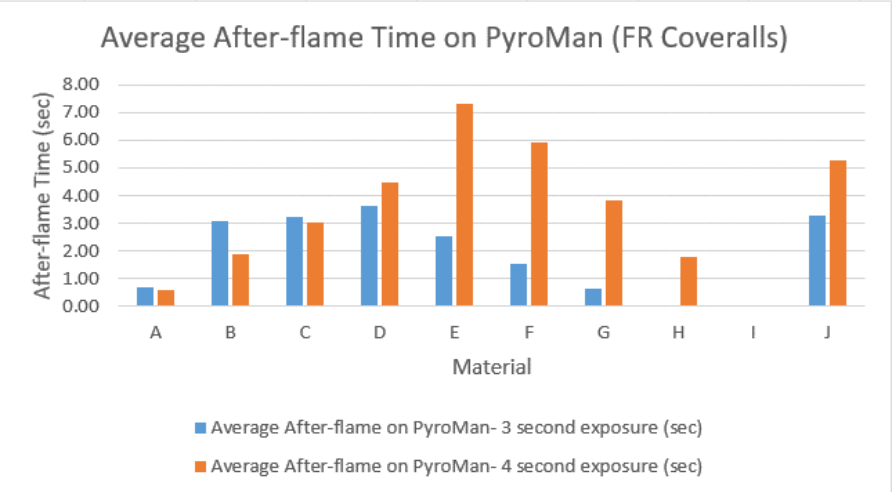

Figure 2.7 Average After-flame time measured in PyroMan testing (FR coveralls)

Data in Table 2.4 show that most FR test materials burn very little, if at all, in most bench-scale flammability tests. However, materials D and E exhibited significant after-flame when tested using the Canadian edge-ignition method. At the same time, after-flame measured in PyroMan™ testing (Figure 2.7), demonstrates that bench-scale flammability tests are not indicative of the after-flame observed in PyroMan™ tests. Half of the FR coverall materials

tested exhibited after-flame greater than 2 seconds in PyroMan™ exposures lasting 3-seconds. Six of the coveralls tested had after-flame greater than 2 seconds in exposure duration of 4-seconds. Another interesting pattern is observed: Figure 2.7 shows that the effects of increasing PyroMan™ exposure time depends on the test material. These data show that, as might be expected, after-flame time increased in most test materials when the duration of the PyroMan™ exposure is increased from 3.0 to 4.0 seconds. However, after-flame slightly decreased or remained about the same in PyroMan™ tests made on aramid test garments (A, B and C) at 3.0 and 4.0 seconds. While not consistent across all test materials, each material class exhibited a similar pattern with regard to the location on the test garment where after-flame occurs in a PyroMan™ test. For example, after-flame on Material J was largely concentrated on the arms

Figure 2.8 (a) After-flame present on the arms of a garment of Material J after a PyroMan™ 3-second exposure; (b) After-flame present on the shoulders and neck of a garment of Material D after a PyroMan™ 3-second exposure.

(Figure 2.8a). The after-flame on the laminate materials initially occurred at multiple areas on the garments, but consistently was reduced to the neck and shoulders at the time the flames were extinguished (Figure 2.8b shows the after-flame for Material D). The after-flame was consistent in replicate tests on PyroMan™ and most of the bench-scale flammability tests. However, the after-flame was much more variable for Materials D and E for the Canadian Flame Test- Edge Ignition than any of the other tests. Materials D and E also exhibited higher variability during the 4-seconds PyroMan™ exposure.

Table 2.5 shows the average peak heat release rate (PHRR) and total heat released (THR) during the total combustion of fabric specimens in the ASTM E1354 cone calorimeter and the PHRR and THR values measured as heat transferred through the garments to the manikin sensors during PyroMan™ tests. Data in Table 2.5 show that the values for the ASTM E1354 cone calorimeter are much higher than the values in the PyroMan™ tests. This is due to the fact that the cone calorimeter test collects these measurements as they relate to the combustion of the entire fabric specimen, rather than as the heat is transferred through the fabric, which is how the measures in PyroMan™ testing are collected. An increase in both the PHRR and THR is exhibited by all FR coverall materials between the 3 seconds and 4-seconds exposure durations in PyroMan™ testing.

2.6.1.1 Prediction of After-flame in PyroMan™ Tests

Multiple statistically based methods were used to determine whether small-scale flammability tests could be used to predict after-flame behavior in PyroMan™ tests. A t-test analysis compared after-flame times measured in the battery of bench-scale tests with the after-flame in coveralls (made from these same materials) tested on PyroMan™. This statistical analysis indicates whether the bench-scale test overestimates, underestimates or accurately

predicts manikin after-flame. The model's hypothesis is as follows: If the bench-scale test after-flame time is neither significantly longer nor shorter than the manikin after-flame time, the bench test is judged to be an accurate predictor of manikin after-flame (Table 2.6).

Table 2.5 Average Peak Heat Release Rate and Total Heat Release in ASTM E1354 Cone Calorimeter and PyroMan™ Testing (FR Coveralls).

ID	Material Class	Cone Calorimeter PHRR (cal/cm2/sec)	3-second PyroMan™ PHRR (cal/cm2/sec)	4-second PyroMan™ PHRR (cal/cm2/sec)	Cone Calorimeter THR (cal/cm2)	3-second PyroMan THR (cal/cm2)	4-second PyroMan THR (cal/cm2)
A	Aramid	2.49	0.71	0.94	45.65	2.59	3.65
B	Aramid	2.68	0.55	0.90	50.24	2.46	3.33
C	Aramid	3.42	0.43	0.67	72.50	2.01	3.18
D	FR Laminate	2.73	0.56	0.94	49.55	2.93	3.98
E	FR Laminate	3.87	0.45	0.68	69.15	2.62	3.84
F	FR Laminate	3.06	0.39	0.74	64.65	2.27	3.70
G	Modacrylic	2.30	0.54	1.10	41.04	2.41	4.34
H	Modacrylic	3.26	0.36	1.09	55.90	1.91	3.95
I	PBI	2.22	0.43	0.51	57.36	1.82	2.85
J	FR Cotton	3.79	0.41	1.32	58.48	2.00	6.26

Table 2.6 T-tests showing grouping of FR coverall materials by statistically significant comparison of bench-scale after-flame to PyroMan™ after-flame

PyroMan™ Exposure Duration	Bench-scale Test	Bench-Scale Overestimates	Bench-Scale Underestimates	Bench-Scale Accurately Estimates
3-seconds	**Vertical Flame Test**		A, B, C, D, E, G, J	F, H, I
	Folded Edge Flame Test	H, I	B, C, D, F, J	A, E, G
	Canadian Test- Edge Ignition		A, B, C, E, G, H, J	D, F, I
	Canadian Test- Surface Ignition		A, B, C, D, E, F, J	G, H, I
	Total for Category	2	26	12
	Percent of Total	5.0%	65.0%	30.0%
4-seconds	**Vertical Flame Test**		B, C, D, E, F, H, J	A, G, I
	Folded Edge Flame Test	I	B, C, D, E, F, H, J	A, G
	Canadian Test- Edge Ignition		B, C, E, F, H, J	A, D, G, I
	Canadian Test- Surface Ignition		B, C, D, E, F, H, J	A, G, I
	Total for Category	1	27	12
	Percent of Total	2.5%	67.5%	30.0%

Table 2.7 Correlations between Bench-Scale Flammability Tests and PyroMan™ After-flame for FR Coverall Fabrics

PyroMan™ Exposure Duration	Bench-Scale Test	Pearson Correlation Coefficient (r)	P-value
3-seconds	Vertical Flame	0.081	0.8233
	Folded Edge Flame Test	-0.019	0.9582
	Canadian Flame Test- Edge Ignition	0.268	0.4534
	Canadian Flame Test- Surface Ignition	0.53	0.1151
	Cone Calorimeter (PHRR)	0.497	0.1438
	Cone Calorimeter (THR)	0.314	0.3764
4-seconds	Vertical Flame	0.721	0.0186*
	Folded Edge Flame Test	0.328	0.3545
	Canadian Flame Test- Edge Ignition	0.639	0.0469*
	Canadian Flame Test- Surface Ignition	0.64	0.0463*
	Cone Calorimeter (PHRR)	0.665	0.0358*
	Cone Calorimeter (THR)	0.422	0.225

*Indicates statistical significance

T-test analysis clearly demonstrates that bench-scale flammability tests do not accurately predict PyroMan™ after-flame. It shows that bench-scale tests tend to underestimate the extent of burning in PyroMan™ tests. This is not a surprising result considering the significant differences in flame intensities, materials configurations and combustion dynamics between bench-scale flame exposures and the PyroMan™ flame environment.

2.6.1.2 Correlation Between Bench-Scale Flammability Tests and After-flame in PyroMan™ Tests

While the t-test analysis shows that bench-scale flammability tests do not accurately predict PyroMan™ after-flame, a relationship may still exist between the bench-scale after-flame and PyroMan™ after-flame. Such a relationship would allow for the ranking of fire protective materials based on bench-scale after-flame. To identify such relationships, correlation analysis is used (Table 2.7). Table 2.7 shows that none of the bench-scale flammability tests produce a statistically significant correlation with 3-seconds PyroMan™ after-flame. Although significant correlations emerged between the ASTM D6413 and the Canadian surface ignition tests with 4-

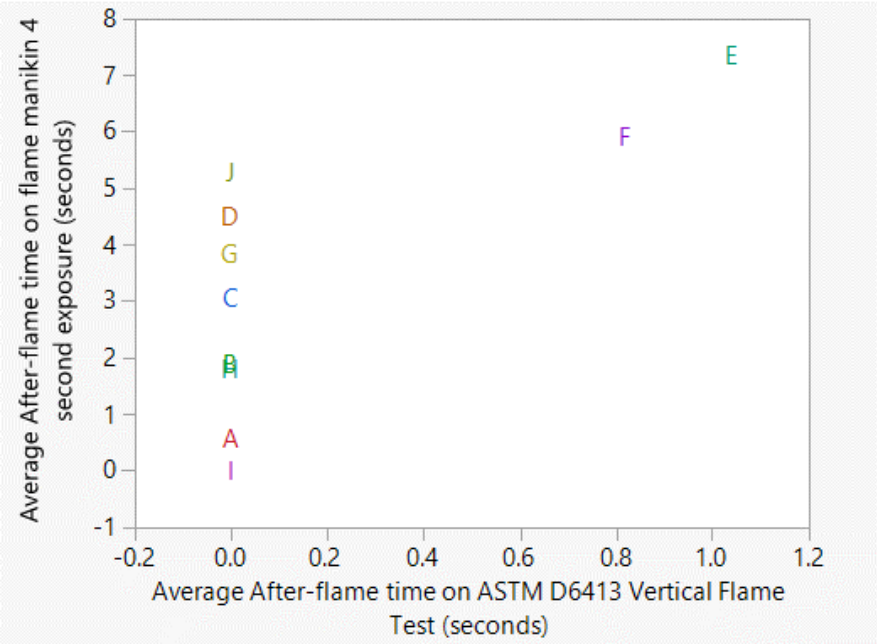

Figure 2.9 Vertical Flame test after-burn vs after-flame in 4-second PyroMan exposure (FR coverall fabrics)

seconds manikin after-flame, these correlations indicate that the relationships are more complex than the coefficients indicate. For example, Figure 2.9 shows the relationship between after-flame measured in the ASTM D6413 vertical flame test and after-flame observed in 4-seconds PyroMan™ exposures. These data show that these FR coverall materials exhibited no after-flame in the ASTM D6413 test, with exception of the two char forming laminates (Materials E and F). These char-forming materials show a slight tendency to after-flame in ASTM D6413, although the amount of after-flame (about 1.0 second) is below the NFPA 2112 criterion of less than 2.0 seconds of after burn [2]. The slight tendency for after-flame indicated by the vertical flammability test forecasts the more significant (7-8 seconds) after-flame time that these same materials (E and F) show in 4.0-seconds PyroMan™ testing. This relationship is considered statistically significant, as indicated in Table 2.7. Without outlier data from Materials E and F, however, no significant relationship would be evident between the ASTM D6413 vertical flame

test and after-flame observed in the 4.0 seconds PyroMan™ test. Similar patterns are observed in the relationships between the two CGSB 27.10 test methods and the 4.0 seconds PyroMan™ test (shown in Appendix A). Other data comparisons tend to demonstrate the insensitivity of the ASTM 6413 test for discriminating among FR materials based on their measured after-flame in fire manikin tests. For example, while none of the aramid fabrics (Materials A, B and C) show after-flame in ASTM D 6413, their after-flame times are distinctly different (they increase with fabric weight) in the PyroMan™ test (Figure 2.9). This analysis generally shows that the ASTM D6413 vertical flame test is not a useful method for ranking materials based on predicted after-flame in fire manikin tests.

While some statistically significant relationships, such as the one in Figure 2.9, do not provide as much information as the correlation coefficients may suggest, other relationships that are not statistically significant may provide useful information of specific classes of materials. Figure 2.10 shows the relationship between after-flame measured in the Canadian surface ignition test (CGSB-4.2, 27.10- Configuration A) and in 3.0-seconds PyroMan™ tests. As

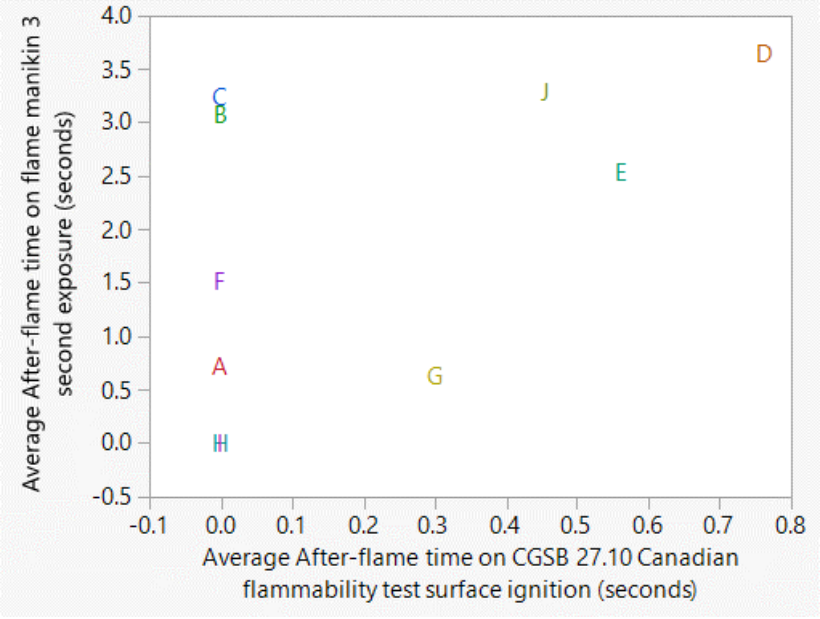

Figure 2.10 Canadian Flame Test (surface ignition) after-flame vs after flame in 3-second PyroMan™ exposure (FR coverall fabrics)

observed for the ASTM D6413 test, the Canadian surface ignition test is unable to forecast difference in after-flame times actually observed in 3.0-seconds PyroMan™ tests. However, the surface ignition method clearly differentiates the after-flame performance of some materials, including the FR modacrylic blends (Materials G and H) and FR cotton/nylon sample (Material J). Trends observed suggest that the Canadian surface ignition test is useful for forecasting after-burn in 3-seconds manikin tests for these materials. However, this test has no apparent utility for predicting manikin after-flame in aramid fabrics.

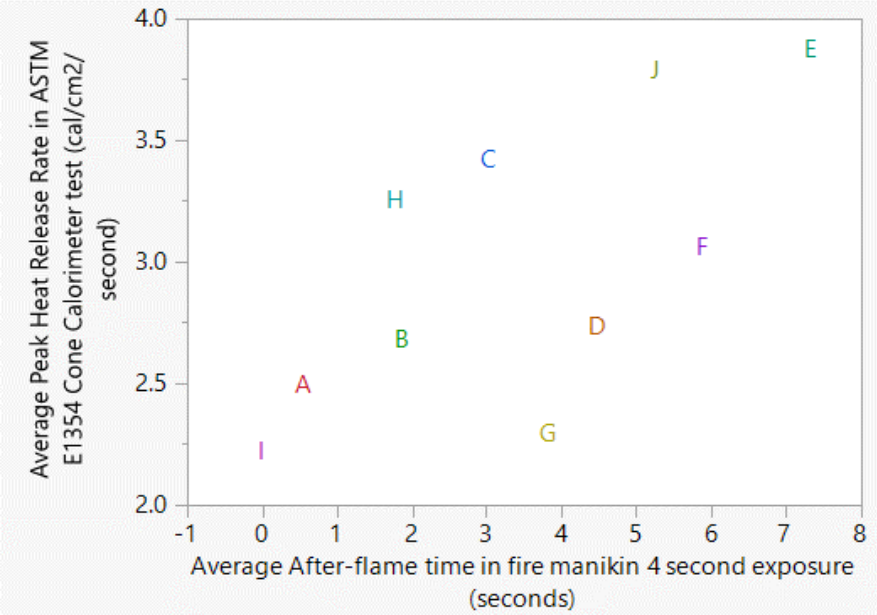

Figure 2.11 PHRR on Cone Calorimeter vs. 4-second PyroMan™ test After-flame for FR coverall fabrics

These correlations do not alter the basic conclusion regarding the inadvisability of using flammability tests to predict after-flame performance in fire manikin exposures. However, correlations analysis (Table 2.7) does show that cone calorimeter peak heat release rate (PHRR) is significantly correlated with after-flame in 4-seconds fire manikin tests. Figure 2.11 shows that the relationship between PHHR and manikin after-flame is complicated. The correlations are

materials dependent: they are better for some materials (aramids and char-forming laminates) than for other fabric types (modacrylic blends).

2.6.1.3 Relationships between After-flame and Thermal Protection

Correlation analysis uncovered no significant relationship between any bench-scale test measure of fabric after-flame and predicted total body burn in PyroMan™ tests of coveralls made from these materials (Table 2.8).

Nor did it reveal a significant relationship between cone calorimeter PHHR and THR and predicted body burn on PyroMan™. The lack of significant relationship for bench-level measures is consistent with the complex relationships observed between after-flame measured on the manikin and predicted % total body burn, in both 3-second and 4-second tests (Figures 2.12 and 2.13). Differences in material characteristics appear to be a factor in the lack of correlation between the after-flame in all flammability tests for protective materials and predicted body burn in PyroMan™ test. These findings do not mean that after-flame has no effect on the burn injury.

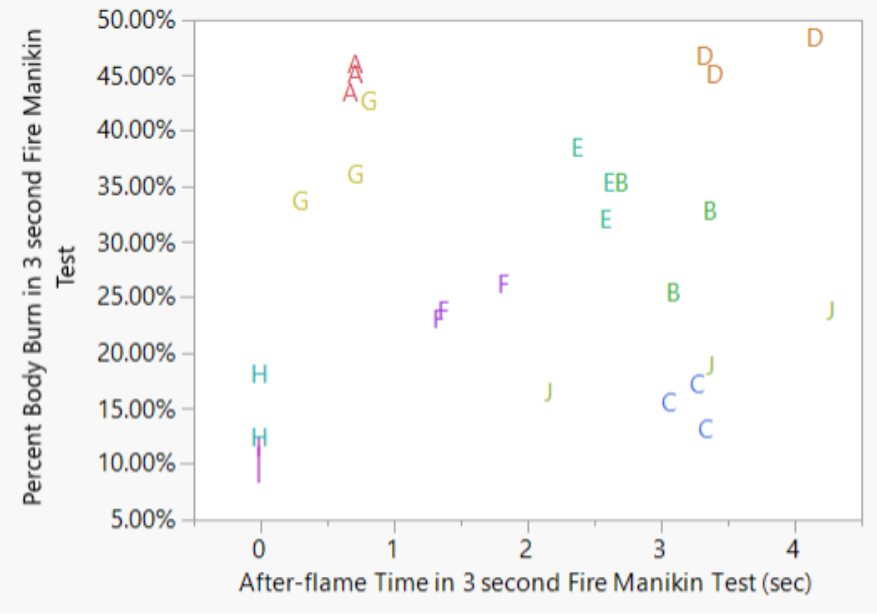

Figure 2.12 After-flame in PyroMan™ 3-second exposure vs. predicted percent body burn in PyroMan™ 3-second exposure (FR coverall fabrics)

They confirm that after-flame is only one of many factors contributing to predicted body burn injury in fire manikin tests.

Table 2.8 Correlation between After-Flame And % Total Body Burn In PyroMan™ Tests of FR Coveralls

PyroMan™ Exposure Duration	Bench-Scale Test	Pearson Correlation Coefficient (r)	P-value
3-seconds	Vertical Flame	0.095	0.7947
	Folded Edge Flame Test	0.006	0.9866
	Canadian Flame Test- Edge Ignition	0.315	0.3746
	Canadian Flame Test- Surface Ignition	0.511	0.1314
	PyroMan™ After-flame	0.235	0.2116
	Cone Calorimeter PHRR	-0.237	0.5094
	Cone Calorimeter THR	-0.5484	0.1007
4-seconds	Vertical Flame	-0.043	0.9065
	Folded Edge Flame Test	-0.318	0.3706
	Canadian Flame Test- Edge Ignition	0.109	0.7646
	Canadian Flame Test- Surface Ignition	0.589	0.0732
	PyroMan™ After-flame	0.384	0.0361*
	Cone Calorimeter PHRR	0.215	0.5503
	Cone Calorimeter THR	-0.46	0.1814

*Indicates statistical significance.

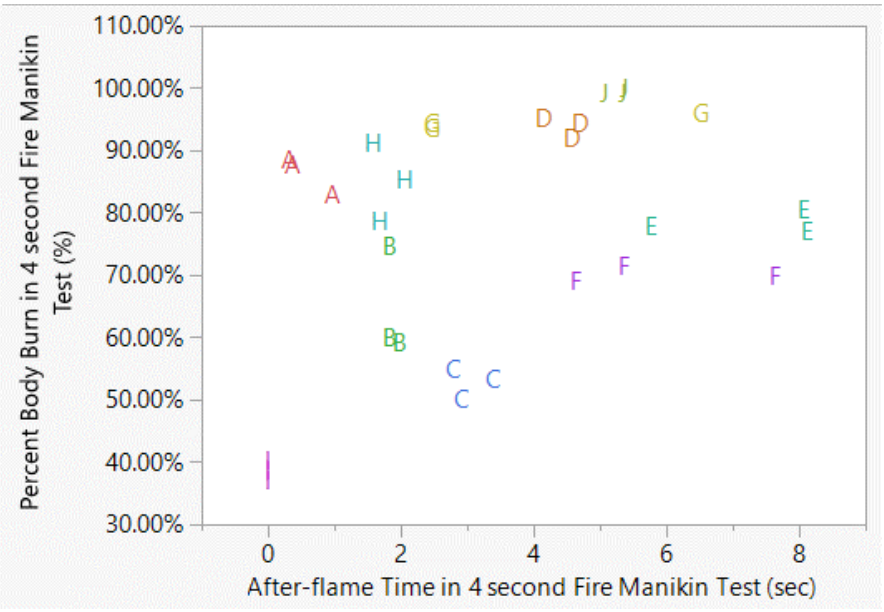

Figure 2.13 After-flame in PyroMan™ 4-second exposure vs. predicted percent body burn in PyroMan™ 4-second exposure (FR coverall fabrics)

2.6.2 FR Rainwear

Table 2.9 shows the average after-flame times measured in bench-scale flammability tests and in PyroMan™ burns for FR rainwear materials.

Table 2.9 Average After-flame Time (Seconds) Measured in Bench-Scale Flammability Tests and in PyroMan™ Burns (FR Rainwear Materials).

Material	Material Type	ASTM D6413 Vertical Flame	ASTM F1358 Folded Edge	Canadian Edge Ignition	Canadian Surface Ignition	PyroMan™ 3-second exposure	PyroMan™ 4-second exposure
D	FR Laminate	0.00	0.87	4.71	0.76	3.64	4.49
E	FR Laminate	1.04	1.93	18.45	0.56	2.53	7.33
F	FR Laminate	0.82	0.86	1.01	0.00	1.52	5.90
K	FR Rainwear	0.30	2.00	5.27	0.64	6.07	15.77
L	FR Rainwear	0.43	1.69	5.45	0.84	34.95	43.17
M	FR Rainwear	0.53	1.00	8.41	0.53	0.29	4.11
N	FR Rainwear	0.27	0.68	0.15	0.24	0.00	0.00
O	FR Rainwear	0.20	0.84	0.00	0.64	1.07	3.99

Figure 2.14 (a) After-flame on Material K rainwear garment after PyroMan 3-second exposure; (b) after-flame on Material L rainwear garment after PyroMan 4-second exposure.

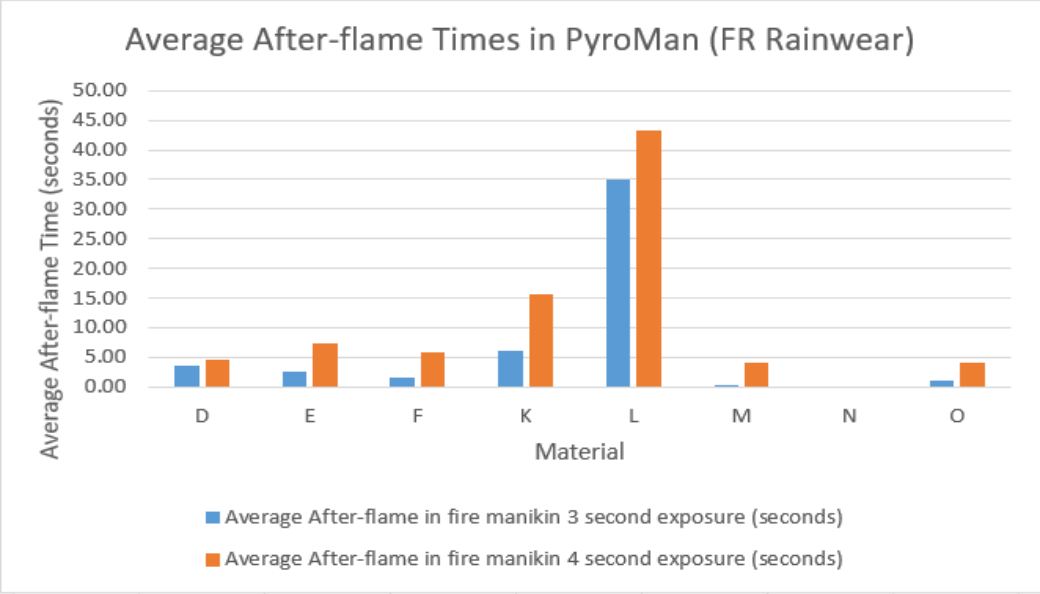

Figure 2.15 Average after-flame times measured in PyroMan testing (FR rainwear materials).

These data show that, for some FR rainwear materials, after-flame observed in PyroMan™ tests is markedly greater than observed in bench-scale flammability tests. For example, PVC Material L exhibited a dramatic increase in after-flame time in PyroMan™ testing, when comparing the bench-scale flammability results. Of the bench-scale tests, the Canadian edge-ignition method provided the most accurate prediction of the flaming response of this material in PyroMan™ tests. With regard to spatial distribution of flames in PyroMan™ tests of these materials, after-flame was observed mainly around the upper body region of the test garment (Figure 2.14a). PVC Material L was the exception to this pattern: for which after-flame concentrated around the midsection and upper legs (Figure 2.14b). Figure 2.15 shows the extensive after-flame observed in the PVC laminates (Materials K and L) in PyroMan™ burns.

Table 2.10 Average Peak Heat Release Rate and Total Heat Release in ASTM E1354 Cone Calorimeter and PyroMan™ Testing (FR Rainwear).

ID	Material Class	Cone Calorimeter PHRR (cal/cm2/sec)	3-second PyroMan™ PHRR (cal/cm2/sec)	4-second PyroMan™ PHRR (cal/cm2/sec)	Cone Calorimeter THR (cal/cm2)	3-second PyroMan THR (cal/cm2)	4-second PyroMan THR (cal/cm2)
D	FR Laminate	2.73	0.56	0.94	49.55	2.93	3.98
E	FR Laminate	3.87	0.45	0.68	69.15	2.62	3.84
F	FR Laminate	3.06	0.39	0.74	64.65	2.27	3.70
K	FR Rainwear	5.27	0.37	0.43	107.15	1.51	2.91
L	FR Rainwear	4.69	0.42	0.50	119.79	2.93	4.45
M	FR Rainwear	2.74	0.27	0.40	66.20	1.28	2.17
N	FR Rainwear	2.93	0.33	0.38	55.17	1.61	2.39
O	FR Rainwear	5.04	0.46	0.64	100.89	1.98	2.92

Table 2.10 shows the average peak heat release rate (PHRR) and total heat release (THR) results from cone calorimeter and PyroMan™ testing. The results from the cone calorimeter are significantly higher than those from PyroMan™ testing due to the fact that the cone calorimeter measures the heat released from the combustion of the entire specimen, while the measurements from PyroMan™ testing are from the heat transferred through the fabric to the manikin sensors during and immediately following flame exposure.

2.6.2.1 Predicting After-flame in PyroMan™ Tests

As observed for FR coveralls, t-test analysis reveals that bench-scale flammability tests have limited ability to predict the PyroMan™ after-flame for FR rainwear materials (Table 2.11). Bench-scale tests most often underestimate, sometimes overestimate, but rarely accurately predict the after-flame measured in PyroMan™ testing of FR rainwear garments.

Table 2.11 T-tests showing grouping of FR rainwear materials by statistically significant comparison of bench-scale after-flame to PyroMan™ after-flame.

PyroMan™ Exposure Duration	Bench-scale Test	Bench-Scale Over-estimate	Bench-Scale Under-estimate	Bench-Scale Accurately Estimates
3-seconds	Vertical Flame Test	N	D, E, K, L, O	F, M
	Folded Edge Flame Test	M, N	D, F, K, L	E, O
	Canadian Flame Test- Edge Ignition	E, M	L, O	D, F, K, N
	Canadian Flame Test- Surface Ignition	N	D, E, F, K, L	M, O
	Total	6	16	10
	Percent of Total	18.8%	50.0%	31.3%
4-seconds	Vertical Flame Test	N	D, E, F, K, L, M, O	
	Folded Edge Flame Test	N	D, E, F, K, L, M, O	
	Canadian Flame Test- Edge Ignition	E	F, K, L, O	D, M, N
	Canadian Flame Test- Surface Ignition	N	D, E, F, K, L, M, O	
	Total	4	25	3
	Percent of Total	12.5%	78.1%	9.4%

2.6.2.2 Correlation between Bench-Scale After-flame and PyroMan™ After-flame

Correlation analysis was used to identify any relationships between the results of bench-scale flammability testing and after-flame measured in PyroMan™ testing (Table 2.12). Table 2.12 shows that only the Total Heat Release (THR) measured in the cone calorimeter exhibits a statistically significant relationship with after-flame measured in PyroMan™ testing. The lack of statistically significant relationships can be attributed to complex burning behavior of FR laminates. FR rainwear materials are composed of various water-resistant membrane/substrate structures that incorporate a variety of FR technologies. This complex behavior is exemplified in Figures 2.16 and 2.17, which both show the relationship between the after-flame measured in the folded edge flammability test and the after-flame in 4-second PyroMan™ testing. The extensive after-flame exhibited by Material L in PyroMan™ testing dramatically impacts the relationship

between the after-flame measured in the folded edge flame test and the 4-second PyroMan™ test for the selected FR rainwear materials.

Table 2.12 Correlations between Small-Scale tests and PyroMan™ After-flame for FR Rainwear

PyroMan™ Exposure Duration	Bench-Scale Test	Pearson Correlation Coefficient (r)	P-value
3-seconds	Vertical Flame	-0.046	0.9143
	Folded Edge Flame Test	0.446	0.2675
	Canadian Flame Test- Edge Ignition	0.037	0.9308
	Canadian Flame Test- Surface Ignition	0.521	0.185
	Cone Calorimeter (PHRR)	0.413	0.3092
	Cone Calorimeter (THR)	0.674	0.0667
	Cone Calorimeter PHRR vs PyroMan™ PHRR	0.128	0.7622
	Cone Calorimeter THR vs PyroMan™ THR	0.04	0.9245
4-seconds	Vertical Flame	0.025	0.9535
	Folded Edge Flame Test	0.576	0.1349
	Canadian Flame Test- Edge Ignition	0.094	0.8257
	Canadian Flame Test- Surface Ignition	0.516	0.19
	Cone Calorimeter (PHRR)	0.518	0.1889
	Cone Calorimeter (THR)	0.759	0.0289*
	Cone Calorimeter PHRR vs PyroMan™ PHRR	-0.25	0.5509
	Cone Calorimeter THR vs PyroMan™ THR	.219	0.602

*Indicates statistical significance.

2.6.2.3 Correlation between After-flame and Thermal Protection

Correlation analysis uncovered no significant relationship between any bench-scale test measure of fabric after-flame and predicted total body burn in PyroMan™ tests of rainwear garments made from these materials (Table 2.13). Although cone calorimeter THR is a significant predictive factor for manikin after-flame (Table 2.12), correlation analysis showed that THR measures do not correlate with predicted manikin skin burn (Table 2.13). Like with FR coverall materials, these findings do not mean that after-flame has no effect on the predicted body burn injury. They confirm that after-flame is only one of many factors contributing to predicted body burn injury in fire manikin tests.

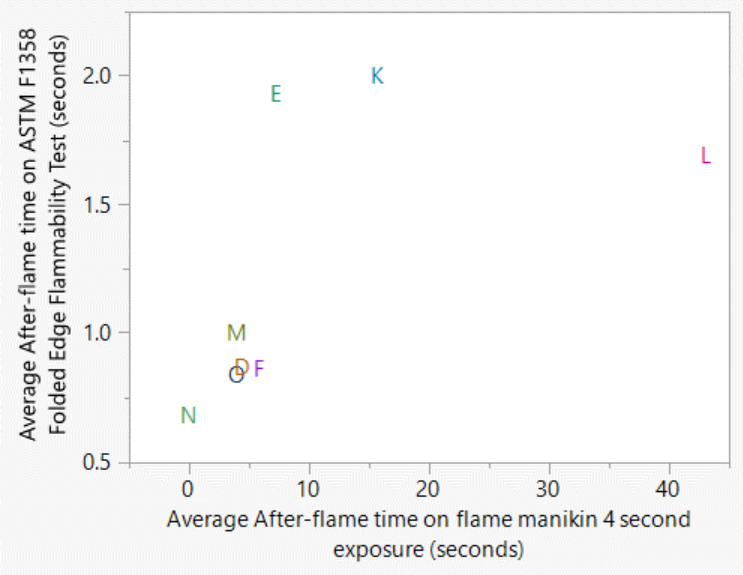

Figure 2.16 After-flame in folded edge flame test vs. after-flame in PyroMan™ 4-second exposure (FR rainwear materials)

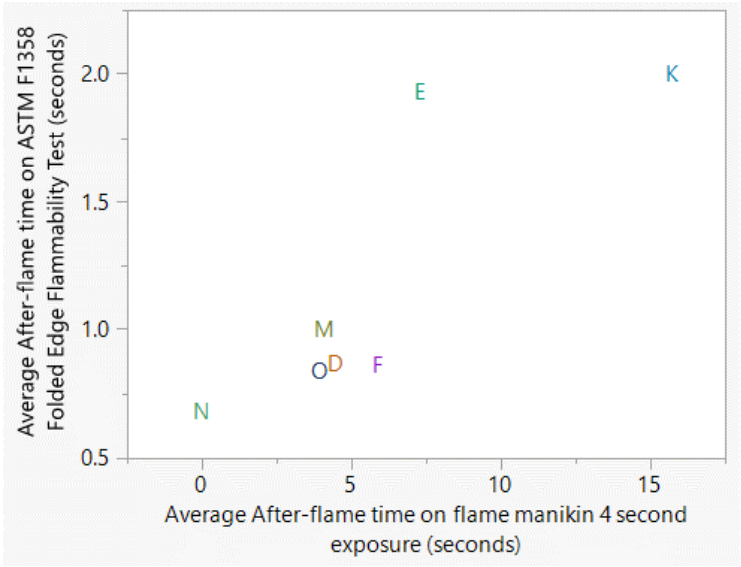

Figure 2.17 After-flame in folded edge flame test vs. after-flame in PyroMan™ 4-second exposure (FR rainwear materials excluding Material L)

Table 2.13 Correlations between After-flame Tests and % Body Burn on PyroMan™ for FR Rainwear

PyroMan™ Exposure Duration	Bench-Scale Test	Pearson Correlation Coefficient (r)	P-value
3-seconds	Vertical Flame	-0.007	0.9868
	Folded Edge Flame Test	0.115	0.7857
	Canadian Flame Test- Edge Ignition	0.294	0.4802
	Canadian Flame Test- Surface Ignition	0.397	0.3298
	Cone Calorimeter (PHRR)	-0.114	0.7882
	Cone Calorimeter (THR)	-0.142	0.738
	PyroMan™ Test	0.327	0.1187
4-seconds	Vertical Flame	0.129	0.7608
	Folded Edge Flame Test	0.194	0.6461
	Canadian Flame Test- Edge Ignition	0.289	0.4872
	Canadian Flame Test- Surface Ignition	0.275	0.5093
	Cone Calorimeter (PHRR)	-0.08	0.8508
	Cone Calorimeter (THR)	-0.092	0.8282
	PyroMan™ Test	0.287	0.1736

2.7 Conclusions

This research has shown that standard bench-scale flammability tests do not provide reliable prediction of the after-flame behavior of FR coveralls or FR rainwear in PyroMan™ tests. This is not surprising considering the significant differences that exist in the variables that control burning in small-scale flammability and manikin tests. Intrinsic differences in burning behavior across the wide range of different fabrics and laminates constructions used in FR coveralls and FR rainwear garments contribute to further confound the relationships between bench-scale flammability and fire manikin tests. At the same time, detailed analysis indicates that some bench-scale flammability tests, such as the Canadian surface-ignition flammability test and the cone calorimeter, may be useful tools for predicting after-flame behavior, or for screening within the same type FR materials for after-flame propensity prior to fire manikin tests. All standardized bench scale tests are useful for screening gross differences between

flammable and non-flammable clothing fabrics. However, full-scale fire manikin tests remain the only reliable means of evaluating after-flame in FR garments in controlled conditions that reasonably simulate field exposures to fire.

The study uncovered no significant correlation between observed garment after-flame time, or bench scale measures of materials after-flame, and the thermal protective performance of FR coveralls or FR rainwear, as indicated by predicted skin burn injury in fire manikin tests. This finding does not exclude heat released by garment after-flame as a factor contributing to potential burn injury. However, it does show that after-flame is just one of many variables that contribute to garment thermal protective performance in PyroMan™ tests.

The findings of this research raise fundamental questions about the use of bench-scale measures of after-flame to differentiate the thermal protective performance of FR workwear and FR rainwear materials. By showing that after-flame time, whether measured on the manikin or in a bench-scale test, does not correlate with garment thermal protective performance (as indicated by predicted manikin skin burn), it raises questions about the inherent value of after-flame requirements for FR materials, beyond broad screening tests for differentiating between FR and non-FR clothing materials. It further questions the use of the ASTM D6413 Vertical Flame Test Methods for determining the after-flame performance requirement in NFPA 2112 and ASTM F2733. It has definitively shown that after-flame time measured using the ASTM D6413 method cannot be used to predict after-flame or thermal protective performance in full-scale fire manikin tests. Furthermore, the use of after-flame requirements as a basis for certifying compliance to these standards could eliminate some FR materials that perform poorly in the ASTM D6413 flammability test, while providing adequate thermal protection in full-scale fire manikin tests.

2.7.1 Recommendations for Future Research

This study has decisively shown that existing standard bench-scale flammability tests for evaluating FR coveralls or FR rainwear have only limited ability to predict the after-flame of these materials in full-scale fire manikin testing. Current bench-scale test methods are unable to accurately reflect after-flame behavior observed in flash fire tests. Multiple variables impact the interaction of the air diffused propane flames with the test garments in fire manikin testing. Such variables include but are not limited to: flame intensity, pressure, velocity, air gaps between the manikin and the test garment, orientation of flame interaction with sheer, direct impingement of flames onto the manikin sensors, and full engulfment of the fabric.

The development of a small-scale test with the ability to accurately and reliably predict the results of fire manikin tests is necessary. Initial studies to more accurately predict after-flame in fire manikin testing could focus on developing a test that exposes a fabric specimen to a flame exposure with similar intensity and contact angle as observed in fire manikin tests.

A study further investigating the impact of after-flame on thermal protection in fire manikin testing is also recommended. Ideally, this study would be able to accurately identify regions of the garment exposed to after-flame and compare the thermal energy transferred in those regions with thermal energy transferred in regions with no after-flame. The impact of different fabric characteristics would be investigated. Such characteristics include but are not limited to: fabric structure (weave, knit, etc.), thickness, air permeability, and fiber composition.

To better predict both the after-flame and thermal protection offered by fire protective fabrics, a test simulating flash fire exposure to an instrumented limb (arm or leg) using small-scale air diffused torches would be suggested. This instrumented limb should be able to be oriented both vertically and horizontally. Such a test would require specialized garments to be

made that can imitate the fit of a full garment. The study should investigate the different variables involved in flash fire testing: flame dynamics, direct flame impingement, full engulfment of the fabric, and orientation of the instrumented limb. The test would be able to provide measures of after-flame, burn injury, thermal energy transfer, and thermal shrinkage.

2.8 References

1. NFPA 2112 Standard on Flame-Resistant Clothing for Protection of Industrial Personnel Against Short-Duration Thermal Exposures from Fire, National Fire Protection Association, Quincy, MA, 2007.

2. NFPA 1971 Standard on Protective Ensembles for Structural Fire Fighting and Proximity Fire Fighting, National Fire Protection Association, Quincy, MA, 2013.

3. ASTM D6413/D6413M-15 Standard Test Method for Flame Resistance of Textiles (Vertical Test), ASTM International, West Conshohocken, PA, 2015.

4. ASTM F1358-16 Standard Test Method for Effects of Flame Impingement on Materials Used in Protective Clothing Not Designated Primarily for Flame Resistance, ASTM International, West Conshohocken, PA, 2016.

5. CAN/CGSB 4.2 NO. 27.10 Textile test methods-Flame resistance, Canadian General Standards Board, 2011.

6. V. Babrauskas, The Cone Calorimeter, in: SFPE Handb. Fire Prot. Eng., Springer, New York, NY, 2016: pp. 952–980. doi:10.1007/978-1-4939-2565-0_28.

7. ASTM E1354-17 Standard Test Method for Heat and Visible Smoke Release Rates for Materials and Products Using an Oxygen Consumption Calorimeter, ASTM International, West Conshohocken, PA, 2017.

8. G. Song, Clothing Air Gap Layers and Thermal Protective Performance in Single Layer Garment, J. Ind. Text. 36 (2007) 193–205. doi:10.1177/1528083707069506.

9. ASTM F2894-14 Standard Test Method for Evaluation of Materials, Protective Clothing and Equipment for Heat Resistance Using a Hot Air Circulating Oven, ASTM International, West Conshohocken, PA, 2014.

10. ASTM F2700-08 Standard Test Method for Unsteady-State Heat Transfer Evaluation of Flame Resistant Materials for Clothing with Continuous Heating, ASTM International, West Conshohocken, PA, 2008.

11. M. Wang, J. Li, Thermal protection retention of fire protective clothing after repeated flash fire exposure, J. Ind. Text. 46 (2016) 737–755. doi:10.1177/1528083715594977.

12. J. Li, M. Zhao, Y. Xie, Y. Wang, Thermal shrinkage of fabrics used for out layer of firefighter protective clothing under flash fire, Fire Mater. 39 (2015) 732–740. doi:10.1002/fam.2260.

13. Barker, R., Geshury, A., Behnke, W. “The Effect of Nomex®/Kevlar® Fiber Blend Ratio and Fabric Weight on Fabric Performance in Static and Dynamic TPP Tests,” Performance of Protective Clothing, Fifth Volume, ASTM STP 1237, James S. Johnson and S. Z. Mansdorf, Eds., American Society for Testing and Materials, Philadelphia, PA (1996).

14. E.M. Crown, J.D. Dale, E. Bitner, A comparative analysis of protocols for measuring heat transmission through flame resistant materials: capturing the effects of thermal shrinkage, Fire Mater. 26 (2002) 207–213. doi:10.1002/fam.797.

15. ASTM F1930-17, Standard Test Method for Evaluation of Flame Resistant Clothing for Protection Against Fire Simulations Using an Instrumented Manikin, ASTM International, West Conshohocken, PA, 2017.

16. X. Li, Y. Lu, L. Zhai, M. Wang, J. Li, Y. Wang, Analyzing Thermal Shrinkage of Fire-Protective Clothing Exposed to Flash Fire, Fire Technol. 51 (2015) 195–211. doi:10.1007/s10694-013-0375-0.

17. M. Wang, X. Li, J. Li, B. Xu, A new approach to quantify the thermal shrinkage of fire protective clothing after flash fire exposure, Text. Res. J. 86 (2016) 580–592. doi:10.1177/0040517515595028.

18. J. Li, M. Zhao, Y. Xie, Y. Wang, Thermal shrinkage of fabrics used for out layer of firefighter protective clothing under flash fire, Fire Mater. 39 (2015) 732–740. doi:10.1002/fam.2260.

19. Pawar, M., Barker, R., Shalev, I., Hamouda, H., Behnke, W., Bender, M., “Analyzing the Performance of Protective Garments in Manikin Fire Tests,” Proceedings of the Fifth Scandinavian Symposium on Protective Clothing, Elsinore, Denmark, May 1997.

20. Wang, X. Li, J. Li, Correlation of bench scale and manikin testing of fire protective clothing with thermal shrinkage effect considered, Fibers Polym. 16 (2015) 1370–1377. doi:10.1007/s12221-015-1370-5.

21. C. Lee, I.Y. Kim, A. Wood, Investigation and correlation of manikin and bench-scale fire testing of clothing systems, Fire Mater. 26 (2002) 269–278. doi:10.1002/fam.808.

22. G. Song, R.L. Barker, H. Hamouda, A.V. Kuznetsov, P. Chitrphiromsri, R.V. Grimes, Modeling the Thermal Protective Performance of Heat Resistant Garments in Flash Fire Exposures, Text. Res. J. 74 (2004)

23. Arifoglu, M., “Innovations in Heat and Flame Protection Using Gore Fabric Technology,” AATCC International Conference Proceedings, Wilmington, NC, March 2017.

24. Adams, D., “Fire Resistant Fabric Testing and Significance,” AATCC Flammability Symposium, Raleigh, NC 2016

25. Structure Sensor- 3D scanning, augmented reality, and more for mobile devices. Available: https://structure.io/.

26. itSeez3D. Available: https://itseez3d.com/.

27. Autodesk. Autodesk Fusion 360. Available: https://www.autodesk.com/.

28. K. Varga et al, "Thermal and sorption study of flame-resistant fibers," Lenzinger Berichte, vol. 89, pp. 50-59, 2011.

29. PBI Products, "PBI Max". Available: https://www.pbiproducts.com/.

30. S. Francis, "Understanding Fibers and Fabrics: The Engineering of Arc Rated/Flame Resistant Fabrics," *Westex by Milliken,* 2018.

31. Gore® Pyrad® fabric technology: durable flame retardant protection. Available: https://www.gore-workwear.co.uk/technologies/gore-pyrad-fabric-technology.

32. B. C. Nutt, J. P. Towey, D. Narasimhan and M. S. Zedalis, "Flexible Lightweight Arc Flash and Flash Fire Resistant Polyvinylchloride Fabric and Garments and Methods Therefor " US 2016.003917OA1, Feb, 2016.

33. ASTM F2733-17 Standard Specification for Flame-Resistant Rainwear for Protection Against Flame Hazards, ASTM International, West Conshohocken, PA, 2017.

34. Backer, Tesoro, Toony, and Moussa, Textile Fabric Flammability, MIT Press, Cambridge, MA

35. Shalev, I. and Barker, R., “Predicting the Thermal Protective Performance of Heat Protective Fabrics from Basic Properties”, Performance of Protective Clothing, Barker and Coletta, Eds., ASTM Special Technical Publication 90, July 1986

36. Yong Wang et al, "Convective Heat Transfer of the Bunsen Flame in the UL94 Vertical Burning Test for Polymers," Journal of Fire Sciences, vol. 28, (4), pp. 337-356, 2010. Available: https://journals.sagepub.com/doi/full/10.1177/0734904109351484. DOI: 10.1177/0734904109351484.

37. S.K. An, R.L. Barker, J.O. Stull, Measurement of The Flammability and Thermal Aging of Chemical Protective Suit Materials, (1989). doi:10.1520/STP22935S.

38. ISO 15025:2016 Protective clothing-Protection against flame-Method of test for limited flame spread, International Organization for Standardization, 2016.

CHAPTER 3: Investigation of Lab Scale Tests for Predicting Garment Shrinkage in Protective Garments in PyroMan™ Tests

3.1 Introduction

Instrumented fire manikin tests provide invaluable evaluation of systems-level thermal protective performance of fire protective clothing. Nevertheless, few studies have focused on predicting garment shrinkage behavior observed in fire manikin testing. Correlations between bench-scale test methods and the garment shrinkage observed in fire manikin tests have yet to be established in scientifically qualified experimental studies. This is a significant gap, since the availability of well-qualified lab-scale tests for predicting the performance of materials in fire manikin tests would be of considerable practical value. These tests would accelerate research and development by identifying promising prototype materials and constructions prior to fire manikin testing.

Standardized bench-scale tests of thermal shrinkage are the primary means of evaluating the suitability of materials for use in fire and heat resistant protective clothing. These tests form the basis of most NFPA performance requirements for fire resistant protective clothing [1-2]. One method stands out: The 500ºF Oven Shrinkage Test [1-2]. In spite of the widespread reliance on this method, apart from screening thermoplastic materials, and identifying materials of normal thermal stability, little scientific basis exits for qualifying the utility of this method for differentiating materials thermal performance in full-scale fires, or for protecting against burn injury in fire exposures.

Instrumented fire manikin technology, PyroMan™, permits assessment of the thermal protective performance of materials and garments in realistic simulations of flash fire exposures. Fire manikin provides an ideal testing platform to address these fundamental questions: How do

bench-scale tests of thermal shrinkage correlate with garment shrinkage observed in realistic simulation of flash fire exposures? If they do not correlate, how can we devise bench-scale tests methods to predict materials response in fire manikin tests?

The objective of this study was to determine the applicability of using thermal shrinkage tests, such as the 500°F oven test, to predict garment shrinkage measured on PyroMan™. This study also sought to qualify the impact of thermal shrinkage on the thermal protective performance, or burn injury prediction, provided by PyroMan™ tests.

3.2 Background

3.2.1 Predicting Thermal Shrinkage in PyroMan™ Tests

An understanding of why fabrics exhibit thermal shrinkage is necessary when attempting to predict the thermal shrinkage performance on any scale. One mechanism that contributes to thermal shrinkage involves the material itself. Oriented polymeric molecules found in fibers, are typically thermodynamically unstable. When the temperature of the fiber is increased, the molecules relax into a more stable, coiled conformation [39]. Another internal factor influencing the thermal shrinkage behavior of fabrics is the fabric structure itself. Rupp and Böhringer found that the thermal shrinkage typically decreases as the yarn density of fabric increases [40]. Li et al found that many external factors, including exposure time, fabric properties, garment size, and body posture, influence the shrinkage behavior of Nomex IIIA garments in manikin testing. They found that the heat flux and air gap size influenced the shrinkage measured at different locations of the test garments [16]. These considerations show the complexity involved in predicting the garment shrinkage in instrumented manikin testing.

Many studies have shown that thermally induced shrinkage can increase the predicted burn injury in instrumented manikin tests. This is largely due to the reduction or elimination of

the insulating air gap layer between the garment and the manikin surface [8]. Garment shrinkage can contribute to burn injury by reducing the insulating air gap layer and by transferring heat directly to the skin from the hot garment.

3.2.2 Measuring Thermal Shrinkage in Bench-Scale Tests

The test method that is most widely used for measuring the thermally induced shrinkage of fabric materials is the 500°F (260°C) hot air circulating oven test, as outlined in ASTM F2894 [4]. Materials compliant to NFPA standards, including NFPA 2112, cannot shrink more than 10% in any direction after a 5-minute exposure in the oven test [1]. The ASTM F2894 standard recognizes that this test is strictly a materials test and "is not intended to simulate the actual exposure of material, clothing or equipment in high heat conditions such as a fire environment" [9]. The main use of the oven test is to differentiate materials that melt, char, or ignite from those that do not exhibit such behaviors at 500°F for use in heat resistant applications. In spite of multiple studies showing that fabric shrinkage reduces the insulating air gap between the skin and the fabric, leading to increased heat transfer, no studies have investigated the correlation between shrinkage data from the 500°F oven test with the thermal protective performance in instrumented manikin testing. Recent industry studies indicate that the 500°F oven test does not correlate with the predicted body burn injury in PyroMan™ instrumented manikin testing for select materials [23-24].

The thermal conditions created in the 500°F oven test are very different from the conditions produced in instrumented manikin testing. Although the 500°F oven test exposes samples to convective heat, there is no significant radiant component in a heated oven exposure. Further, test materials are not exposed to flames in the oven test. This removes the possibility of flash ignition during the test as well as any additional thermal shrinkage that may result from

increased temperatures caused by the burning fabric itself. The 5-minute exposure in the 500°F oven test is much longer than the typical 3 or 4-second exposure durations used in fire manikin testing. Additionally, the shrinkage of garments in instrumented manikin testing is limited by the manikin form. There is no such limiting constraint in the oven test, meaning that test materials can theoretically shrink as much as possible during testing. Therefore, the many differences between the 500°F oven test and fire manikin testing indicate that the 500°F oven test may not be an optimum predictor of thermal shrinkage in fire manikin exposures.

3.2.2.1 Measuring Thermal Shrinkage in Thermal Protective Performance (TPP) Tests

Multiple studies have used the thermal protective performance (TPP) test and its variants to measure the thermally induced shrinkage of protective textiles. The TPP test (Figure 3.1), as described in ASTM F2700, employs a quartz tube bank and a pair of Meker burners to produce a convective-radiant heat flux of approximately 2 cal/cm^2/sec (84 kW/m^2) [10]. This heat flux is the same as called for by the ASTM F1930 instrumented manikin flash fire test, which may allow for test materials to shrink in a similar manner to the garments in the instrumented manikin test. Abbott measured the temperature rise behind different fabrics exposed to flames generated by a JP-4 fuel burner. He found that as the fabrics shrink in heat, they contact the thermal sensor,

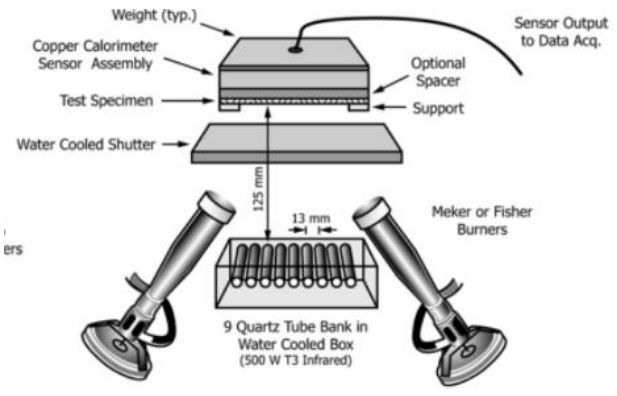

Figure 3.1 Schematic illustration of TPP burner and sensor assembly (Redrawn from [10]).

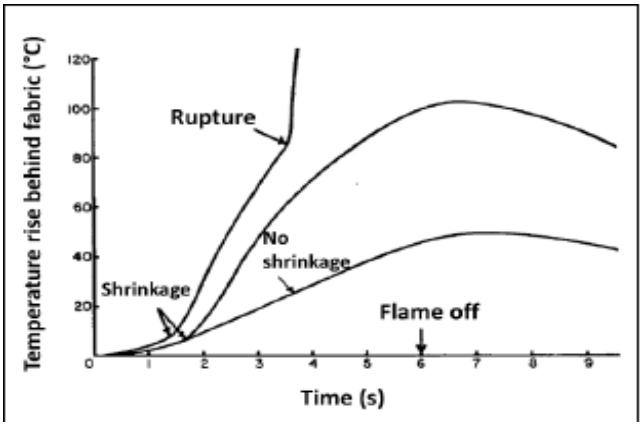

Figure 3.2 Comparison of temperature rise behind fabric with and without shrinkage (redrawn from [21])

causing a rapid increase in the rate of temperature rise (Figure 3.2). Other fabrics exhibited shrinkage sufficient to cause the fabric to break open, resulting in a further increase of the heat transfer [41]. Therefore, Abbott's study clearly shows that material shrinkage has an effect on the thermal protective capabilities of FR fabrics and suggest that the TPP test may be useful in determining the shrinkage behaviors of fabrics when exposed to flash fire conditions. One potential drawback of standardized TPP tests, as described by Crown et al, is that the specified test end point is typically based on the time required for the heat transferred through the fabric to cause a second-degree burn in human skin [14]. However, the flash fire exposure may continue beyond the test endpoint, as the end point of flash fire exposure is not defined in standardized test methods. This lack of definition may result in inconsistent material shrinkage measurements as the duration of exposure beyond the test end point may vary. The instrumented manikin test calls for a predetermined exposure duration, typically ranging from 3 to 10 seconds, and the energy transferred to the sensors is measured up to 60 seconds after the exposure. The continued data collection after the flash fire exposure is necessary as skin damage may still occur after the exposure ends [14]. This difference in both the exposure duration and the data collection period

between the bench-scale and full-scale tests may lead to a lack of relationship between the thermal shrinkage measured in the tests despite both standardized tests prescribing the same flash fire intensity.

While Abbott's study suggests that shrinkage plays an important role in the thermal protection offered by FR materials, the measurement of material shrinkage is not a requirement in the standardized TPP test, which provides much better bench-scale simulation of the PyroMan™ flame test than does the 500°F oven test. Researchers have measured the material shrinkage exhibited on the TPP test. Behnke found that certain heat-resistant materials experience shrinkage-induced break-open when restrained by the TPP sample holder [42]. Wang and Li used an image processing technique to characterize the change in surface area of TPP samples after repeated 3-second exposures. A 230g frame was used to partially restrain the samples to keep them from shrinking so much that they may drop down into the flash fire during the exposure. In spite of their significant shrinkage, Nomex IIIA and polysulfonamide (PSA)

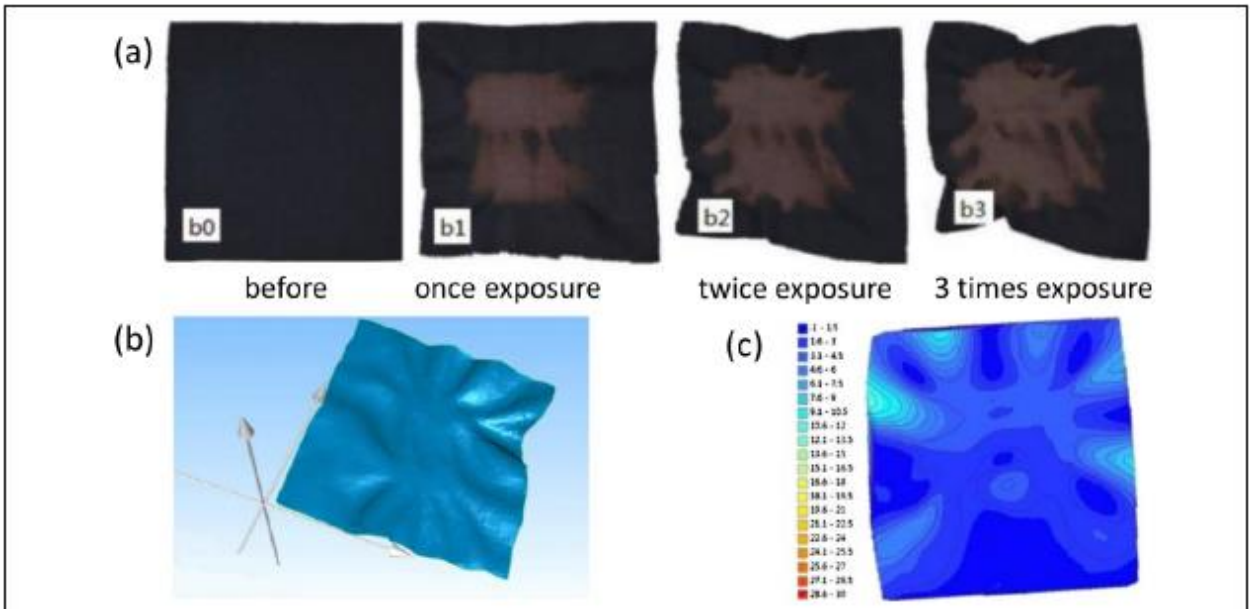

Figure 3.3 (a) Photographs of Polysulfonamide (PSA) fabric, unexposed and after repeated exposure times [11]; (b) the slope image of fabric after exposure [11]; and (c) Image of fabric acquired by Handyscan 3D after processing by Geomagic software [12].

fabrics tested in the study exhibited an increase the their respective TPP values. The increase in TPP values was attributed to an increase in the fabric thickness that was a result of the flash fire exposure [11]. In another study, Li et al measured the surface appearance of burned TPP samples using a handheld laser scanner and was able to quantify the material shrinkage of the samples using 3D software. To eliminate any restriction of shrinkage, the copper sensor was not used during the test [12]. One drawback of both of these studies is that the shrinkage measurements were taken over the entire sample rather than only measuring the area that was exposed to the flash fire conditions. As shown in Figure 3.3, the area of exposure on the polysulfonamide (PSA) fabric sample makes up a portion of the entire sample. The unexposed part of the sample does not experience any shrinkage and including this area in the measurement may led to inaccurate shrinkage calculations.

There are significant differences between the TPP test and fire manikin testing. Many TPP tests have a defined “end point”, calling for the end of the test either the point at which a predicted second-degree burn injury is reached or a 24°C rise in temperature at the sensor occurs.

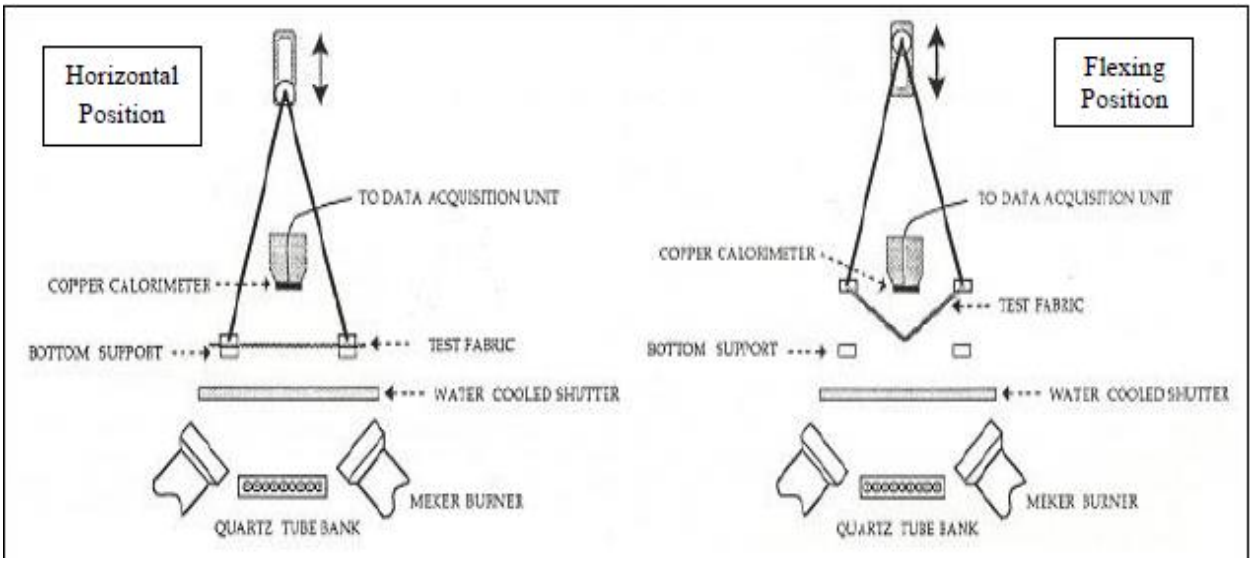

Figure 3.4 Schematic diagram of dynamic thermal protective performance (DTPP) tester.

These approaches are different from the predetermined exposure durations in the instrumented manikin test [14]. Fabric specimens in the TPP test are restricted from shrinking, even in the

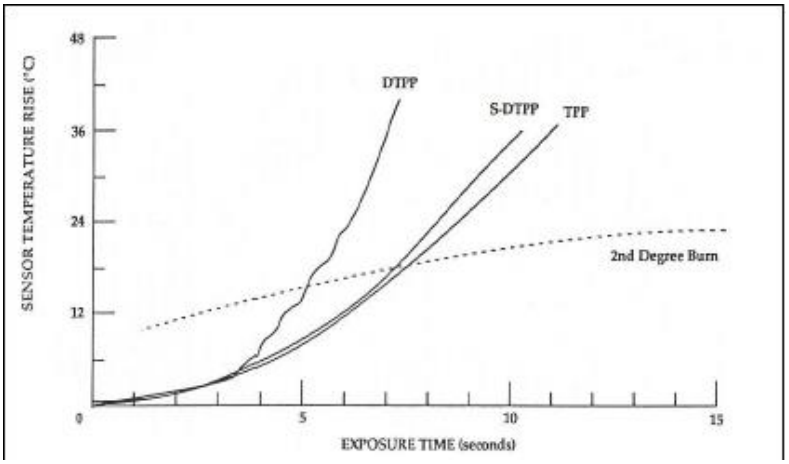

Figure 3.5 Thermal Protective Performance graph of Nomex® IIIA (redrawn from [13]).

'relaxed' configuration, due to the weight of the sensor. While the manikin form limits shrinkage in fire manikin testing, the garment shrinkage is not restricted until the air gap between the garment and the manikin is eliminated around the entire garment.

Variations of the TPP test have been developed which further investigate the influence of material shrinkage on the thermal protective performance. The dynamic TPP test (DTPP) allows

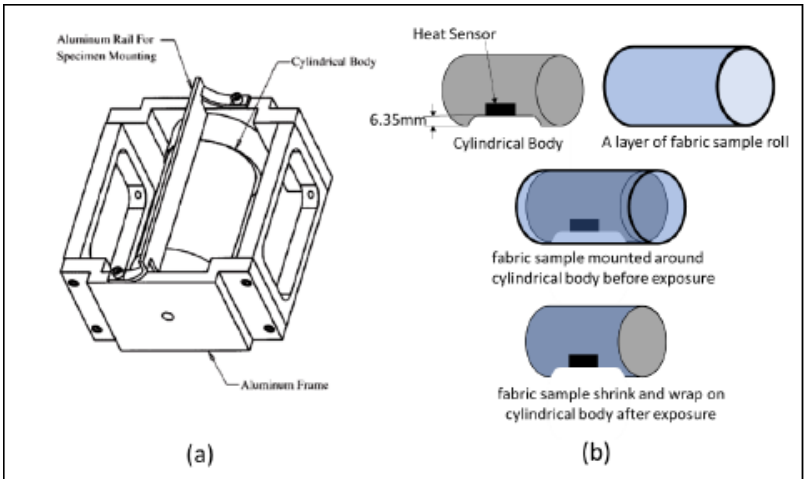

Figure 3.6 (a) Cylindrical TPP test device; (b) cylindrical test principle (redrawn from [14]).

for the effects of dynamic movement as well as thermal shrinkage to be studied. A novel specimen holder is mounted to the TPP tester, as shown in Figure 3.4, which subjects the fabric to a dynamic force during the flash fire exposure. The heat sensor used during the DTPP test is different from the one used during standard TPP testing to accommodate the dynamic sample holder. The study also investigated the effect of Nomex®/Kevlar® fiber blend ratio and fabric weight on the thermal protective performance of the fabrics and found that the TPP value of Nomex IIIA® fabric is greatly reduced in the DTPP test when compared to the static TPP test as shown in Figure 3.5. The stepped increase in the rate of heat transfer observed during the DTPP test was attributed to the reduction of the insulating air gap between the fabric and the sensor that resulted from fabric shrinkage [13]. This study did not measure the material shrinkage that resulted from the flash fire exposure.

Crown et al developed a cylindrical sensor apparatus for the TPP test as shown in Figure 3.6 to measure the effect of shrinkage on the thermal protective performance. The fabric specimen is wrapped around the cylinder, which contains a 6.35 mm (0.25 inch) spacer. Samples were also tested in a contact configuration. Thermal shrinkage eliminates the resulting air gap, thus increasing the rate of heat transfer to the sensor [14]. There is no measurement of the thermal shrinkage in the study.

3.2.3 Measuring Garment Shrinkage in PyroMan™ Tests

While measuring the garment shrinkage is not incorporated into the ASTM F1930 standard manikin test method, researchers have employed multiple methods to obtain a numerical measurement of garment shrinkage. Garment shrinkage has been measured largely through two distinct methods: physical marks on the garments and 3-D scanning technology. Li et al sealed stamps on the backside of test garments at locations of the garment that matched the

heat sensor locations on the manikin to investigate how different body postures impact the thermal shrinkage and thermal protective performance of FR garments. These circular stamps were marked to measure the thermal shrinkage in the warp, fill, and ±45 degrees to the warp direction of woven test fabrics [16]. While the markers were able to provide an accurate measurement of the garment shrinkage, the area covered by the markers only contains a portion of the garment and may not give the best representation of the overall shrinkage exhibited by the garment material.

The second method of measuring the thermal shrinkage of garments used in flame manikin testing is 3-D scanning. Song used 3-D body scanning technology to measure the reduction in the insulative air gap layer that results from garment shrinkage [8]. In more recent studies, Wang and Li employed a portable 3-D scanner mounted in the manikin test chamber to obtain 3-D images of the nude manikin and the clothed manikin immediately prior to and following flash fire exposure. The shrinkage was measured by superimposing the scans of the clothed manikin onto the scans of the nude manikin. The length and girth of the garment was

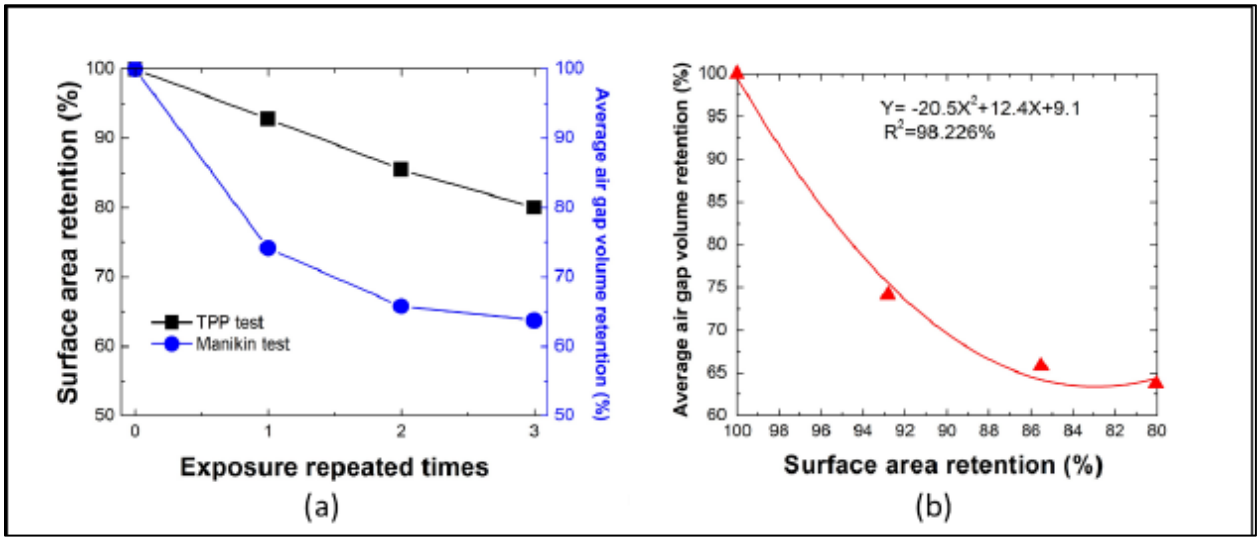

Figure 3.7 (a) Comparison between bench-scale TPP tested Nomex IIIA fabric (surface area retention) and manikin tested Nomex® IIIA garment shrinkage (average air gap volume retention) of; (b) correlation between fabric shrinkage in TPP test and garment shrinkage in manikin test (redrawn from [12]).

measured by the surface area change, while the change in insulative air gap was calculated by the volume change and air gap thickness change [17-18]. Each of these studies has shown the importance of garment shrinkage in maintaining the thermal protective performance in full-scale testing. The use of 3-D scanning technology has clearly shown to be a useful process in the studies that employed the technology and may contain an advantage to the marker measurement method as the scanners can measure the entire garment. However, the scanning technology used in the studies is very complex and may not be practical for use in routine testing.

3.2.4 Correlation of Bench-Scale Thermal Shrinkage with PyroMan™ Tests

Many studies have shown the importance of the thermal stability and shrinkage of FR materials and thermal protection measured in fire manikin tests. Most have focused on correlating TPP tests with predicted body burn in fire manikin exposures [8, 16, 19, 20-22]. Several studies conducted at NC State have investigated the relationship between clothing air layers and the role of garment shrinkage on distributed body burn measured on PyroMan™ [18-19]. TPP tests, measured in both sample contact or sample spaced test configurations, have been found to provide localized prediction of PyroMan™ burn. TPP tests correlate with manikin burn predictions when they are precisely matched with the spatial configuration (spaced or contact) found between the manikin thermal sensor and test garment. These findings were consistent with Crown and Dale's study that demonstrated the importance of thermal shrinkage, as measured using a cylindrical TPP test arrangement. Crown and Dale's research demonstrated a good correlation using a predictive model that combined 70% spaced configuration and 30% contact configuration [14].

In a recent study, Wang and Li used a portable 3D body scanner to measure shrinkage in Nomex® IIIA test garments as a function of exposure time in fire manikin tests [17-18]. They

assessed the effects of thermal shrinkage as reductions in the fabric surface area in the TPP test, and by thermally induced changes in the garment/manikin interface air volume in the fire manikin test. Figure 3.7a shows the strong relationship between thermally induced physical changes in small-scale TPP tests, and full-scale fire manikin tests. Li and Wang's data are plotted in Figure 3.7b. They show the connection between shrinkage effects measured in TPP tests (fabric surface retention) and air volume reduction in fire manikin (air-gap volume retention). These data confirm the utility of using the TPP test as a platform for predicting thermal shrinkage effects observed in PyroMan™ testing.

Therefore, previous research studies provide a strong basis for using TPP testing variants to evaluate materials thermal shrinkage in order to predict shrinkage in PyroMan™ tests. At the same time, scientifically based studies demonstrating a similar utility for the 500ºF oven test were not found. On the other hand, recent corporate studies seem to show that the 500ºF oven shrinkage test does not correlate with thermal shrinkage and burn protection measured on PyroMan™ for some materials. Arifoglu presented data indicating that reliance on the 500ºF oven test limits choices in FR materials used for thermal protection to aramid-based materials [23]. Adams presented data indicating that thermal shrinkage measured in the 500ºF oven test does not correlate with predicted PyroMan™ body burn: 100% aramid fabrics that show low shrinkage in the oven test record higher body burn in comparison with similar weight aramid/FR and a modacrylic blend fabrics [24]. Although these limited data cannot be viewed as a definitive assessment of the value of the 500ºF oven test as a predictor of PyroMan™ performance, they do indicate the need to better qualify the relationships between thermal shrinkage and garment-level thermal protective performance measured in fire manikin tests.

3.3 Test Materials

A variety of different fire protective fabric materials were selected for this study. Table 1 provides a summarized description of the test materials. Test materials fall into two broad categories: one group was selected to represent a range of flammability and thermal shrinkage characteristics found in single-layer woven FR industrial workwear or military uniform fabrics. The other group represented FR rainwear laminates.

3.3.1 Aramids

Three different aramid fabrics: 4.5osy (Material A), 6.0osy (Material B), and 7.5osy (Material C). Temperatures above the glass transition temperature (T_g) of meta-aramid fibers are observed in flash fires causing fabrics made with meta-aramid fibers to shrink [28]. To improve high temperature thermal stability, meta-aramid fibers are blended with other more heat-resistant fibers, including para-aramid fibers. Meta-aramid fibers have a glass transition temperature (T_g) of 275°C, while para-aramid fibers have a T_g of 327°C. Meta-aramid fibers swell in high-heat exposures, which seals openings in the fabric reducing heat transfer to the skin [28].

3.3.2 Polybenzimidazole (PBI)

A 7osy twill-weave fabric of 70%/30% “PBI-dominant” para-aramid blend/para-aramid filament (Material I). PBI has a high T_g (400°C) and thermal decomposition temperature (1175°C), indicating thermal stability (shrinkage resistance) in flash fire conditions [29].

3.3.3 Modacrylic Blends

Two twill-weave variants composed of blends of 45% modacrylic/35% Lyocell/ 20% aramid in a 7osy (Materials G) and 8.5 osy (Materials H) basis weight. Both fabrics are NFPA 2112 certified, indicating that they exhibit less than 2 seconds of after-flame time on the vertical

flame test and less than 10% shrinkage in the 500°F oven test. Because modacrylic fibers are composed of an acrylic and modacrylic co-polymer composition, they undergo a two-stage degradation at temperatures of 236°C and 503°C. The acrylic component protects by char formation, while the modacrylic flame retardant component suppresses burning via vapor-phase free radical (halogen) reactions [28].

3.3.4 FR Cotton

The FR cotton fabric used in this study is a 7osy twill construction incorporating an 88/12% blend of cotton and nylon fibers (Materials J). This test fabric uses a FR finish containing tetrakis (hydroxymethylol) phosphonium salts to achieve flame resistance. It is NFPA 2112 certified, meaning that it has less than 2 seconds after-flame time in the vertical flame test, and less than 10% shrinkage in the 500°F oven test. Once the FR finish is consumed during a flame exposure, the cotton will quickly degrade, rapidly increasing after-flame and heat transfer [30].

3.3.5 FR Laminate

Proprietary technology FR laminate materials incorporate a char-forming FR component. Three different substrate constructions and weights were studied: Material D used a 100% nylon plain weave substrate in a 4osy construction, Material E used a twill rip-stop weave made of 100% nylon 6,6, and Material F featured a 100% polyester twill weave 100% polyester substrate fabric. These laminate constructions form stable char contributing to increased structural integrity in flame exposures [31]. They have less than 2 seconds after-flame time in the vertical flame test but exhibit high levels of thermal shrinkage in the 500°F oven test [31]. Because these laminate materials are used in rainwear ensembles, these three FR laminates were included in both the FR coverall and FR rainwear categories of garment test materials.

Table 3.1 Summarized Description of Test Materials.

ID	**Material**	**Fiber Content**	**Construction**	**Fabric Weight** (osy)	(1) **Nominal After-flame** (sec)	(2) **Nominal Shrinkage** (%)
A	Aramid	93% meta-aramid/ 5% para-aramid/ 2% antistat	Plain Weave	4.5	< 2	< 10%
B	Aramid	93% meta-aramid/ 5% para-aramid/ 2% antistat	Plain Weave	6.0	< 2	< 10%
C	Aramid	93% meta-aramid/ 5% para-aramid/ 2% antistat	Plain Weave	7.5	< 2	< 10%
D	FR Laminate	100% nylon	Plain Weave	4.0	< 2	high
E	FR Laminate	100% nylon 6,6	Rip-stop	5.3	< 2	high
F	FR Laminate	100% polyester	Twill Weave	6.5	< 2	high
G	Modacrylic	45% modacrylic/ 35% Lyocell/ 20% aramid	Twill Weave	7.0	< 2	< 10%
H	Modacrylic	45% modacrylic/ 35% Lyocell/ 20% aramid	Twill Weave	8.5	< 2	< 10%
I	PBI	70% PBI/ 30% para-aramid	Twill Weave	7.0	< 2	< 10%
J	FR Cotton	88% FR cotton/ 12% nylon	Twill Weave	7.0	< 2	< 10%
K	FR Rainwear	100% meta-aramid	FR PVC/ on meta-aramid nonwoven	11.3	< 2	
L	FR Rainwear	100% meta-aramid	FR PVC on meta-aramid nonwoven	9.5	< 2	
M	FR Rainwear	100% polyester	Twill Weave	8.3	< 2	high
N	FR Rainwear	93% meta-aramid/ 5% para-aramid/ 2% antistat	FR neoprene on plain weave meta-aramid	13.5	< 2	
O	FR Rainwear	100% FR cotton	FR polyurethane on FR cotton knit	10.0	< 2	

3.3.6 FR Rainwear

This study included materials used in FR rainwear garments (rain jacket and bibs/overalls). Rainwear material M is a proprietary char-forming laminate technology

incorporated in a 8.3osy construction. Other FR rainwear test materials consisted of a FR poly(vinyl) chloride (PVC) barrier laminated on a nonwoven meta-aramid fabric in a 11.3osy construction (Material K), and in 9.5osy laminate (Material L). The low T_g and low flash point of PVC material means that they will burn and propagate flame more readily than other FR rainwear materials. Additionally, phthalates are often used as PVC plasticizers and may be present in these materials. The presence of phthalate plasticizers could affect how the material burns and propagates flames [32]. Another of the rainwear test materials (Material N) used a FR neoprene coating on meta-aramid fabric in a 13.5osy construction. The halogens in the neoprene coating produce radical reactions when exposed to a flame, the source of the FR properties in this material. Finally, rainwear garment Material O is a laminate composed of a FR polyurethane coating on 10osy 100% knit FR cotton. Each of the rainwear test materials is compliant with the ASTM F2733 standard, meaning that they exhibit less than 2 seconds of after-flame in the ASTM D6413 vertical flame test.

Table 3.2 Battery of Bench-Scale Test Methods for Predicting PyroMan™ Garment Shrinkage

Test Method	Rationale
ASTM F2894 (500°F Oven)	Test used in NFPA standards
TPP Test	Convective-radiant heat flux level comparable to PyroMan™
Cylindrical TPP Test	Convective -radiant heat flux level comparable to PyroMan™; Thermal shrinkage experienced in the sample can eliminate air gap, increasing rate of heat transfer

3.4 Test Methods

Table 3.2 shows the battery of bench-scale shrinkage tests used to evaluate the thermal shrinkage of the test materials described in Table 3.1.

Test materials were used to construct FR coveralls and rainwear garments for testing on PyroMan™. Triplicate tests were made for each of garment types. Table 3.3 shows the PyroMan™ measurement parameters.

Table 3.3 PyroMan™ Test Measurements (3, 4-second exposures)

Report	Measurements
% Body burn	Recorded temperature data
Duration of after-flame	Video recordings (front and rear)
Garment Shrinkage	Markers on backside of garments; 3-D Scanning

3.4.1 Bench-Scale Test Methods

3.4.1.1 500°F Oven Test

The 500°F circulating air oven test (ASTM F2894) required by the NFPA 2112 standard. Compliant materials must exhibit less than 10% shrinkage in any direction in this test.

3.4.1.2 Thermal Protective Performance (TPP) Test

We used the ASTM F2700 TPP standard test method to measure thermal protective insulation. This procedure measures time to second-degree burn in continuous flame exposure. In addition, we tested at 3.0- and 4.0-seconds exposure durations to produce test conditions similar to manikin flame exposure. We used spaced and contact sample testing configurations. We measured thermal shrinkage in TPP exposures as follows: we marked a 2.0 x 2.5-inch rectangular grid in the area of the test specimen directly exposed to heat (Figure 3.8). We

Figure 3.8 Photograph of marked fabric sample before and after TPP exposure

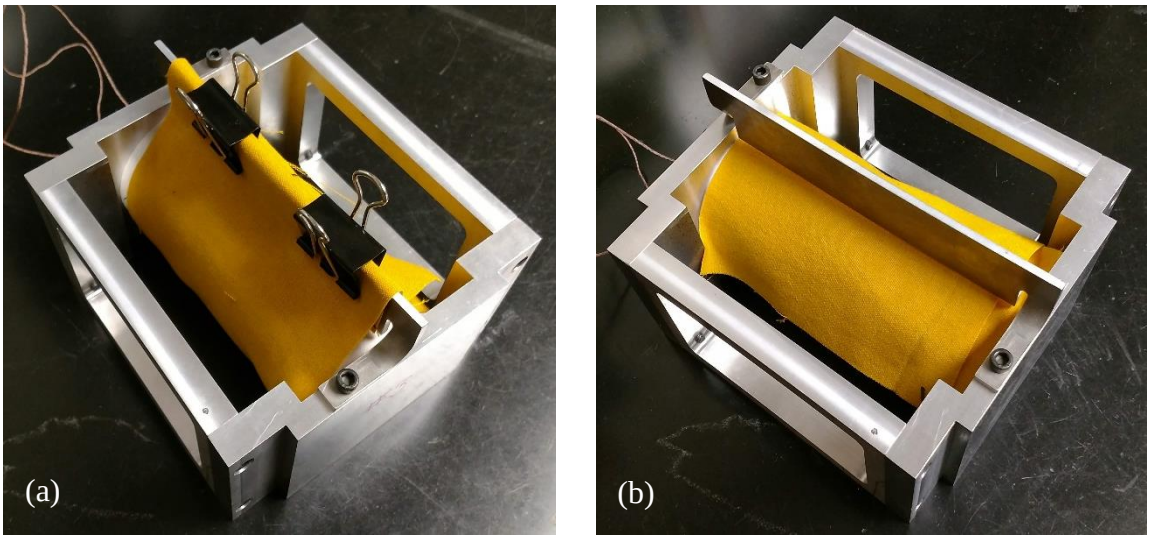

Figure 3.9 Specimen mounting technique used (a) in [14] and (b) in this study.

calculated thermal shrinkage as the percent dimensional change before and after exposure. We estimated areal shrinkage as the percent change of the area.

3.4.1.3 Cylindrical TPP Test

A variant of Dale's cylindrical TPP test method was used to evaluate thermal shrinkage in TPP exposures [14]. Dale's method replaced the flat TPP thermal sensing block and sample holder arrangement with a cylindrical sample holder and thermal sensor arrangement (Figure 3.6a). The cylinder incorporates a 6.35mm (0.25 inch) spacer between the test fabric and thermal sensor. While Dale's method restrained the specimens by clamping the ends of the specimens to the mounting rail, this study kept the ends of the specimens underneath the mounting rail and did not restrain the specimens [14]. Figure 3.9 shows the difference in sample mounting between the method used in Dale's study and the variant used in this study. Dale's study ended the TPP exposure after a 24°C rise in temperature was reached [14]. Wrapped around the cylindrical apparatus, unrestrained test fabric samples exhibit the full extent of thermal shrinkage caused by 3.0 and 4.0-seconds exposures to 84 kW/m2 incident heat.

3.4.2 Measuring Garment Shrinkage in PyroMan™ Tests

This study developed several different methods to evaluate garment thermal shrinkage in PyroMan™ tests. The first method used a variant of the procedure described by Li: circular markers of known size (12.7 cm diameter for coveralls and 7.6 cm diameter for rainwear) were drawn at selected locations of the manikin test garment (Figures 3.10a and 3.10b) [16]. The circular section was marked in the warp and filling directions to enable shrinkage measurement (Figure 3.10c). Markers were drawn at 38 locations on FR coveralls and 18 locations on FR rainwear, avoiding seams, reflective striping and pockets. The percent thermal shrinkage was estimated by measuring changes in the circular marker dimensions (warp and filling direction) following garment exposure in PyroMan™ tests.

The other method used in evaluating the garment shrinkage in fire manikin testing was 3-D scanning. This study used the Structure Sensor 3D scanner by Occipital, a portable 3-D scanner that attaches to an iPad, along with itSeez3D software to capture three-dimensional scans of the dressed manikin before and after flash fire exposure [26-27]. To ensure accuracy, each test garment was scanned three times before and after the exposure. Each of the scans were exported into Autodesk Fusion 360 modeling software, where any part of the scans not covered by the garment was removed (Figure 3.11), the scans were set to the correct scale, and the scan file was converted from a mesh to a solid body [28]. The correct scale for the scan was set based on the height of the manikin in the initial scan (not including the stabilizing block underneath the foot) and the total height of the manikin as specified in the ASTM F1930 standard [15]. The Autodesk Fusion 360 software then measures the surface area and volume of the manikin. These measurements are recorded and used to calculate the areal and volumetric shrinkage exhibited by each garment.

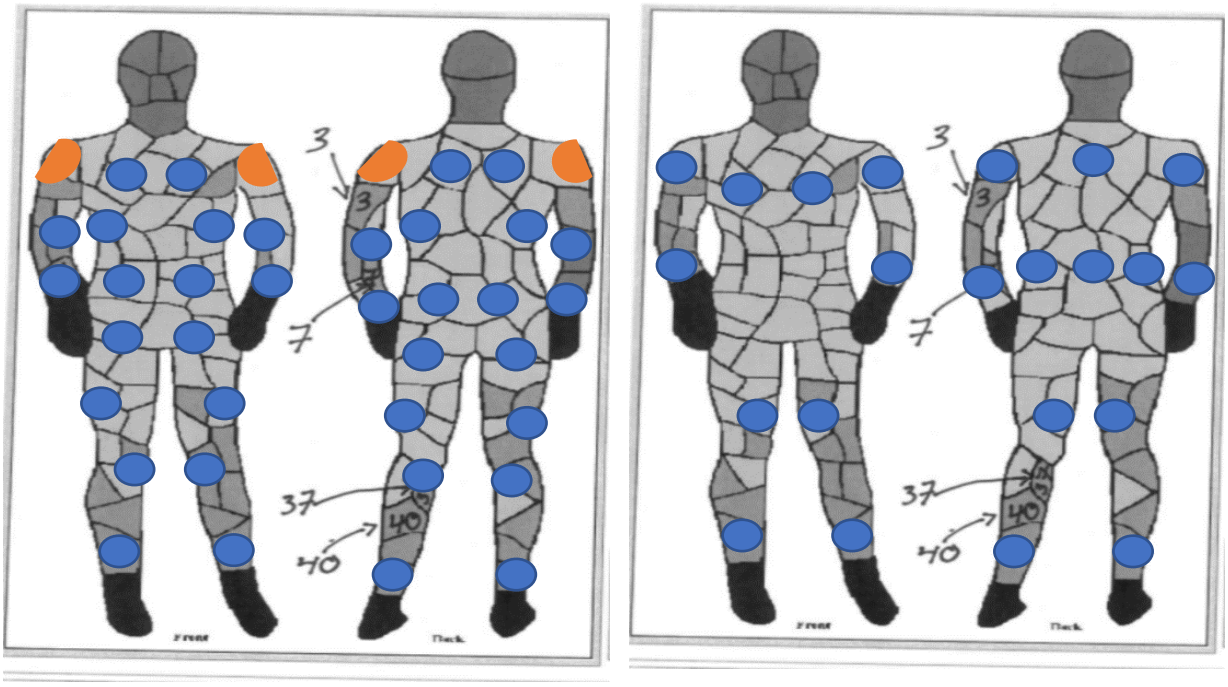

(a) (b)

(c)

Figure 3.10 (a) Approximate locations of markers on FR coverall garments used in fire manikin testing; (b) approximate locations of markers on FR rainwear garments used in fire manikin testing; (c) drawing of the marker used in measuring dimensional shrinkage in fire manikin testing

There are multiple advantages to using a 3-D scanning technique to measure garment shrinkage rather than physical markers. The scanner is able to measure the surface area and volume of the entire garment ensemble rather than a small sample, as is the case with the marker measurements, which ensures that the true amount of shrinkage is being measured. The methods of measuring both coveralls and rainwear are the same, which eliminates any potential

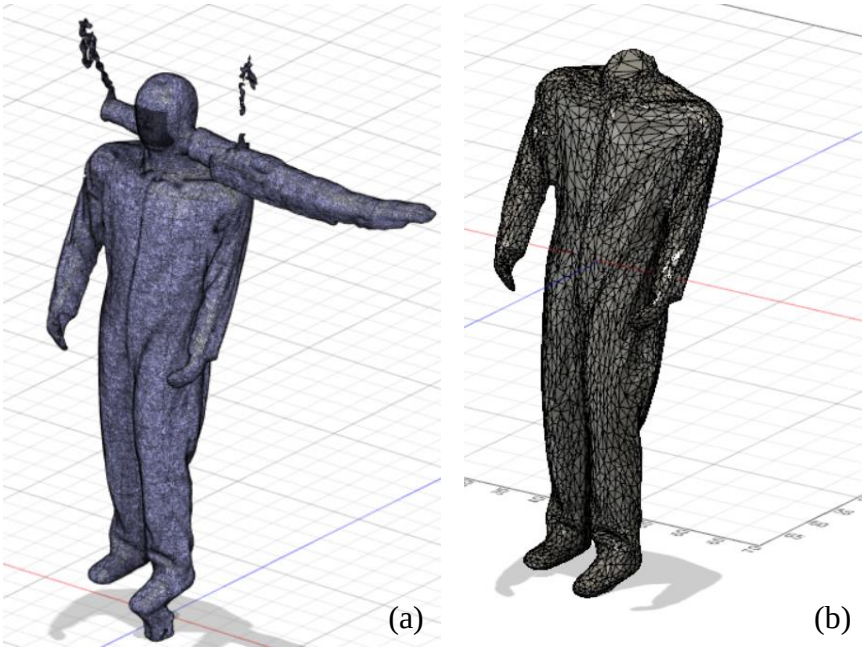

Figure 3.11 (a) Unedited 3-D scan inserted in Autodesk Fusion 360 Software; (b) 3-D scan in Autodesk Fusion 360 Software after removal of areas not covered by garment, scaling, and file conversion for surface area and volume measurements.

differences in results caused by different methodologies. The areal and volumetric shrinkage may better represent the reduction in the insulating air gap between the garment and manikin than the dimensional shrinkage measurements evaluated by the markers.

In spite of the advantages that 3-D scanning holds over the marker measurements, there are drawbacks to the scanning method. The accuracy and precision of the scanner is unknown, which may impact the repeatability of the results. Although the areal and volumetric shrinkage may be more telling about the reduction of the air gap, the ASTM F2894 500°F oven test measures dimensional shrinkage, so a direct comparison of shrinkage values is not available through standardized bench-scale test methods. ASTM and NFPA performance standards also call for dimensional shrinkage requirements rather than areal or volumetric shrinkage, so the 3-D scanning results are not directly applicable to the current performance requirements. When

compared to the marker measurements, 3-D scanning also carries a higher cost, which limits the practicality of the method.

3.5 Results and Discussion

3.5.1 FR Coveralls

Table 3.4 summarizes dimensional thermal shrinkage data measured in bench-scale tests and in PyroMan™ burns of FR coverall materials (500°F Oven, 3-seconds exposures in Cylindrical TPP, TPP and PyroMan™). Summarized data for the dimensional shrinkage measured in 4-seconds exposures on the Cylindrical TPP, TPP, and PyroMan™ tests as well as summarized tables for the surface area and volumetric shrinkage data can be found in Appendix B.

These data show that test materials (A, B, C, G, H, I, J) meet minimum thermal NFPA 2112 requirements. They exhibit less than 10% shrinkage in the ASTM F2894 500°F oven test, with less than 10% dimensional shrinkage in 3-seconds PyroMan™ exposure. However, the difference between the shrinkage measured in the 500°F oven test and the 3-seconds exposure in PyroMan™ testing varies for each material. The laminate materials (Materials D, E, F) consistently had the highest levels of thermal shrinkage. NFPA 2112 compliant Materials A and H shrink more than 10% in the Cylindrical TPP test. This result was not predicted by the 500°F oven test. Material H shrinks more than 10% in the TPP test (continuous exposure).

Figure 3.12 shows shrinkage observed in Material D (char-forming laminate) in a 3.0 second PyroMan™ exposure. In PyroMan™ testing, the highest levels of shrinkage were typically measured on the arms and lower legs of the test garments.

Figure 3.13 shows the average dimensional shrinkage observed in rainwear test garments in 3.0 and 4.0 PyroMan™ tests. As expected, thermal shrinkage increased with flame exposure,

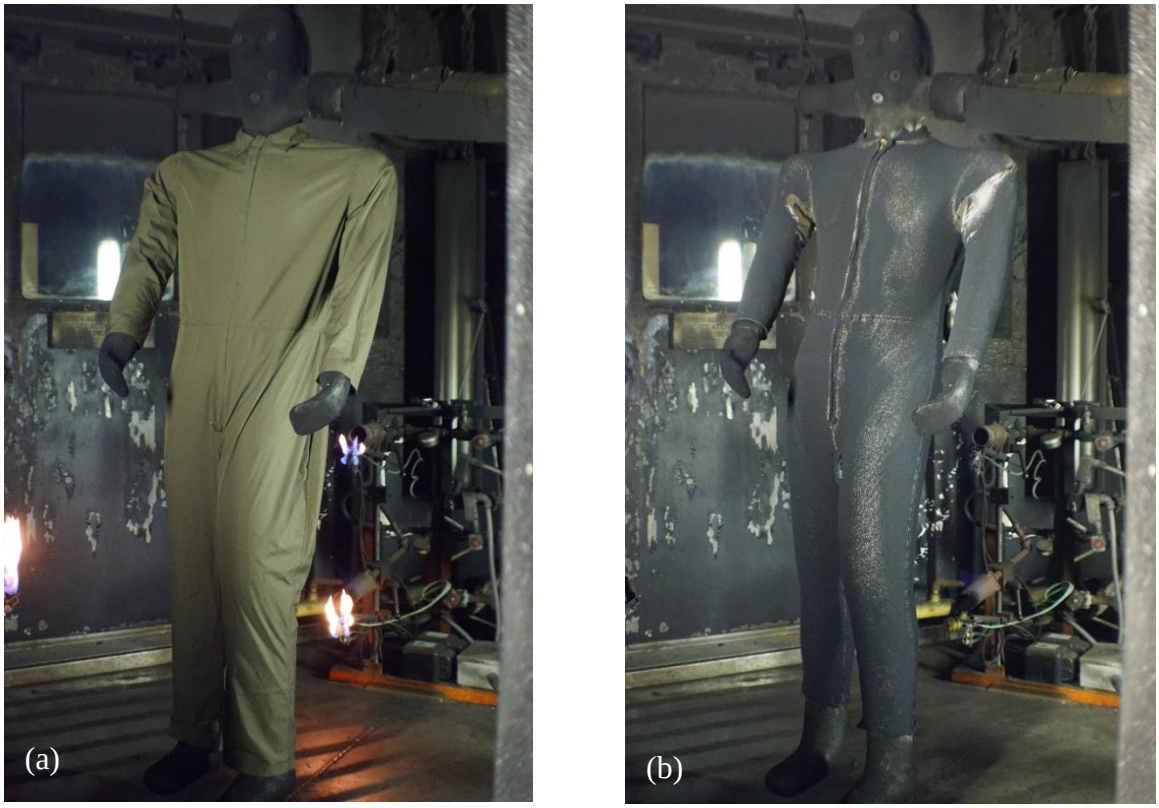

Figure 3.12 Shrinkage in coverall D- (a) before and (b) after a PyroMan™ 3-seconds exposure.

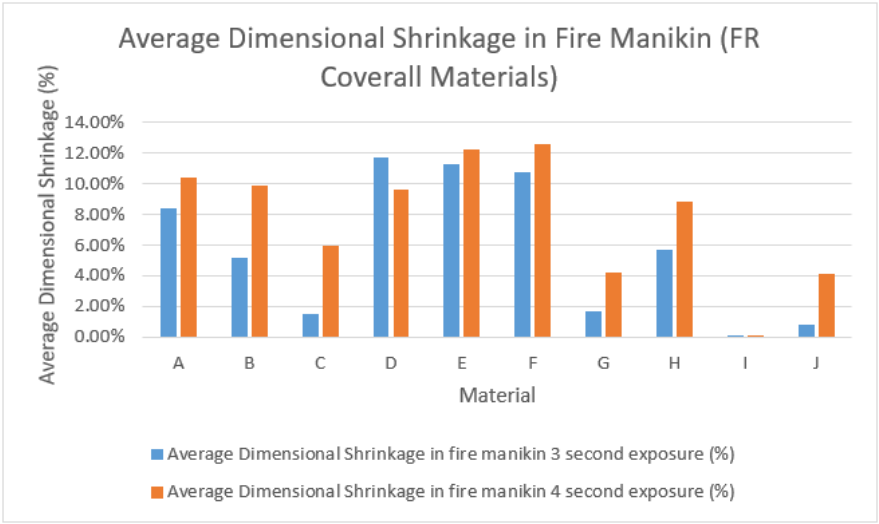

Figure 3.13 Average dimensional shrinkage measured in PyroMan™ testing (FR coverall fabrics).

with the amount of the increase depending on the specific test material. However, shrinkage measured in PyroMan™ testing of these laminate materials is limited by constrains of the

manikin itself. Figure 3.14 clearly shows that the coverall fits very tightly around the manikin form after a 3.0 second flash fire exposure. This physical limitation undoubtedly limits the maximum shrinkage that occurs in some of these materials.

Table 3.4 Dimensional Shrinkage (%) Measured in Bench-Scale tests and PyroMan™ (FR Coveralls).

ID	Material Type	ASTM F2894 500° F Oven	Cylindrical TPP		TPP		Average Dimensional Shrinkage in TPP continuous exposure		Average Dimensional Shrinkage in fire manikin
			Spaced 3 sec	Contact 3sec	Spaced 3 sec	Contact 3sec	Spaced (%)	Contact (%)	3 sec exposure (%)
A	Aramid	1.11%	14.52%	10.92%	7.28%	7.56%	5.80%	6.14%	8.40%
B	Aramid	2.14%	6.14%	7.68%	5.56%	5.58%	6.26%	8.34%	5.13%
C	Aramid	1.36%	4.00%	4.88%	4.68%	4.34%	6.62%	6.98%	1.50%
D	FR Laminate	21.81%	17.16%	29.24%	9.66%	6.62%	9.40%	12.24%	11.70%
E	FR Laminate	19.36%	11.74%	18.66%	5.76%	4.86%	13.36%	10.80%	11.30%
F	FR Laminate	19.92%	13.28%	19.76%	4.68%	5.40%	14.68%	10.82%	10.73%
G	Modacrylic	2.67%	7.24%	7.90%	5.52%	5.84%	8.10%	7.32%	1.70%
H	Modacrylic	8.56%	10.60%	11.16%	7.64%	7.18%	11.50%	10.04%	5.73%
I	PBI	1.17%	4.20%	4.50%	4.28%	3.98%	5.50%	5.44%	0.03%
J	FR Cotton	7.44%	3.83%	4.84%	4.72%	4.78%	7.08%	5.10%	0.83%

3.5.1.1 Predicting Garment Shrinkage in PyroMan™ Testing

Multiple statistically based methods were used to determine whether small-scale thermal shrinkage tests could be used to predict garment shrinkage behavior in PyroMan™ tests. A t-test analysis compared thermal shrinkage measured in the battery of bench-scale tests with the thermal shrinkage in FR coveralls (made from these same materials) tested on PyroMan™. This statistical analysis indicates whether the bench-scale test overestimates, underestimates or accurately predicts manikin garment shrinkage. The model's hypothesis is as follows: If the

bench-scale test shrinkage is neither significantly greater nor less than the manikin shrinkage, the bench test is judged to be an accurate predictor of manikin shrinkage.

T-test correlation analysis showed that bench scale thermal shrinkage tests tend to overestimate garment dimensional and areal shrinkage in PyroMan™ tests (Table 3.5, areal shrinkage table is found in Appendix B). This is an expected result in light of known differences in the physical restraint placed on the test materials in small-scale tests and in manikin tests. Test materials shrink without restriction in oven and cylindrical TPP tests of thermal shrinkage. The weight of the sensor apparatus in TPP testing restrains the ability for test specimens to shrink. The presence of the manikin form limits the maximum shrinkage of test garments in PyroMan™ tests.

3.5.1.2 Correlation Between Bench-Scale Tests and Garment Shrinkage in PyroMan™ Tests

While the t-test analysis shows that bench-scale shrinkage tests does not accurately predict PyroMan™ garment shrinkage, a relationship may still exist between the bench-scale shrinkage and PyroMan™ shrinkage. If it exists, this relationship could be used to rank fire protective materials based on bench-scale shrinkage. Therefore, it is significant that Pearson correlation analysis revealed statistically significant correlations between bench-scale thermal shrinkage tests and dimensional and areal garment shrinkage in 3.0 and 4.0 second manikin flame exposures (Table 3.6).

Table 3.5 T-Tests Showing Grouping of FR Coverall Materials by Statistically Significant Comparison of Bench-Scale Dimensional Shrinkage to PyroMan™ Dimensional Shrinkage

PyroMan™ Exposure Duration	Bench-Scale			
	Test	**Overestimate**	**Underestimate**	**Accurately Estimates**
3-seconds	Oven Test	D, E, F, H, I, J	A, B	C, G
	Cylindrical TPP- 3 sec contact	A, C, D, E, F, G, H, I, J		B
	Cylindrical TPP- 3 sec spaced	A, C, D, F, G, H, I, J		B, E
	TPP- 3 sec Contact	C, G, H, I, J	D, E, F	A, B
	TPP- 3 sec spaced	G, H, I, J	C, D, E, F	A, B
	TPP- continuous exposure contact	B, C, G, H, I, J	A	D, E, F
	TPP- continuous exposure spaced	C, F, G, H, I, J	A	B, D, E, K
	Total	43	11	16
	Percent of Total	61.4%	15.7%	22.9%
4-seconds	Oven Test	D, E, F, J, I	A, B, C, G	H
	Cylindrical TPP- 4 sec contact	A, B, C, D, E, F, G, I		H, J
	Cylindrical TPP- 4 sec spaced	A, B, C, D, E, F, G, I		H, J
	TPP- 4 sec Contact	G	B, E, F, H, I	A, C, D, J
	TPP- 4 sec spaced	D, I	E, F, H	A, B, C, G, J
	TPP- continuous exposure contact	C, D, G, I	A, E	B, F, H, J
	TPP- continuous exposure spaced	G, I	A, B	C, D, E, F, H, J
	Total	30	16	24
	Percent of Total	42.9%	22.9%	34.3%

Table 3.6 Correlations between Bench-Scale Tests of Dimensional Shrinkage and PyroMan™ Dimensional Shrinkage for FR Coveralls

PyroMan™ Exposure Duration	Bench-Scale Test	Pearson Correlation Coefficient (r)	P-value
3-seconds	Forced Air Oven Test	0.796	0.0059*
	Cylindrical TPP- 3-seconds Spaced	0.914	0.0002*
	Cylindrical TPP- 3-seconds Contact	0.903	0.0003*
	TPP- 3-seconds Spaced	0.583	0.0769
	TPP- 3-seconds Contact	0.481	0.1588
	TPP- Continuous Exposure Spaced	0.67	0.0339*
	TPP- Continuous Exposure Contact	0.825	0.0033*
4-seconds	Forced Air Oven Test	0.604	0.0643
	Cylindrical TPP- 4-seconds Spaced	0.65	0.0418*
	Cylindrical TPP- 4-seconds Contact	0.733	0.0158*
	TPP- 4-seconds Spaced	0.652	0.041*
	TPP- 4-seconds Contact	0.469	0.1719
	TPP- Continuous Exposure Spaced	0.645	0.044*
	TPP- Continuous Exposure Contact	0.724	0.0179*

*Indicates statistical significance.

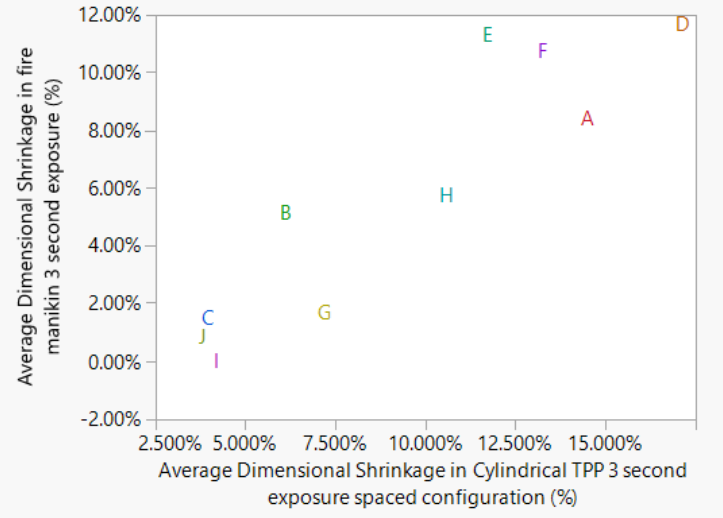

Figure 3.14 Relationship between 3-second cylindrical TPP (spaced configuration) test and 3-second PyroMan test (FR coverall materials)

These data show that thermal shrinkage measured in the 500°F oven test strongly correlates with manikin dimensional shrinkage in 3-second exposures; but, not in 4-second fire exposures. On the other hand, thermal shrinkage measured in the cylindrical TPP test provides a

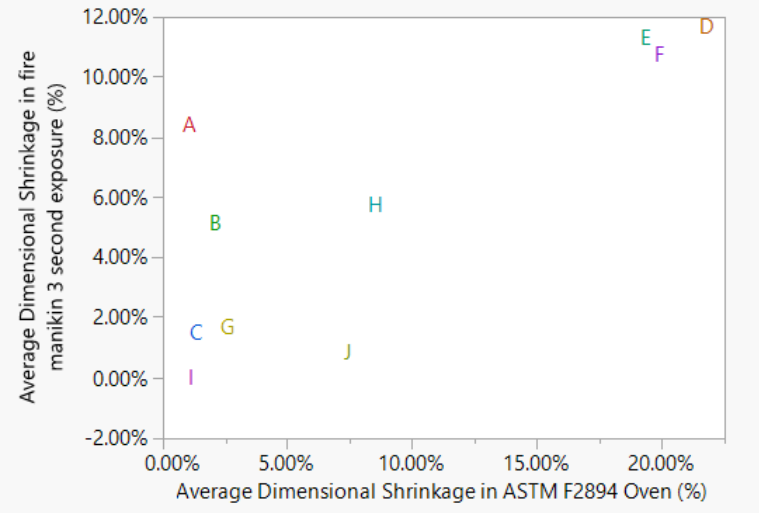

Figure 3.15 Average Dimensional Shrinkage in ASTM F2894 500F oven vs. Average Dimensional Shrinkage in 3-second PyroMan Tests (FR coverall materials)

stronger correlation with garment shrinkage on the manikin, in both 3.0 and 4.0-seconds flame exposures. Figure 3.14 shows the relationship between the dimensional shrinkage in 3.0 second cylindrical TPP tests (spaced configuration) and the dimensional garment shrinkage in 3.0 second manikin tests. At the same time, the 500°F oven test does not correlate with manikin shrinkage at the 4.0-seconds flame exposure condition. The correlations observed between bench-scale measures of areal shrinkage are similar to the correlations with dimensional shrinkage (table B.15 in Appendix B). Therefore, the cylindrical TPP shrinkage test provides the strongest correlations with manikin shrinkage at both 3.0- and 4.0-second manikin exposure levels.

Figure 3.15 shows the relationship between 500°F oven test and garment shrinkage in a 3-seconds PyroMan™ exposure. The correlation for the oven test is not as strong as the TPP cylinder shrinkage test, mainly because of the relatively low level of thermal shrinkage exhibited by the aramid fabrics (Materials A, B and C) in the oven test. All the FR coverall test materials

except the char-forming laminate constructions (Materials D, E and F) achieve less than 10% shrinkage in the 500°F oven test.

3.5.1.3 Relationship Between Thermal Shrinkage and Thermal Protection

Correlation analysis showed no significant relationship between the 500° F oven thermal shrinkage and thermal protective performance measured in 3.0 or 4.0-seconds fire manikin tests. On the other hand, this analysis showed statistically significant correlations between predicted manikin body burn and thermal shrinkage measured in the cylindrical TPP shrinkage test (Table 3.7).

Table 3.7 Correlations between Bench-Scale Dimensional Shrinkage Tests and Percent Body Burn (FR Coveralls)

PyroMan™ Exposure Duration	Bench-Scale Test	Pearson Correlation Coefficient (r)	P-value
3-seconds	500°F Oven Test	0.318	0.3704
	Cylindrical TPP- 3-seconds Spaced	0.709	0.0218*
	Cylindrical TPP- 3-seconds Contact	0.606	0.0633
	TPP- 3-seconds Spaced	0.636	0.0479*
	TPP- 3-seconds Contact	0.595	0.0698
	TPP- Continuous Exposure Spaced	0.067	0.8531
	TPP- Continuous Exposure Contact	0.38	0.2789
	PyroMan™ Marker Measurements	0.619	0.0003*
4-seconds	500°F Oven Test	0.327	0.3565
	Cylindrical TPP- 4-seconds Spaced	0.366	0.2983
	Cylindrical TPP- 4-seconds Contact	0.313	0.3788
	TPP- 4-seconds Spaced	0.268	0.4537
	TPP- 4-seconds Contact	0.291	0.4147
	TPP- Continuous Exposure Spaced	0.221	0.5392
	TPP- Continuous Exposure Contact	0.219	0.5431
	PyroMan™ Marker Measurements	0.332	0.0784

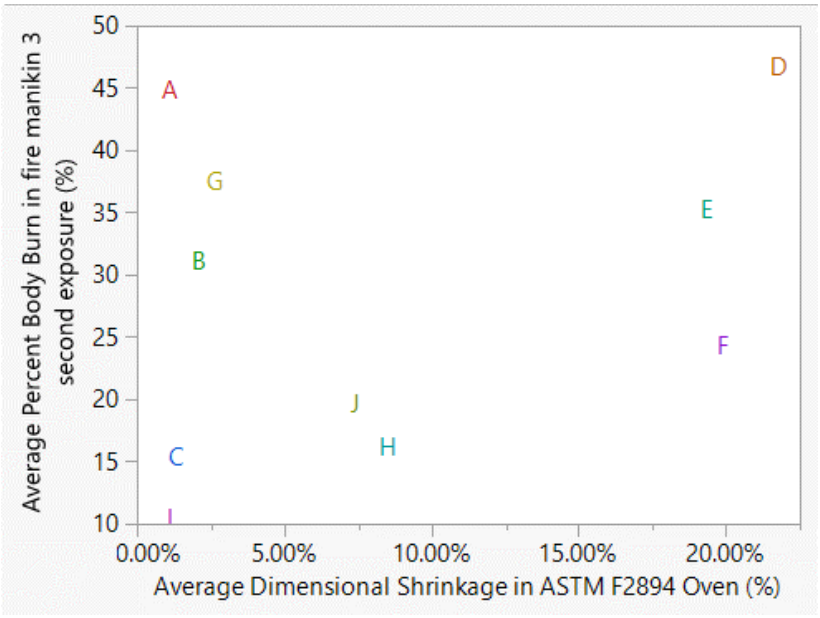

Figure 3.16 Dimensional shrinkage in ASTM F2894 Oven vs. percent body burn in PyroMan™ 3-seconds exposure (FR coveralls).

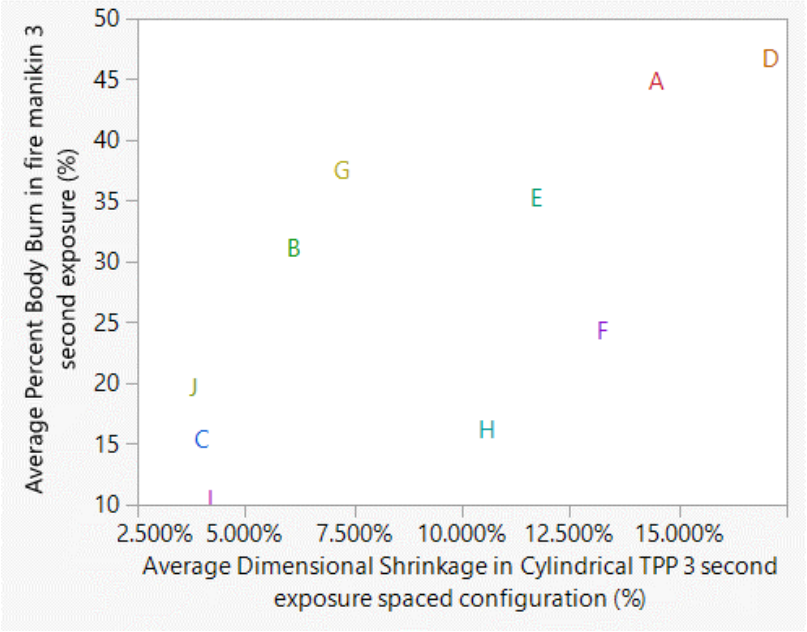

Figure 3.17 Dimensional shrinkage in Cylindrical TPP 3-seconds exposure spaced configuration vs. percent body burn in PyroMan™ 3-seconds exposure (FR coveralls).

Figure 3.16 shows the relationship between the dimensional shrinkage measured in the 500°F oven and the predicted percent body burn in the PyroMan™ 3-seconds exposure for FR

coverall fabrics. The plot shows three distinct groups based on the shrinkage measured in the 500°F oven test. The first group of fabrics contains materials that exhibit low shrinkage in the 500°F oven (all below 3% shrinkage) and a wide variety of protective ability (10-45% body burn).

The second group of materials, comprised entirely of the three laminates, exhibits high shrinkage (all greater than 15%) and a wide span of thermal protection (24-47% body burn). The final group, which is made up of Materials H and J, exhibits moderate shrinkage on the 500°F oven test and good thermal protection (16-20% body burn). The wide variety in protection offered by materials with a similar level of shrinkage indicates that the shrinkage measured in the 500°F oven test does not predict the protective performance offered by the FR coverall test garments. Furthermore, the char-forming laminate materials, which fail the NFPA 2112 shrinkage requirement, pass the NFPA 2112 manikin test requirement of exhibiting less than 50% predicted body burn even though testing was done without cotton t-shirt and briefs as required in NFPA 2112 [2]. This result shows that the current standards may screen out materials that are effective at protecting the wearer. The many differences in the test conditions is likely the reason for the lack of a correlation between the shrinkage measured in the 500°F oven test and the predicted percent body burn in the PyroMan™ 3-seconds exposure.

By contrast, the shrinkage in the Cylindrical TPP 3-second exposure in the spaced configuration exhibits a statistically significant relationship with the predicted body burn in the PyroMan™ 3-second exposure (Figure 3.17). Even though the aramid materials are the only class of fabrics that shows an upward trend on its own, the general upward trend of all the FR coverall materials suggests that the shrinkage measured in the Cylindrical TPP 3-second exposure spaced configuration can predict the percent body burn in the PyroMan™ 3-second

exposure. The similar conditions that are produced in the Cylindrical TPP and PyroMan™ tests are likely an important factor in the correlation between the shrinkage measured in the Cylindrical TPP 3-second exposure spaced configuration and the predicted percent body burn in the PyroMan™ 3-second exposure.

3.5.2 FR Rainwear

Table 3.8 summarizes thermal shrinkage data measured in bench-scale tests and in PyroMan™ burns of FR rainwear materials. The table includes dimensional shrinkage data from the 500°F oven test as well as 3-seconds exposures of the cylindrical TPP, TPP, and PyroMan™ tests and the TPP continuous exposure. Tables summarizing the data from areal shrinkage and the 4-seconds exposure of the cylindrical TPP, TPP, and PyroMan™ tests are located in Appendix B.

Table 3.8 Dimensional Shrinkage (%) Measured in Bench-Scale tests and PyroMan™ (FR Coveralls).

ID	Material Type	Average Dimensional Shrinkage							
		ASTM F2894	Cylindrical TPP (3 sec)		TPP (3 sec)		TPP (continuous)		Fire Manikin (3 sec)
		Oven (%)	spaced (%)	contact (%)	spaced (%)	contact (%)	spaced (%)	contact (%)	(%)
D	FR Laminate	21.81%	17.16%	29.24%	9.66%	6.62%	9.40%	12.24%	11.70%
E	FR Laminate	19.36%	11.74%	18.66%	5.76%	4.86%	13.36%	10.80%	11.30%
F	FR Laminate	19.92%	13.28%	19.76%	4.68%	5.40%	14.68%	10.82%	10.73%
K	FR Rainwear	2.31%	3.15%	3.98%	4.22%	3.90%	2.70%	5.70%	1.00%
L	FR Rainwear	2.11%	2.67%	4.82%	3.62%	3.26%	0.65%	6.82%	4.93%
M	FR Rainwear	16.61%	11.80%	12.38%	4.10%	5.42%	-0.53%	6.34%	9.30%
N	FR Rainwear	2.14%	2.14%	3.22%	3.36%	3.28%	3.80%	5.72%	1.33%
O	FR Rainwear	3.22%	3.75%	4.36%	3.92%	3.34%	3.48%	3.98%	1.60%

Figure 3.18 Shrinkage observed by Material M rainwear garment (a) before and (b) after PyroMan™ 3-seconds exposure.

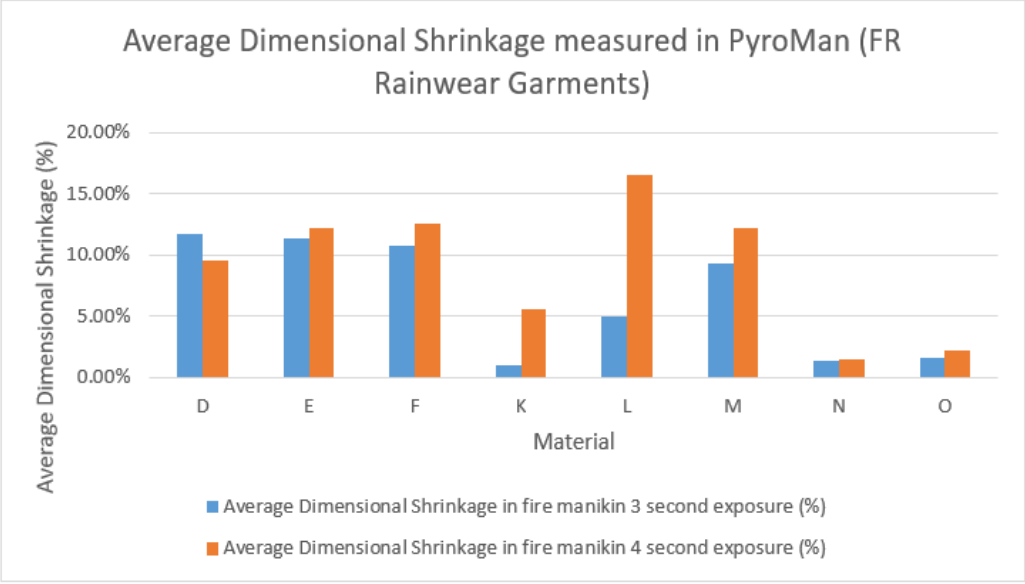

Figure 3.19 Average dimensional shrinkage measured in PyroMan™ testing (FR rainwear materials).

An initial review of the thermal shrinkage results for the FR rainwear materials shows that each of the FR rainwear materials exhibit a low level of shrinkage apart from the laminate materials and Material M (Figure 3.20), which is expected. Although the ASTM F2733 standard does not call for a shrinkage performance requirement, the FR rainwear materials apart from the laminate materials and Material M would pass the 10% shrinkage requirement called for by the NFPA 2112 standard for FR coveralls. In fact, shrinkage measured in the 500°F oven is not as dramatically different from the shrinkage measured in PyroMan™ 3-second exposure as was observed with the FR coveralls. Material M, which consistently exhibited high levels of shrinkage, showed significantly less shrinkage in the TPP tests than in the other bench-scale and PyroMan™ testing, which was expected as the weight of the TPP sensor restricts the sample from shrinking. Materials K and L both experienced a dramatic increase in the shrinkage measured in PyroMan™ between the 3-second and 4-second exposures, which can be seen in Figure 3.19. As with FR coveralls, the highest levels of shrinkage in PyroMan™ testing occurred around the arms and the legs of the FR rainwear garments.

3.5.2.1 Predicting Shrinkage of Rainwear Garments in PyroMan™ Tests

As discovered for FR coverall materials, t-test analysis showed that bench-scale thermal shrinkage tests generally overestimate the shrinkage of rainwear garments measured in fire manikin tests (Table 3.9, areal shrinkage shown in Appendix B). In TPP testing, where fabric specimens are restrained from shrinking due to the weight of the sensor apparatus, the garment shrinkage in PyroMan™ was generally underestimated. Specific relationships appear to associate with differences in the thermal response of different types of rainwear laminates.

Table 3.9 T-Tests Showing Grouping of FR Rainwear Materials with Statistically Significant Comparison Bench-Scale Dimensional Shrinkage to PyroMan™ Dimensional Shrinkage

PyroMan™ Exposure Duration	Bench-Scale			
	Test	**Overestimate**	**Underestimate**	**Accurately Estimates**
3-seconds	Oven Test	D, E, F, M, N, O	L	K
	Cylindrical TPP- 3-seconds contact	D, E, F, K, N, O		L, M
	Cylindrical TPP- 3-seconds spaced	D, F, K, N, O	L	E, M
	TPP- 3-seconds Contact	K, N, O	D, E, F, L, M	
	TPP- 3-seconds spaced	K, N, O	D, E, F, L	M
	TPP- continuous exposure contact	K, N, O		D, E, F, L, M
	TPP- continuous exposure spaced	F, N, O	L, M	D, E, K
	Total	29	13	14
	Percent of Total	51.8%	23.2%	25.0%
4-seconds	Oven Test	D, E, F, M, O	K, L	N
	Cylindrical TPP- 4-seconds contact	D, E, F, N, O	L	K, M
	Cylindrical TPP- 4-seconds spaced	D, E, F, O	L	K, M, N
	TPP- 4-seconds Contact	N, O	E, F, L, M	D, K
	TPP- 4-seconds spaced	D, N, O	E, F, L, M	K
	TPP- continuous exposure contact	D, N, O	E, L, M	F, K
	TPP- continuous exposure spaced	N, O	K, L, M	D, E, F
	Total	24	18	14
	Percent of Total	42.9%	32.1%	25.0%

3.5.2.2 Correlation Between Bench-Scale Thermal Shrinkage and Shrinkage of Rainwear Garments in PyroMan™ Tests

Correlation analysis was used to identify relationships between thermal shrinkage in bench-scale tests and garment shrinkage in PyroMan™ testing that would allow materials to be ranked based on bench-scale shrinkage. Table 3.10 summarizes the results of correlation analysis of relationships between the dimensional shrinkage measured in bench-scale tests and in

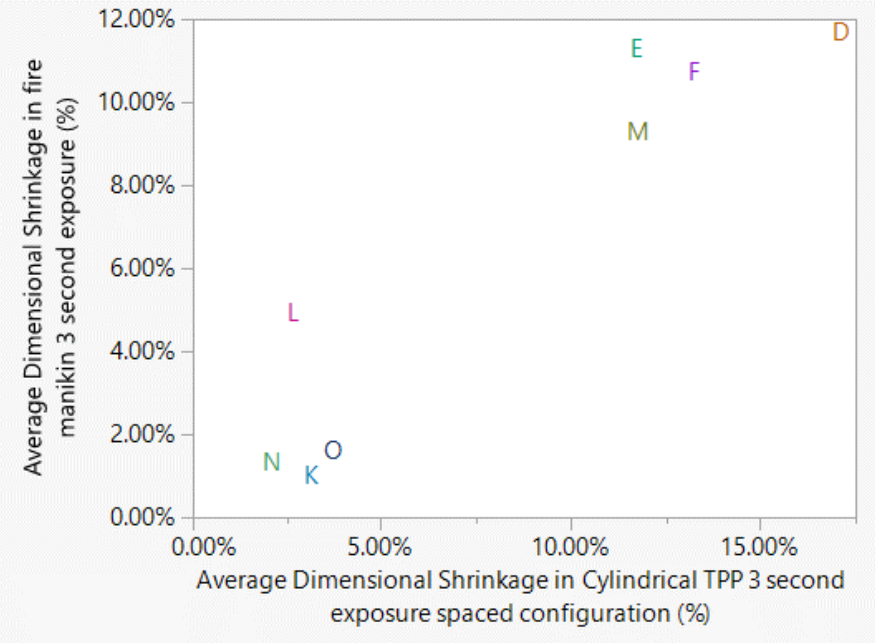

Figure 3.20 Dimensional shrinkage in Cylindrical TPP 3-seconds exposure spaced configuration vs. dimensional shrinkage in PyroMan™ 3-seconds exposure (FR Rainwear materials).

Table 3.10 Correlations between Bench-Scale Dimensional Shrinkage Tests and PyroMan™ Dimensional Shrinkage for FR Rainwear

PyroMan™ Exposure Duration	Bench-Scale Test	Pearson Correlation Coefficient (r)	P-value
3-seconds	Forced Air Oven Test	0.963	0.0001*
	Cylindrical TPP- 3-seconds Spaced	0.937	0.0006*
	Cylindrical TPP- 3-seconds Contact	0.911	0.0017*
	TPP- 3-seconds Spaced	0.645	0.0842
	TPP- 3-seconds Contact	0.869	0.0051*
	TPP- Continuous Exposure Spaced	0.63	0.094
	TPP- Continuous Exposure Contact	0.877	0.0042*
4-seconds	Forced Air Oven Test	0.473	0.237
	Cylindrical TPP- 4-seconds Spaced	0.427	0.2908
	Cylindrical TPP- 4-seconds Contact	0.355	0.3869
	TPP- 4-seconds Spaced	0.35	0.3948
	TPP- 4-seconds Contact	0.224	0.5941
	TPP- Continuous Exposure Spaced	0.184	0.6632
	TPP- Continuous Exposure Contact	0.52	0.1861

*Indicates statistical significance

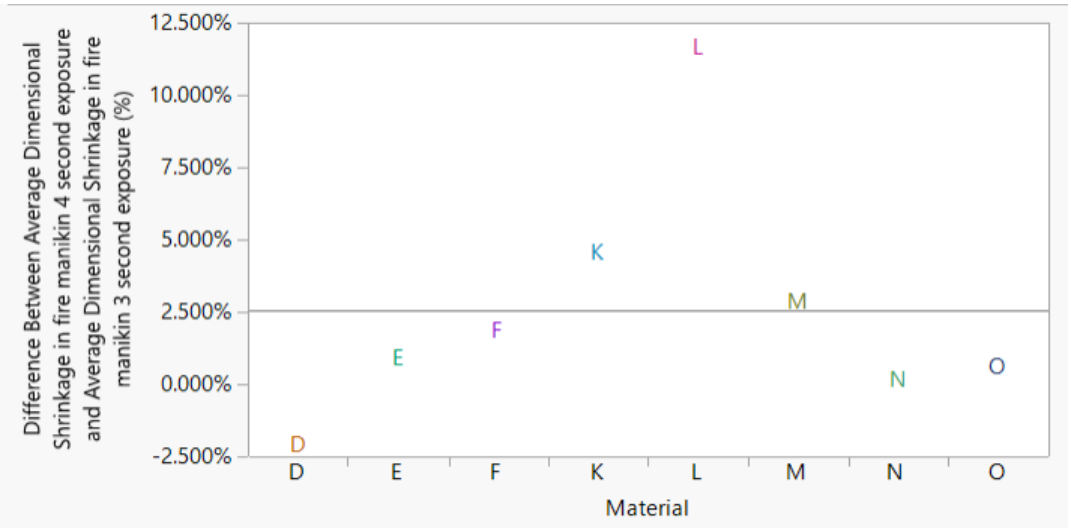

Figure 3.21 Difference between average dimensional shrinkage on fire manikin 4-seconds exposure and average dimensional shrinkage in fire manikin 3-seconds exposure (FR Rainwear)

PyroMan™ testing (areal shrinkage shown in Appendix B). These data show that statistically significant relationships exist between several bench-scale measures of thermal shrinkage and garment shrinkage in 3-second PyroMan™ tests.

Figure 3.20 shows that a strong relationship exists between cylindrical TPP shrinkage and dimensional shrinkage in FR rainwear garments in 3-seconds PyroMan™ tests. The relationship shows two distinct groups: materials that employ char-forming technology (D, E, F, M) and the other FR rainwear laminates (K, L, N, O). Figure 3.21 shows the difference in garment shrinkage between the 3- and 4- second exposure durations in PyroMan™ testing. The dramatic increase in garment shrinkage for Material L may explain why the correlations are strong for 3-second exposures, but weak for 4-second exposures.

3.5.2.3 Relationship Between Thermal Shrinkage and Thermal Protection in FR Rainwear

Table 3.11 shows the correlations analysis between bench-scale measures of thermal shrinkage and thermal protective performance (% predicted body burn) in PyroMan™ tests. These results show that no statistically significant correlation exists between thermal shrinkage

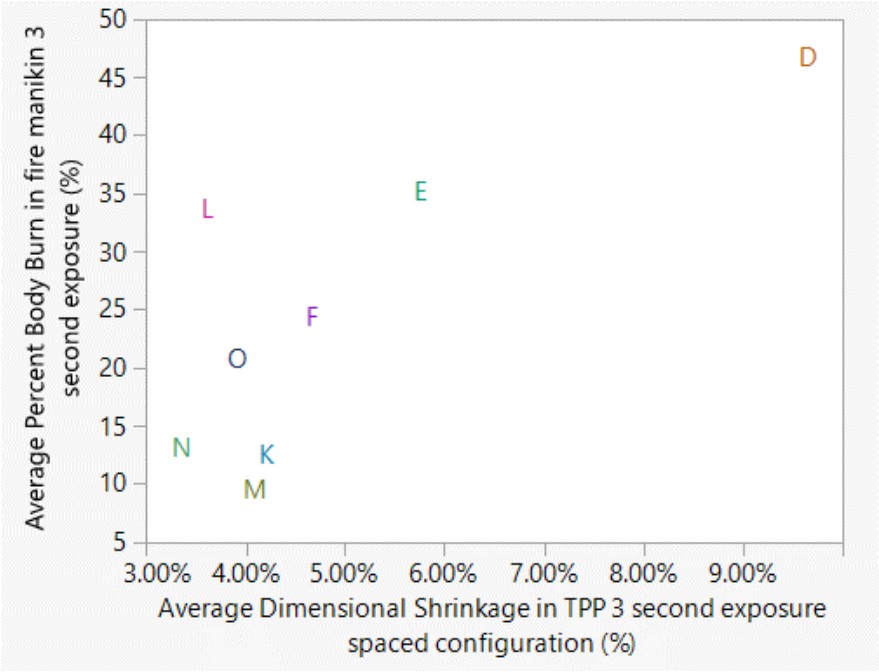

Figure 3.22 Dimensional shrinkage in TPP 3-second exposure spaced configuration vs. predicted percent body burn in PyroMan™ 3-second exposure (FR rainwear materials).

Table 3.11 Correlations between dimensional shrinkage tests and % Body Burn (FR Rainwear).

PyroMan™ Exposure Duration	Bench-Scale Test	Pearson Correlation Coefficient (r)	P-value
3-seconds	Forced Air Oven Test	0.471	0.2384
	Cylindrical TPP- 3-seconds Spaced	0.513	0.1933
	Cylindrical TPP- 3-seconds Contact	0.685	0.0611
	TPP- 3-seconds Spaced	0.768	0.026*
	TPP- 3-seconds Contact	0.445	0.2694
	TPP- Continuous Exposure Spaced	0.519	0.187
	TPP- Continuous Exposure Contact	0.742	0.0349*
	PyroMan™- Marker Measurements	0.547	0.0057*
4-seconds	Forced Air Oven Test	0.504	0.2025
	Cylindrical TPP- 4-seconds Spaced	0.692	0.0573
	Cylindrical TPP- 4-seconds Contact	0.698	0.054
	TPP- 4-seconds Spaced	0.811	0.0146*
	TPP- 4-seconds Contact	0.787	0.0205*
	TPP- Continuous Exposure Spaced	0.618	0.1024
	TPP- Continuous Exposure Contact	0.802	0.0166*
	PyroMan™- Marker Measurements	0.526	0.0083*

*Indicates statistical significance

in the 500°F oven test and PyroMan™ predicted burn injury for FR rainwear materials. However, they do indicate that a statistically significant correlation exists between shrinkage measured in standard TPP tests.

Figure 3.22 shows the relationship between thermal shrinkage measured in 3-second TPP exposures and predicted manikin body burn in 3-seconds flame exposures. These data show the influence of the char-forming laminates (Materials D, E, F, and M) on the correlation between shrinkage in TPP tests and predicted manikin body burn. Therefore, this finding that thermal shrinkage measured on these tests may not be useful for ranking other FR rainwear materials on the predicted body burn injury in the PyroMan™ test.

3.6 Conclusions

Because they overestimate thermal shrinkage, bench-scale shrinkage tests do not provide accurate prediction of the thermal shrinkage exhibited by FR coveralls or FR rainwear materials in PyroMan™ tests. At the same time, our analysis indicates that some small-scale shrinkage measures correlate well with garment shrinkage in manikin tests on these materials. In this regard, our study shows that shrinkage measured in the cylindrical TPP tests more strongly correlates with manikin measures of shrinkage than the 500°F oven test. We have further shown that the 500°F oven shrinkage test is not a useful tool for predicting burn protection assessed in fire manikin tests.

For FR coverall materials, thermal shrinkage measured on the cylindrical TPP test in 3-seconds flame exposure provided the best prediction of manikin burn protection. The standard spaced configuration TPP test provided the best burn prediction for FR rainwear. However, complex differences in the thermal response of different types of FR rainwear laminates made

identifying correlations between small-scale measures of thermal shrinkage and performance of garments in PyroMan™ tests is more challenging.

The findings are of interest when considering the NFPA 2112 standard performance requirements. They have shown that thermal shrinkage measured using a cylindrical TPP method would be a more useful test for establishing thermal shrinkage requirements for FR coveralls than the 500°F oven test. The cylindrical TPP method would therefore deserve consideration as a standard test method. This study indicates that incorporating a TPP-type thermal shrinkage requirement in the FR rainwear standards may be more useful, since we have demonstrated that this test can rank FR rainwear materials based on garment shrinkage and thermal protective performance in fire manikin tests.

3.6.1 Recommendations for Future Research

This study has decisively shown that existing standard bench-scale test methods for measuring after-flame or thermal shrinkage in FR coveralls or FR rainwear provide only limited ability to predict thermal shrinkage of these materials in full-scale fire manikin testing. The current bench-scale test methods cannot accurately reflect the thermal shrinkage behavior that can occur with a flash fire test. When testing with a flash fire manikin system, the air diffused propane flames interact with the garment with multiple variables. These include but are not limited to pressure, air gaps, velocity, and orientation of the flame interaction with sheer, direct impingement and full engulfment of the fabric.

Future research is proposed to develop a small-scale test method that would more reliably predict results obtained in fire manikin tests. Ideally, this study would simulate these characteristics using an instrumented simulated human limb (arm or leg) that can be oriented in the vertical and horizontal direction while surrounded by small scale air diffused propane

torches. Special garments would be made to mimic how the garment fits and drapes on the flame manikin. This would better predict the fabric characteristics of thermal shrinkage and after-flame when exposed to a high intensity flash fire.

The study would investigate how a fabric reacts to flame dynamics with sheer flow, direct impingement, full engulfment of the fabric, pressure, velocity and orientation of the simulated human limb in a horizontal and vertical orientation. Using multiple fabrics and three styles of sensors (modified copper slug, embedded thermocouple and surface thermocouple) we could provide measurements of thermal shrinkage, after-flame, 2nd degree burn, and transferred thermal energy.

3.8 References

1. NFPA 2112 Standard on Flame-Resistant Clothing for Protection of Industrial Personnel Against Short-Duration Thermal Exposures from Fire, National Fire Protection Association, Quincy, MA, 2007.

2. NFPA 1971 Standard on Protective Ensembles for Structural Fire Fighting and Proximity Fire Fighting, National Fire Protection Association, Quincy, MA, 2013.

3. ASTM D6413/D6413M-15 Standard Test Method for Flame Resistance of Textiles (Vertical Test), ASTM International, West Conshohocken, PA, 2015.

4. ASTM F1358-16 Standard Test Method for Effects of Flame Impingement on Materials Used in Protective Clothing Not Designated Primarily for Flame Resistance, ASTM International, West Conshohocken, PA, 2016.

5. CAN/CGSB 4.2 NO. 27.10 Textile test methods-Flame resistance, Canadian General Standards Board, 2011.

6. V. Babrauskas, The Cone Calorimeter, in: SFPE Handb. Fire Prot. Eng., Springer, New York, NY, 2016: pp. 952–980. doi:10.1007/978-1-4939-2565-0_28.

7. ASTM E1354-17 Standard Test Method for Heat and Visible Smoke Release Rates for Materials and Products Using an Oxygen Consumption Calorimeter, ASTM International, West Conshohocken, PA, 2017.

8. G. Song, Clothing Air Gap Layers and Thermal Protective Performance in Single Layer Garment, J. Ind. Text. 36 (2007) 193–205. doi:10.1177/1528083707069506.

9. ASTM F2894-14 Standard Test Method for Evaluation of Materials, Protective Clothing and Equipment for Heat Resistance Using a Hot Air Circulating Oven, ASTM International, West Conshohocken, PA, 2014.

10. ASTM F2700-08 Standard Test Method for Unsteady-State Heat Transfer Evaluation of Flame Resistant Materials for Clothing with Continuous Heating, ASTM International, West Conshohocken, PA, 2008.

11. M. Wang, J. Li, Thermal protection retention of fire protective clothing after repeated flash fire exposure, J. Ind. Text. 46 (2016) 737–755. doi:10.1177/1528083715594977.

12. J. Li, M. Zhao, Y. Xie, Y. Wang, Thermal shrinkage of fabrics used for out layer of firefighter protective clothing under flash fire, Fire Mater. 39 (2015) 732–740. doi:10.1002/fam.2260.

13. Barker, R., Geshury, A., Behnke, W. “The Effect of Nomex®/Kevlar® Fiber Blend Ratio and Fabric Weight on Fabric Performance in Static and Dynamic TPP Tests,” Performance of Protective Clothing, Fifth Volume, ASTM STP 1237, James S. Johnson and S. Z. Mansdorf, Eds., American Society for Testing and Materials, Philadelphia, PA (1996).

14. E.M. Crown, J.D. Dale, E. Bitner, A comparative analysis of protocols for measuring heat transmission through flame resistant materials: capturing the effects of thermal shrinkage, Fire Mater. 26 (2002) 207–213. doi:10.1002/fam.797.

15. ASTM F1930-17, Standard Test Method for Evaluation of Flame Resistant Clothing for Protection Against Fire Simulations Using an Instrumented Manikin, ASTM International, West Conshohocken, PA, 2017.

16. X. Li, Y. Lu, L. Zhai, M. Wang, J. Li, Y. Wang, Analyzing Thermal Shrinkage of Fire-Protective Clothing Exposed to Flash Fire, Fire Technol. 51 (2015) 195–211. doi:10.1007/s10694-013-0375-0.

17. M. Wang, X. Li, J. Li, B. Xu, A new approach to quantify the thermal shrinkage of fire protective clothing after flash fire exposure, Text. Res. J. 86 (2016) 580–592. doi:10.1177/0040517515595028.

18. J. Li, M. Zhao, Y. Xie, Y. Wang, Thermal shrinkage of fabrics used for out layer of firefighter protective clothing under flash fire, Fire Mater. 39 (2015) 732–740. doi:10.1002/fam.2260.

19. Pawar, M., Barker, R., Shalev, I., Hamouda, H., Behnke, W., Bender, M., “Analyzing the Performance of Protective Garments in Manikin Fire Tests,” Proceedings of the Fifth Scandinavian Symposium on Protective Clothing, Elsinore, Denmark, May 1997.

20. Wang, X. Li, J. Li, Correlation of bench scale and manikin testing of fire protective clothing with thermal shrinkage effect considered, Fibers Polym. 16 (2015) 1370–1377. doi:10.1007/s12221-015-1370-5.

21. C. Lee, I.Y. Kim, A. Wood, Investigation and correlation of manikin and bench-scale fire testing of clothing systems, Fire Mater. 26 (2002) 269–278. doi:10.1002/fam.808.

22. G. Song, R.L. Barker, H. Hamouda, A.V. Kuznetsov, P. Chitrphiromsri, R.V. Grimes, Modeling the Thermal Protective Performance of Heat Resistant Garments in Flash Fire Exposures, Text. Res. J. 74 (2004)

23. Arifoglu, M., “Innovations in Heat and Flame Protection Using Gore Fabric Technology,” AATCC International Conference Proceedings, Wilmington, NC, March 2017.

24. Adams, D., “Fire Resistant Fabric Testing and Significance,” AATCC Flammability Symposium, Raleigh, NC 2016

25. Structure Sensor- 3D scanning, augmented reality, and more for mobile devices. Available: https://structure.io/.

26. itSeez3D. Available: https://itseez3d.com/.

27. Autodesk. Autodesk Fusion 360. Available: https://www.autodesk.com/.

28. K. Varga et al, "Thermal and sorption study of flame-resistant fibers," Lenzinger Berichte, vol. 89, pp. 50-59, 2011.

29. PBI Products, "PBI Max". Available: https://www.pbiproducts.com/.

30. S. Francis, "Understanding Fibers and Fabrics: The Engineering of Arc Rated/Flame Resistant Fabrics," *Westex by Milliken*, 2018.

31. Gore® Pyrad® fabric technology: durable flame retardant protection. Available: https://www.gore-workwear.co.uk/technologies/gore-pyrad-fabric-technology.

32. B. C. Nutt, J. P. Towey, D. Narasimhan and M. S. Zedalis, "Flexible Lightweight Arc Flash and Flash Fire Resistant Polyvinylchloride Fabric and Garments and Methods Therefor " US 2016.003917OA1, Feb, 2016.

33. ASTM F2733-17 Standard Specification for Flame-Resistant Rainwear for Protection Against Flame Hazards, ASTM International, West Conshohocken, PA, 2017.

34. Backer, Tesoro, Toony, and Moussa, Textile Fabric Flammability, MIT Press, Cambridge, MA

35. Shalev, I. and Barker, R., “Predicting the Thermal Protective Performance of Heat Protective Fabrics from Basic Properties”, Performance of Protective Clothing, Barker and Coletta, Eds., ASTM Special Technical Publication 90, July 1986

36. Yong Wang et al, "Convective Heat Transfer of the Bunsen Flame in the UL94 Vertical Burning Test for Polymers," Journal of Fire Sciences, vol. 28, (4), pp. 337-356, 2010. Available: https://journals.sagepub.com/doi/full/10.1177/0734904109351484. DOI: 10.1177/0734904109351484.

37. S.K. An, R.L. Barker, J.O. Stull, Measurement of The Flammability and Thermal Aging of Chemical Protective Suit Materials, (1989). doi:10.1520/STP22935S.

38. ISO 15025:2016 Protective clothing-Protection against flame-Method of test for limited flame spread, International Organization for Standardization, 2016.

39. M. Trznadel and M. Kryszewski, "Thermal Shrinkage Of Oriented Polymers," Journal of Macromolecular Science, Part C: Polymer Reviews, vol. 32, (3-4), pp. 259-300, 1992. . DOI: 10.1080/15321799208021428.

40. J. Rupp and A. Böhringer, "Yarns and fabrics containing elastane," International Textile Bulletin, vol. 45, (1), pp. 10-30, 1999.

41. N.J. Abbott, S. Schulman, Protection From Fire: Nonflammable Fabrics and Coatings*, J. Coat. Fabr. 6 (1976) 48–64. doi:10.1177/152808377600600106.

42. W.P. Behnke, Predicting flash fire protection of clothing from laboratory tests using second-degree burn to rate performance, Fire Mater. 8 (1984) 57–63. doi:10.1002/fam.810080202.

CHAPTER 4: Relationship Between Garment Shrinkage and Protective Performance of Heat-Resistant Workwear in PyroMan™ Tests

4.1 Abstract

This study investigated the relationship between garment shrinkage and protective performance, in terms of predicted percent body burn, measured in PyroMan™ tests of fire protective coveralls. Two methods of measuring the garment shrinkage in fire manikin testing were used: physical markers on the back side of the garments and portable 3-D scanning. Results of correlation analysis revealed that the garment shrinkage has a statistically significant relationship with the percent body burn in 3-second PyroMan™ test exposures of FR workwear materials, but no such relationship exists in 4-second PyroMan™ test exposures of the same materials. The lack of a correlation in the 4-second PyroMan™ test exposures is attributed to differences in flame retardancy mechanisms among the variety of test materials.

4.2 Introduction

Instrumented fire manikin tests provide invaluable evaluation of systems-level thermal protective performance of fire protective clothing. Thermally induced shrinkage has been identified as an important factor in the thermal protection of fire protective garments. Garment shrinkage can potentially contribute to burn injury by reducing the clothing air-gap insulation and by contributing stored thermal energy from the hot material directly to the skin. Multiple studies have identified this impact and several factors that influence the garment shrinkage experienced in manikin testing. Therefore, a study of the relationship between garment shrinkage and thermal protective performance for a variety of fire protective materials is needed to confirm that the relationship between garment shrinkage and thermal protective performance is not simply a characteristic of one class of fire protective fabric. This study sought to qualify the

relationship between garment shrinkage and thermal protection for a variety of fire protective workwear materials.

4.3 Background

4.3.1 Measuring Garment Shrinkage in Fire Manikin Testing

While measuring the garment shrinkage is not incorporated into the ASTM F1930 standard manikin test method, previous experimental studies have employed multiple methods to obtain a numerical measurement of garment shrinkage. Garment shrinkage has been measured largely through two distinct methods: physical marks on the garments and 3-D scanning technology. Li et al sealed stamps on the backside of test garments at locations of the garment that matched the heat sensor locations on the manikin (Figure 4.1) to investigate how different body postures impact the thermal shrinkage and thermal protective performance of FR garments. These circular stamps were marked to measure the thermal shrinkage in the warp, fill, and ±45

Figure 4.1 Markers on test garment prior to flash fire exposure [1].

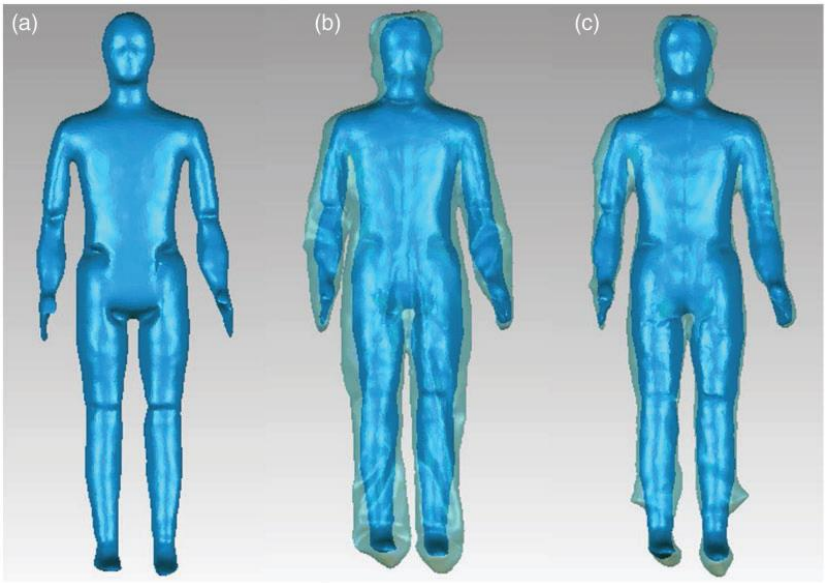

Figure 4.2 Three dimensional images of (a) nude manikin and manikin dressed in a test garment (b) before and (c) after exposure [3].

degrees to the warp direction of woven test fabrics [1]. While the markers were able to provide an accurate measurement of the garment shrinkage, the area covered by the markers only contains a portion of the garment and may not give the best representation of the overall shrinkage exhibited by the garment material.

The second method of measuring the thermal shrinkage of garments used in flame manikin testing is 3-D scanning. Song used 3-D body scanning technology to measure the reduction in the insulative air gap layer that results from garment shrinkage [2]. In more recent studies, Wang and Li employed a portable 3-D scanner mounted in the manikin test chamber to obtain 3-D images of the nude manikin and the clothed manikin immediately prior to and following flash fire exposure (Figure 4.2). The shrinkage was measured by superimposing the scans of the clothed manikin onto the scans of the nude manikin. The length and girth of the garment was measured by the surface area change, while the change in insulative air gap was calculated by the volume change and air gap thickness change [3-4]. The use of 3-D scanning

technology has clearly shown to be a useful process in the studies that employed the technology and may contain an advantage to the marker measurement method as the scanners can measure the entire garment. However, the scanning technology used in the studies is very complex and may not be practical for use in routine testing.

4.3.2 Correlating Garment Shrinkage with Thermal Protection in Fire Manikin Tests

In addition to pioneering methods of evaluating the garment shrinkage exhibited in full-scale fire manikin tests, each of the studies referenced above related the garment shrinkage to the thermal protection offered by the garments. Each of the studies also identified the impact of factors such as garment size and manikin posture on the exhibited shrinkage. Song showed that the air gap size and shrinkage rate impact the thermal protection of PBI/para-aramid and meta-aramid garments [2]. Wang et al found that garments of meta-aramid, PBI/para-aramid, and polysulfonamide (PSA) exhibited a strong correlation between the air gap thickness reduction and the percentage of burn injury [3]. Li et al examined the impact of garment size, garment fabric weight, body posture, and motion on the garment shrinkage of para-aramid garments. The study also found that garment shrinkage exhibited significant correlations with heat flux at different regions of the body [1].

Each of these studies have shown that garment shrinkage has a significant impact on the thermal protective performance in fire manikin testing. However, the studies have tested garments of only three different fiber compositions, leaving a knowledge gap in the relationship between garment shrinkage and thermal protection of other FR materials. Currently, it is assumed that a relationship between garment shrinkage and thermal protection exists for the general population of FR materials.

4.4 Experimental Methods

This study is centered around the PyroMan™ instrumented fire manikin test, as outlined by the ASTM F1930 standard test method [5]. Two methods for evaluating the thermal shrinkage in fire manikin testing were employed in this study: physical markers on the garments and 3-D scanning. Both methods follow precedent established in studies by Li et al and Wang et al, respectively [1, 3-4], and each method provides valuable information that the other method cannot. Each method also has drawbacks that the other method does not.

4.4.1 Marker Measurements

The first method of measuring the garment shrinkage in fire manikin testing was the marker measurements. Predicated on work completed by Li et al, the method involved drawing markers of known size at multiple locations (Figure 4.3) on the back side of each test garment [1]. Each marker, as seen in Figure 4.4, is a circle with lines in the vertical and horizontal

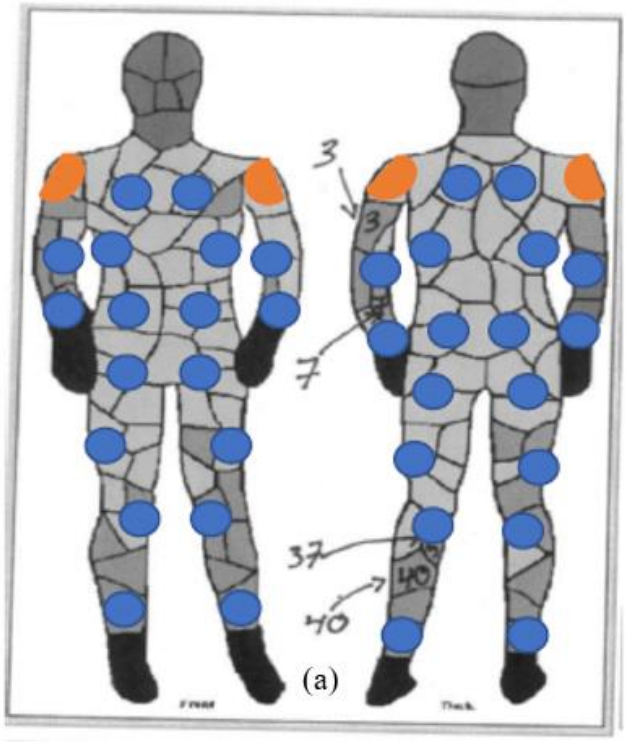

Figure 4.3 Locations of markers on PyroMan test garments. Orange semicircles denote that the marker is on the side of the shoulder.

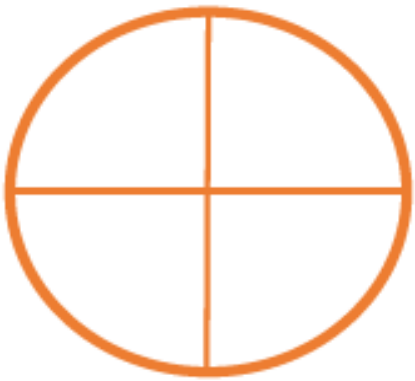

Figure 4.4 Schematic of marker drawn on PyroMan™ test garments

direction to match the warp and fill fiber directions, respectively. Each marker was 5 inches (12.7 cm) in diameter and 38 markers were drawn on the garment.

The marker measurement method is useful in determining the dimensional shrinkage exhibited by the materials. Shrinkage performance requirements found in NFPA standards call for the evaluation of dimensional shrinkage, so evaluating the dimensional shrinkage in fire manikin testing allows for direct comparison to the required values for performance in the 500°F oven test. The cost for evaluating the garment shrinkage via marker measurements is low, making the method a financially practical option for measuring the shrinkage measurements.

There are, however, several drawbacks to the marker measurement method that are important to consider. Because the markers are physically drawn onto the garments, they are vulnerable to any damage that may accompany the degradation of garments during testing. While the markers are well distributed on the garment, there are significant portions of the garment that are not measured, which may result in inaccurate measurements. Dimensional shrinkage may not be the best indicator of the change in the insulating air gap layer between the garment and the manikin. The reduction in the air gap layer, which has shown to be an indicator of thermal protective performance, may be better described with a measure of areal or volumetric shrinkage.

Although the method has a low cost, it can be time consuming, which weakens its case as a practical method for evaluating the thermal shrinkage.

4.4.2 3-D Scanning

The other method used in evaluating the garment shrinkage in fire manikin testing was 3-D scanning. This study used the Structure Sensor 3D scanner by Occipital, a portable 3-D scanner that attaches to an iPad, along with itSeez3D software to capture three-dimensional scans of the dressed manikin before and after flash fire exposure [6-7]. To ensure accuracy, each test garment was scanned three times before and after the exposure. Each of the scans were exported into Autodesk Fusion 360 modeling software, where any part of the scans not covered by the garment was removed (Figure 4.5), the scans were set to the correct scale, and the scan file was converted from a mesh to a solid body [8]. The correct scale for the scan was set based on the height of the manikin in the initial scan (not including the stabilizing block underneath the foot) and the total height of the manikin as specified in the ASTM F1930 standard [5]. The Autodesk Fusion 360 software then measures the surface area and volume of the manikin. These measurements are recorded and used to calculate the areal and volumetric shrinkage exhibited by each garment.

There are multiple advantages to using a 3-D scanning technique to measure garment shrinkage rather than physical markers. The scanner is able to measure the surface area and volume of the entire garment ensemble rather than a small sample, as is the case with the marker measurements, which ensures that the true amount of shrinkage is being measured. The methods of measuring both coveralls and rainwear are the same, which eliminates any potential

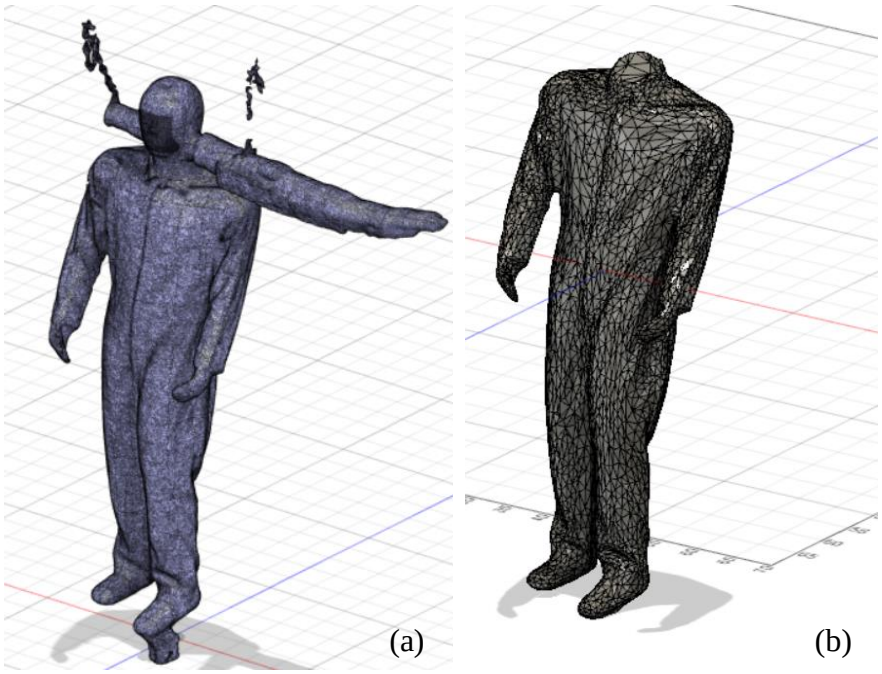

Figure 4.5 (a) Unedited 3-D scan inserted in Autodesk Fusion 360 Software; (b) 3-D scan in Autodesk Fusion 360 Software after removal of areas not covered by garment, scaling, and file conversion for surface area and volume measurements.

differences in results caused by different methodologies. The areal and volumetric shrinkage may better represent the reduction in the insulating air gap between the garment and manikin than the dimensional shrinkage measurements evaluated by the markers. Despite these advantages that 3-D scanning holds over the marker measurements, the accuracy and precision of the scanner is unknown, which may impact the reproducibility of the results.

4.5 Test Materials

A variety of different fire protective fabric materials were selected for this study. Table 4.1 provides a summarized description of the test materials. The materials consist of single layer, woven fabrics and a group of three specialty FR laminate materials. Each material was tested as a standard coverall as outlined in ASTM F1930 [5]. Three replicates of each garment were tested with no undergarments. Prior to use in testing, each test material was washed for one cycle with

a water temperature of 140°F using the AATCC standard reference detergent. Each test specimen was dried at a temperature of 155°F.

Table 4.1 Summarized Description of Test Materials.

ID	**Material Class**	**Fiber Content**	**Construction**	**Fabric Weight** (osy)	(1)**Nominal After-flame** (sec)	(2)**Nominal Shrinkage** (%)
A	Aramid	93% meta-aramid/ 5% para-aramid/ 2% antistat	Plain Weave	4.5	< 2	< 10%
B	Aramid	93% meta-aramid/ 5% para-aramid/ 2% antistat	Plain Weave	6.0	< 2	< 10%
C	Aramid	93% meta-aramid/ 5% para-aramid/ 2% antistat	Plain Weave	7.5	< 2	< 10%
D	FR Laminate	100% nylon	Plain Weave	4.0	< 2	high
E	FR Laminate	100% nylon 6,6	Rip-stop	5.3	< 2	high
F	FR Laminate	100% polyester	Twill Weave	6.5	< 2	high
G	Modacrylic	45% modacrylic/ 35% Lyocell/ 20% aramid	Twill Weave	7.0	< 2	< 10%
H	Modacrylic	45% modacrylic/ 35% Lyocell/ 20% aramid	Twill Weave	8.5	< 2	< 10%
I	PBI	70% PBI/ 30% para-aramid	Twill Weave	7.0	< 2	< 10%
J	FR Cotton	88% FR cotton/ 12% nylon	Twill Weave	7.0	< 2	< 10%

4.5.1 Aramids

Three different aramid fabrics: 4.5osy (Material A), 6.0osy (Material B), and 7.5osy (Material C). Temperatures above the glass transition temperature (T_g) of meta-aramid fibers are observed in flash fires causing fabrics made with meta-aramid fibers to shrink [9]. To improve high temperature thermal stability, meta-aramid fibers are blended with other more heat-resistant fibers, including para-aramid fibers. Meta-aramid fibers have a glass transition temperature (T_g)

of 275°C, while para-aramid fibers have a T_g of 327°C. Meta-aramid fibers swell in high-heat exposures, which seals openings in the fabric reducing heat transfer to the skin [9].

4.5.2 FR Laminate

Proprietary technology FR laminate materials incorporate a char-forming FR component. Three different substrate constructions and weights were studied: Material D used a 100% nylon plain weave substrate in a 4osy construction, Material E used a twill rip-stop weave made of 100% nylon 6,6, and Material F featured a 100% polyester twill weave 100% polyester substrate fabric. These laminate constructions form stable char contributing to increased structural integrity in flame exposures [10]. They have less than 2 seconds after-flame time in the vertical flame test but exhibit high levels of thermal shrinkage in the 500°F oven test [10]. Because these laminate materials are used in rainwear ensembles, these three FR laminates were included in both the FR coverall and FR rainwear categories of garment test materials.

4.5.3 Modacrylic Blends

Two twill-weave variants composed of blends of 45% modacrylic/35% Lyocell/ 20% aramid in a 7osy (Materials G) and 8.5 osy (Materials H) basis weight. Both fabrics are NFPA 2112 certified, indicating that they exhibit less than 2 seconds of after-flame time on the vertical flame test and less than 10% shrinkage in the 500°F oven test. Because modacrylic fibers are composed of an acrylic and modacrylic co-polymer composition, they undergo a two-stage degradation at temperatures of 236°C and 503°C. The acrylic component protects by char formation, while the modacrylic flame retardant component suppresses burning via vapor-phase free radical (halogen) reactions [9].

4.5.4 Polybenzimidazole (PBI)

A 7osy twill-weave fabric of 70%/30% “PBI-dominant” para-aramid blend/para-aramid filament (Material I). PBI has a high T_g (400°C) and thermal decomposition temperature (1175°C), indicating thermal stability (shrinkage resistance) in flash fire conditions [11].

4.5.5 FR Cotton

The FR cotton fabric used in this study is a 7osy twill construction incorporating an 88/12% blend of cotton and nylon fibers (Material J). This test fabric uses a FR finish containing tetrakis(hydroxymethylol) phosphonium salts to achieve flame resistance. It is NFPA 2112 certified, meaning that it has less than 2 seconds after-flame time in the vertical flame test, and less than 10% shrinkage in the 500°F oven test. Once the FR finish is consumed during a flame exposure, the cotton will quickly degrade, rapidly increasing after-flame and heat transfer [12].

4.6 Results and Discussion

Table 4.2 summarizes the results of PyroMan™ flash fire testing of the protective coveralls. While many of the garments exhibited a significant increase in shrinkage between the 3 and 4-second PyroMan™ tests, as expected, some of the garments exhibited a similar level of shrinkage between the exposure times, suggesting that the selected materials exhibit a variety of shrinkage responses. All of the test garments exhibit a significant increase in percent body burn between the 3 and 4-second PyroMan™ tests (Figure 4.6). The FR cotton garment Material J exhibited the largest increase in percent body burn, which suggests that the FR finish is entirely consumed at some point during the final second of the 4-second PyroMan™ test. Only the PBI/para-aramid material experienced a percent body burn of less than 50% in the 4-second PyroMan™ test.

Table 4.2 Summarized Garment Shrinkage (%) and Percent Body Burn results of Fire Protective Workwear

	Average Dimensional Shrinkage (%)		Average Areal Shrinkage (%)		Average Volumetric Shrinkage (%)		Average Body Burn (%)	
Material ID	3-seconds	4-seconds	3-seconds	4-seconds	3-seconds	4-seconds	3-seconds	4-seconds
A	8.40%	10.40%	9.27%	9.90%	12.97%	15.13%	44.81%	86.34%
B	5.13%	9.90%	4.10%	10.43%	2.80%	15.70%	31.15%	64.48%
C	1.50%	5.93%	1.40%	6.20%	-3.03%	6.50%	15.30%	52.73%
D	11.70%	9.60%	10.83%	9.93%	16.17%	16.67%	46.72%	93.71%
E	11.30%	12.20%	8.53%	10.47%	12.93%	16.33%	35.25%	78.42%
F	10.73%	12.57%	11.00%	10.73%	14.07%	15.93%	24.32%	69.94%
G	1.70%	4.20%	0.93%	2.27%	-5.70%	-3.07%	37.43%	94.53%
H	5.73%	8.87%	6.03%	8.13%	4.67%	8.70%	16.12%	84.97%
I	0.03%	0.07%	2.23%	2.70%	0.10%	-2.83%	10.39%	38.52%
J	0.83%	4.10%	-0.30%	3.20%	-3.13%	-5.03%	19.67%	99.45%

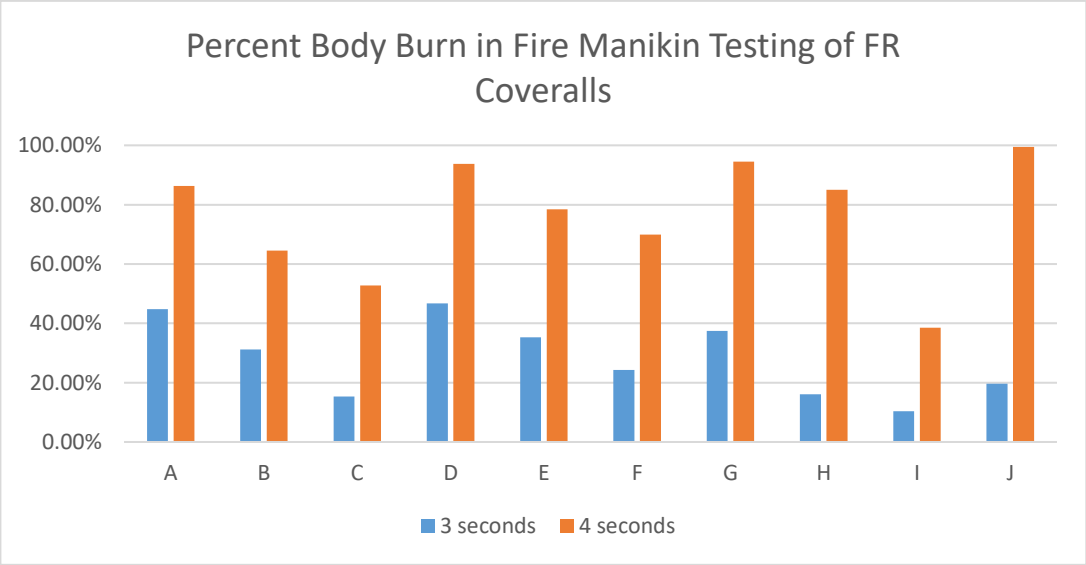

Figure 4.6 Percent Body Burn in Fire Manikin Testing of FR Coveralls (3, 4-second exposures).

While the dimensional shrinkage (marker method) produced similar shrinkage results as the areal shrinkage (3-D scans), the volumetric shrinkage (3-D scans) results appear to exaggerate the results: when the dimensional and areal shrinkage is higher (> 9%), the volumetric measurements tend to show a higher shrinkage response than the dimensional and

areal measurements, and when the shrinkage is lower (< 5%), the volumetric measurements tend to show a lower shrinkage response than the dimensional and areal shrinkage measurements.

Table 4.3 Correlations Between Garment Shrinkage (Dimensional Areal, and Volumetric) and Predicted Percent Body Burn in PyroMan™ Tests

PyroMan™ Exposure Duration	Shrinkage Dimension	Pearson Correlation Coefficient (r)	p-value
3-seconds	Dimensional	0.6198	0.0003*
	Areal	0.5247	0.0029*
	Volumetric	0.5281	0.0027*
4-seconds	Dimensional	0.3321	0.0784
	Areal	0.0761	0.6982
	Volumetric	0.0463	0.8079

*Indicates statistical significance.

Correlation analysis was used to investigate the relationship between garment shrinkage and percent body burn in PyroMan™ tests. Table 4.3 provides the Pearson correlation coefficient and corresponding p-value for the relationships between garment shrinkage (dimensional, areal, and volumetric) and percent body burn in FR coveralls. The relationship between garment shrinkage (dimensional, areal, and volumetric) and percent body burn is statistically significant for the 3-second PyroMan™ exposure, which confirms that the relationship between garment shrinkage and thermal protection is significant for the general population of FR materials in 3-second fire manikin tests. However, no significant correlation was found between the garment shrinkage and thermal protection for 4-second PyroMan™ tests, which indicates that the assumption of a significant relationship between garment shrinkage and thermal protection does not remain true for the general population of FR materials at exposure durations other than 3-seconds. This result does not suggest that garment shrinkage has no impact on the thermal protective performance of FR materials at 4-second fire manikin exposures. It does suggest,

however, that the differences in material characteristics such as the flame retardancy mechanism may become more pronounced as the exposure duration increases.

4.7 Conclusions

This study provided useful insight into the techniques used to measure the garment shrinkage in PyroMan™ tests. Both techniques proved to be viable methods of measuring garment shrinkage. It is important to consider the strengths and weaknesses of both techniques before deciding on one measurement technique or the other.

This study also confirmed that the relationship between garment shrinkage and thermal protective performance is significant for 3-second fire manikin tests of the general population of FR materials. However, no significant relationship was found for the same materials in 4-second fire manikin tests. This result is attributed to differences in material characteristics, such as flame retardancy mechanisms, becoming more pronounced as the fire manikin exposure duration is increased.

4.8 References

1. Li X, Lu Y, Zhai L, Wang M, Li J, Wang Y. Analyzing Thermal Shrinkage of Fire-Protective Clothing Exposed to Flash Fire. Fire Technology 2015 Jan;51(1):195-211.

2. Song G. Clothing Air Gap Layers and Thermal Protective Performance in Single Layer Garment. Journal of Industrial Textiles 2007 Jan;36(3):193-205.

3. Wang M, Li X, Li J, Xu B. A new approach to quantify the thermal shrinkage of fire protective clothing after flash fire exposure. Textile Research Journal 2016 Apr;86(6):580-592.

4. Wang M, Li X, Li J. Correlation of bench scale and manikin testing of fire protective clothing with thermal shrinkage effect considered. Fibers Polym 2015 Jun;16(6):1370-1377.

5. ASTM International. ASTM F1930 Standard Test Method for Evaluation of Flame Resistant Clothing for Protection Against Fire Simulations Using an Instrumented Manikin.

6. Structure Sensor- 3D scanning, augmented reality, and more for mobile devices. Available at: https://structure.io/.

7. itSeez3D. Available at: https://itseez3d.com/.

8. Autodesk. Autodesk Fusion 360.

9. Varga K, Noisternig MF, Griesser UJ, Aljaz L, Koch T. Thermal and sorption study of flame-resistant fibers. Lenzinger Berichte 2011;89:50-59.

10. Gore® Pyrad® fabric technology: durable flame retardant protection. Available at: https://www.gore-workwear.co.uk/technologies/gore-pyrad-fabric-technology.

11. PBI Performance Products I. PBI Max. Available at: https://pbiproducts.com/fabrics/product/pbi-max/.

12. Francis S. Understanding Fibers and Fabrics: The Engineering of Arc Rated/Flame Resistant Fabrics. Westex by Milliken 2018.

APPENDICES

Appendix A. Supplementary Information for Chapter 2

TABLE A.1 Summarized After-flame Test Data

ID	Material Class	Average After-flame in ASTM D6413 Vertical Flame Test (seconds)	Average After-flame in ASTM F1358 Folded Edge Flame Test (seconds)	Average After-flame in CGSB 27.10 Canadian Flame Test Edge Ignition (seconds)	Average After-flame in CGSB 27.10 Canadian Flame Test Surface Ignition (seconds)	Average After-flame in fire manikin 3-second exposure (seconds)	Average After-flame in fire manikin 4-second exposure (seconds)	Average Percent Body Burn in fire manikin 3-second exposure (%)	Average Percent Body Burn in fire manikin 4-second exposure (%)
A	Aramid	0.00	0.79	0.00	0.00	0.71	0.56	44.81	86.34
B	Aramid	0.00	0.77	0.00	0.00	3.07	1.89	31.15	64.48
C	Aramid	0.00	0.82	0.15	0.00	3.23	3.04	15.30	52.73
D	FR Laminate	0.00	0.87	4.71	0.76	3.64	4.49	46.72	93.71
E	FR Laminate	1.04	1.93	18.45	0.56	2.53	7.33	35.25	78.42
F	FR Laminate	0.82	0.86	1.01	0.00	1.52	5.90	24.32	69.94
G	Modacrylic	0.00	0.82	0.00	0.30	0.62	3.84	37.43	94.53
H	Modacrylic	0.00	0.65	0.17	0.00	0.00	1.78	16.12	84.97
I	PBI	0.00	1.41	0.00	0.00	0.00	0.00	10.39	38.52
J	Cotton	0.00	0.74	0.00	0.46	3.28	5.26	19.67	99.45
K	FR Rainwear	0.30	2.00	5.27	0.64	6.07	15.77	12.57	42.35
L	FR Rainwear	0.43	1.69	5.45	0.84	34.95	43.17	33.61	76.78
M	FR Rainwear	0.53	1.00	8.41	0.53	0.29	4.11	9.57	29.51
N	FR Rainwear	0.27	0.68	0.15	0.24	0.00	0.00	13.12	34.15
O	FR Rainwear	0.20	0.84	0.00	0.64	1.07	3.99	20.76	47.27

TABLE A.2 Average Peak Heat Release Rate and Total Heat Release in ASTM E1354 Cone Calorimeter and PyroMan™ Tests

ID	Material Class	Cone Calorimeter PHRR (cal/cm2/sec)	3-second PyroMan™ PHRR (cal/cm2/sec)	4-second PyroMan™ PHRR (cal/cm2/sec)	Cone Calorimeter THR (cal/cm2)	3-second PyroMan™ THR (cal/cm2)	4-second PyroMan™ THR (cal/cm2)
A	Aramid	2.49	0.71	0.94	45.65	2.59	3.65
B	Aramid	2.68	0.55	0.90	50.24	2.46	3.33
C	Aramid	3.42	0.43	0.67	72.50	2.01	3.18
D	FR Laminate	2.73	0.56	0.94	49.55	2.93	3.98
E	FR Laminate	3.87	0.45	0.68	69.15	2.62	3.84
F	FR Laminate	3.06	0.39	0.74	64.65	2.27	3.70
G	Modacrylic	2.30	0.54	1.10	41.04	2.41	4.34
H	Modacrylic	3.26	0.36	1.09	55.90	1.91	3.95
I	PBI	2.22	0.43	0.51	57.36	1.82	2.85
J	FR Cotton	3.79	0.41	1.32	58.48	2.00	6.26
K	FR Rainwear	5.27	0.37	0.43	107.15	1.51	2.91
L	FR Rainwear	4.69	0.42	0.50	119.79	2.93	4.45
M	FR Rainwear	2.74	0.27	0.40	66.20	1.28	2.17
N	FR Rainwear	2.93	0.33	0.38	55.17	1.61	2.39
O	FR Rainwear	5.04	0.46	0.64	100.89	1.98	2.92

TABLE A.3 T-tests Showing Grouping of FR coverall materials by statistically significant comparison of bench-scale after-flame to PyroMan™ after-flame

PyroMan™ Exposure Duration	Bench-scale Test	Bench-Scale Overestimates	Bench-Scale Underestimates	Bench-Scale Accurately Estimates
3-seconds	Vertical Flame Test		A, B, C, D, E, G, J	F, H, I
	Folded Edge Flame Test	H, I	B, C, D, F, J	A, E, G
	Canadian Flame Test- Edge Ignition		A, B, C, E, G, H, J	D, F, I
	Canadian Flame Test- Surface Ignition		A, B, C, D, E, F, J	G, H, I
	Total for Category	2	26	12
	Percent of Total	5.0%	65.0%	30.0%
4-seconds	Vertical Flame Test		B, C, D, E, F, H, J	A, G, I
	Folded Edge Flame Test	I	B, C, D, E, F, H, J	A, G
	Canadian Flame Test- Edge Ignition		B, C, E, F, H, J	A, D, G, I
	Canadian Flame Test- Surface Ignition		B, C, D, E, F, H, J	A, G, I
	Total for Category	1	27	12
	Percent of Total	2.5%	67.5%	30.0%

TABLE A.4 Correlations Between Bench-Scale Flammability Tests and PyroMan™ After-flame for FR Coverall Fabrics

PyroMan™ Exposure Duration	Bench-Scale Test	Pearson Correlation Coefficient (r)	P-value
3-seconds	Vertical Flame	0.081	0.8233
	Folded Edge Flame Test	-0.019	0.9582
	Canadian Flame Test- Edge Ignition	0.268	0.4534
	Canadian Flame Test- Surface Ignition	0.53	0.1151
	Cone Calorimeter (PHRR)	0.497	0.1438
	Cone Calorimeter (THR)	0.314	0.3764
4-seconds	Vertical Flame	0.721	0.0186*
	Folded Edge Flame Test	0.328	0.3545
	Canadian Flame Test- Edge Ignition	0.639	0.0469*
	Canadian Flame Test- Surface Ignition	0.64	0.0463*
	Cone Calorimeter (PHRR)	0.665	0.0358*
	Cone Calorimeter (THR)	0.422	0.225

*Indicates statistical significance

TABLE A.5 Correlations Between After-flame and % Total Body Burn in PyroMan™ tests for FR Coveralls

PyroMan™ Exposure Duration	Bench-Scale Test	Pearson Correlation Coefficient (r)	P-value
3-seconds	Vertical Flame	0.095	0.7947
	Folded Edge Flame Test	0.006	0.9866
	Canadian Flame Test- Edge Ignition	0.315	0.3746
	Canadian Flame Test- Surface Ignition	0.511	0.1314
	PyroMan™ After-flame	0.235	0.2116
	Cone Calorimeter PHRR	-0.237	0.5094
	Cone Calorimeter THR	-0.5484	0.1007
4-seconds	Vertical Flame	-0.043	0.9065
	Folded Edge Flame Test	-0.318	0.3706
	Canadian Flame Test- Edge Ignition	0.109	0.7646
	Canadian Flame Test- Surface Ignition	0.589	0.0732
	PyroMan™ After-flame	0.384	0.0361*
	Cone Calorimeter PHRR	0.215	0.5503
	Cone Calorimeter THR	-0.46	0.1814

*Indicates statistical significance

TABLE A.6 T-tests showing grouping of FR rainwear materials by statistically significant comparison of bench-scale after-flame to PyroMan™ after-flame

PyroMan™ Exposure Duration	Bench-scale Test	Bench-Scale Overestimates	Bench-Scale Underestimates	Bench-Scale Accurately Estimates
3-seconds	Vertical Flame Test	N	D, E, K, L, O	F, M
	Folded Edge Flame Test	M, N	D, F, K, L	E, O
	Canadian Flame Test- Edge Ignition	E, M	L, O	D, F, K, N
	Canadian Flame Test- Surface Ignition	N	D, E, F, K, L	M, O
	Total	6	16	10
	Percent of Total	18.8%	50.0%	31.3%
4-seconds	Vertical Flame Test	N	D, E, F, K, L, M, O	
	Folded Edge Flame Test	N	D, E, F, K, L, M, O	
	Canadian Flame Test- Edge Ignition	E	F, K, L, O	D, M, N
	Canadian Flame Test- Surface Ignition	N	D, E, F, K, L, M, O	
	Total	4	25	3
	Percent of Total	12.5%	78.1%	9.4%

TABLE A.7 Correlations between Bench-Scale Tests and PyroMan™ After-flame for FR Rainwear

PyroMan™ Exposure Duration	Bench-Scale Test	Pearson Correlation Coefficient (r)	P-value
3-seconds	Vertical Flame	-0.046	0.9143
	Folded Edge Flame Test	0.446	0.2675
	Canadian Flame Test- Edge Ignition	0.037	0.9308
	Canadian Flame Test- Surface Ignition	0.521	0.185
	Cone Calorimeter (PHRR)	0.413	0.3092
	Cone Calorimeter (THR)	0.674	0.0667
	Cone Calorimeter PHRR vs PyroMan™ PHRR	0.128	0.7622
	Cone Calorimeter THR vs PyroMan™ THR	0.04	0.9245
4-seconds	Vertical Flame	0.025	0.9535
	Folded Edge Flame Test	0.576	0.1349
	Canadian Flame Test- Edge Ignition	0.094	0.8257
	Canadian Flame Test- Surface Ignition	0.516	0.19
	Cone Calorimeter (PHRR)	0.518	0.1889
	Cone Calorimeter (THR)	0.759	0.0289*
	Cone Calorimeter PHRR vs PyroMan™ PHRR	-0.25	.5509
	Cone Calorimeter THR vs PyroMan™ THR	.219	.602

*Indicates statistical significance

TABLE A.8 Correlations between After-flame Tests and % Body Burn on PyroMan™ for FR Rainwear

PyroMan™ Exposure Duration	Bench-Scale Test	Pearson Correlation Coefficient (r)	P-value
3-seconds	Vertical Flame	-0.007	0.9868
	Folded Edge Flame Test	0.115	0.7857
	Canadian Flame Test- Edge Ignition	0.294	0.4802
	Canadian Flame Test- Surface Ignition	0.397	0.3298
	Cone Calorimeter (PHRR)	-0.114	0.7882
	Cone Calorimeter (THR)	-0.142	0.738
	PyroMan™ Test	0.327	0.1187
4-seconds	Vertical Flame	0.129	0.7608
	Folded Edge Flame Test	0.194	0.6461
	Canadian Flame Test- Edge Ignition	0.289	0.4872
	Canadian Flame Test- Surface Ignition	0.275	0.5093
	Cone Calorimeter (PHRR)	-0.08	0.8508
	Cone Calorimeter (THR)	-0.092	0.8282
	PyroMan™ Test	0.287	0.1736

Appendix B: Supplemental Information for Chapter 3

TABLE B.1 Average Bench-Scale Dimensional Shrinkage Test Data (3-second exposures in Cylindrical TPP and TPP testing)

ID	Material Class	Dimensional Shrinkage in ASTM F2894 Oven (%)	Dimensional Shrinkage in spaced Cylindrical TPP 3-second exposure (%)	Dimensional Shrinkage in contact Cylindrical TPP 3-second exposure (%)	Dimensional Shrinkage in spaced TPP 3-second exposure (%)	Dimensional Shrinkage in contact TPP 3-second exposure (%)	Dimensional Shrinkage in spaced TPP continuous exposure (%)	Dimensional Shrinkage in contact TPP continuous exposure (%)
A	Aramid	1.11%	14.52%	10.92%	7.28%	7.56%	5.80%	6.14%
B	Aramid	2.14%	6.14%	7.68%	5.56%	5.58%	6.26%	8.34%
C	Aramid	1.36%	4.00%	4.88%	4.68%	4.34%	6.62%	6.98%
D	FR Laminate	21.81%	17.16%	29.24%	9.66%	6.62%	9.40%	12.24%
E	FR Laminate	19.36%	11.74%	18.66%	5.76%	4.86%	13.36%	10.80%
F	FR Laminate	19.92%	13.28%	19.76%	4.68%	5.40%	14.68%	10.82%
G	Modacrylic	2.67%	7.24%	7.90%	5.52%	5.84%	8.10%	7.32%
H	Modacrylic	8.56%	10.60%	11.16%	7.64%	7.18%	11.50%	10.04%
I	PBI	1.17%	4.20%	4.50%	4.28%	3.98%	5.50%	5.44%
J	Cotton	7.44%	3.83%	4.84%	4.72%	4.78%	7.08%	5.10%
K	FR Rainwear	2.31%	3.15%	3.98%	4.22%	3.90%	2.70%	5.70%
L	FR Rainwear	2.11%	2.67%	4.82%	3.62%	3.26%	0.65%	6.82%
M	FR Rainwear	16.61%	11.80%	12.38%	4.10%	5.42%	-0.53%	6.34%
N	FR Rainwear	2.14%	2.14%	3.22%	3.36%	3.28%	3.80%	5.72%
O	FR Rainwear	3.22%	3.75%	4.36%	3.92%	3.34%	3.48%	3.98%

TABLE B.2 Average Bench-Scale Dimensional Shrinkage Test Data (4-second exposures in Cylindrical TPP and TPP testing)

ID	Material Class	Dimensional Shrinkage in ASTM F2894 Oven (%)	Dimensional Shrinkage in Cylindrical TPP 4-second exposure spaced (%)	Dimensional Shrinkage in Cylindrical TPP 4-second exposure contact (%)	Dimensional Shrinkage in TPP 4-second exposure spaced (%)	Dimensional Shrinkage in TPP 4-second exposure contact (%)	Dimensional Shrinkage in TPP continuous exposure spaced (%)	Dimensional Shrinkage in TPP continuous exposure contact (%)
A	Aramid	1.11%	23.93%	17.18%	11.72%	13.96%	5.80%	6.14%
B	Aramid	2.14%	17.67%	14.68%	9.98%	6.80%	6.26%	8.34%
C	Aramid	1.36%	8.07%	8.24%	5.70%	5.52%	6.62%	6.98%
D	FR Laminate	21.81%	26.22%	36.56%	13.14%	10.06%	9.40%	12.24%
E	FR Laminate	19.36%	15.68%	22.12%	9.48%	6.60%	13.36%	10.80%
F	FR Laminate	19.92%	15.67%	24.78%	6.22%	5.66%	14.68%	10.82%
G	Modacrylic	2.67%	5.74%	8.28%	4.82%	5.36%	8.10%	7.32%
H	Modacrylic	8.56%	10.93%	11.14%	6.50%	5.86%	11.50%	10.04%
I	PBI	1.17%	4.52%	4.42%	4.48%	4.68%	5.50%	5.44%
J	Cotton	7.44%	5.59%	6.42%	4.44%	4.28%	7.08%	5.10%
K	FR Rainwear	2.31%	4.80%	5.44%	4.26%	5.20%	2.70%	5.70%
L	FR Rainwear	2.11%	3.94%	3.90%	5.22%	4.74%	0.65%	6.82%
M	FR Rainwear	16.61%	13.51%	12.80%	5.06%	4.22%	-0.53%	6.34%
N	FR Rainwear	2.14%	2.41%	3.60%	3.66%	4.14%	3.80%	5.72%
O	FR Rainwear	3.22%	3.79%	5.06%	4.10%	4.22%	3.48%	3.98%

TABLE B.3 Average Bench-Scale Areal Shrinkage Test Data (3-second exposures in Cylindrical TPP and TPP)

ID	Material Class	Areal Shrinkage in ASTM F2894 Oven (%)	Areal Shrinkage in spaced Cylindrical TPP 3-second exposure (%)	Areal Shrinkage in contact Cylindrical TPP 3-second exposure (%)	Areal Shrinkage in spaced TPP 3-second exposure (%)	Areal Shrinkage in contact TPP 3-second exposure (%)	Areal Shrinkage in spaced TPP continuous exposure (%)	Areal Shrinkage in contact TPP continuous exposure (%)
A	Aramid	2.21%	26.88%	20.63%	14.00%	14.53%	11.32%	11.96%
B	Aramid	4.23%	11.90%	14.70%	10.83%	10.87%	12.32%	15.97%
C	Aramid	2.70%	7.80%	9.56%	9.19%	8.56%	12.80%	13.46%
D	FR Laminate	38.93%	31.38%	49.42%	18.38%	12.80%	18.16%	23.00%
E	FR Laminate	35.07%	22.14%	33.66%	11.23%	9.53%	24.99%	20.49%
F	FR Laminate	36.00%	24.84%	35.58%	9.22%	10.53%	27.22%	20.48%
G	Modacrylic	5.27%	13.96%	15.16%	10.76%	11.36%	15.52%	14.07%
H	Modacrylic	16.38%	20.26%	21.16%	14.68%	13.81%	21.67%	19.09%
I	PBI	2.32%	8.27%	8.86%	8.40%	7.87%	10.73%	10.61%
J	Cotton	14.33%	7.48%	9.52%	9.26%	9.38%	13.63%	9.97%
K	FR Rainwear	4.55%	6.20%	7.88%	8.34%	7.74%	5.35%	11.09%
L	FR Rainwear	4.16%	5.30%	9.20%	7.17%	6.48%	1.39%	13.18%
M	FR Rainwear	30.46%	22.24%	23.38%	8.13%	10.56%	-1.22%	12.27%
N	FR Rainwear	4.23%	4.22%	6.32%	6.63%	6.44%	7.49%	11.11%
O	FR Rainwear	6.36%	7.36%	8.58%	7.77%	6.55%	6.89%	7.85%

TABLE B.4 Average Bench-Scale Areal Shrinkage Test Data (4-second exposures in Cylindrical TPP and TPP)

ID	Material Class	Areal Shrinkage in ASTM F2894 Oven (%)	Areal Shrinkage in spaced Cylindrical TPP 4-second exposure (%)	Areal Shrinkage in contact Cylindrical TPP 4-second exposure (%)	Areal Shrinkage in spaced TPP 4-second exposure (%)	Areal Shrinkage in contact TPP 4-second exposure (%)	Areal Shrinkage in spaced TPP continuous exposure (%)	Areal Shrinkage in contact TPP continuous exposure (%)
A	Aramid	2.21%	42.10%	31.33%	22.12%	25.94%	11.32%	11.96%
B	Aramid	4.23%	32.14%	27.06%	18.98%	13.12%	12.32%	15.97%
C	Aramid	2.70%	15.50%	15.76%	11.10%	10.76%	12.80%	13.46%
D	FR Laminate	38.93%	44.82%	59.78%	24.56%	19.16%	18.16%	23.00%
E	FR Laminate	35.07%	28.88%	38.98%	18.09%	12.76%	24.99%	20.49%
F	FR Laminate	36.00%	28.96%	43.44%	12.08%	11.02%	27.22%	20.48%
G	Modacrylic	5.27%	11.20%	15.84%	9.43%	10.44%	15.52%	14.07%
H	Modacrylic	16.38%	20.80%	21.14%	12.57%	11.39%	21.67%	19.09%
I	PBI	2.32%	8.84%	8.68%	8.82%	9.19%	10.73%	10.61%
J	Cotton	14.33%	10.88%	12.46%	8.70%	8.45%	13.63%	9.97%
K	FR Rainwear	4.55%	9.32%	10.46%	8.30%	10.14%	5.35%	11.09%
L	FR Rainwear	4.16%	7.72%	7.60%	10.14%	9.26%	1.39%	13.18%
M	FR Rainwear	30.46%	25.24%	23.92%	9.91%	8.34%	-1.22%	12.27%
N	FR Rainwear	4.23%	4.72%	7.10%	7.24%	8.19%	7.49%	11.11%
O	FR Rainwear	6.36%	7.44%	9.88%	8.05%	8.34%	6.89%	7.85%

TABLE B.5 Average Shrinkage Data in PyroMan™ testing

ID	Material Class	Dimensional Shrinkage in fire manikin 3-second exposure (%)	Areal Shrinkage in fire manikin 3-second exposure (%)	Volumetric Shrinkage in fire manikin 3-second exposure (%)	Dimensional Shrinkage in fire manikin 4-second exposure (%)	Areal Shrinkage in fire manikin 4-second exposure (%)	Volumetric Shrinkage in fire manikin 4-second exposure (%)
A	Aramid	8.40%	9.27%	12.97%	10.40%	9.90%	15.13%
B	Aramid	5.13%	4.10%	2.80%	9.90%	10.43%	15.70%
C	Aramid	1.50%	1.40%	-3.03%	5.93%	6.20%	6.50%
D	FR Laminate	11.70%	10.83%	16.17%	9.60%	9.93%	16.67%
E	FR Laminate	11.30%	8.53%	12.93%	12.20%	10.47%	16.33%
F	FR Laminate	10.73%	11.00%	14.07%	12.57%	10.73%	15.93%
G	Modacrylic	1.70%	0.93%	-5.70%	4.20%	2.27%	-3.07%
H	Modacrylic	5.73%	6.03%	4.67%	8.87%	8.13%	8.70%
I	PBI	0.03%	2.23%	0.10%	0.07%	2.70%	-2.83%
J	Cotton	0.83%	-0.30%	-3.13%	4.10%	3.20%	-5.03%
K	FR Rainwear	1.00%	1.37%	-2.27%	5.53%	6.70%	8.30%
L	FR Rainwear	4.93%	6.47%	9.63%	16.60%	13.10%	22.23%
M	FR Rainwear	9.30%	8.20%	10.40%	12.17%	10.47%	14.77%
N	FR Rainwear	1.33%	1.97%	0.93%	1.50%	3.57%	1.10%
O	FR Rainwear	1.60%	1.40%	1.13%	2.20%	1.90%	1.77%

TABLE B.6 T-tests showing grouping of FR coverall materials by statistically significant comparison of bench-scale dimensional shrinkage to PyroMan™ dimensional shrinkage

PyroMan™ Exposure Duration	Bench-scale Test	Bench-Scale Overestimates	Bench-Scale Underestimates	Bench-Scale Accurately Estimates
3-seconds	ASTM F2894 Oven Test	D, E, F, H, I, J	A, B	C, G
	Cylindrical TPP- 3-seconds contact	A, C, D, E, F, G, H, I, J		B
	Cylindrical TPP- 3-seconds spaced	A, C, D, F, G, H, I, J		B, E
	TPP- 3-seconds Contact	C, G, H, I, J	D, E, F	A, B
	TPP- 3-seconds spaced	G, H, I, J	C, D, E, F	A, B
	TPP- continuous exposure contact	B, C, G, H, I, J	A	D, E, F
	TPP- continuous exposure spaced	C, F, G, H, I, J	A	B, D, E
	Total	44	11	15
	Percent of Total	62.9%	15.7%	21.4%
4-seconds	ASTM F2894 Oven Test	D, E, F, J, I	A, B, C, G	H
	Cylindrical TPP- 4-seconds contact	A, B, C, D, E, F, G, I		H, J
	Cylindrical TPP- 4-seconds spaced	A, B, C, D, E, F, G, I		H, J
	TPP- 4-seconds Contact	G	B, E, F, H, I	A, C, D, J
	TPP- 4-seconds spaced	D, I	E, F, H	A, B, C, G, J
	TPP- continuous exposure contact	C, D, G, I	A, E	B, F, H, J
	TPP- continuous exposure spaced	G, I	A, B	C, D, E, F, H, J
	Total	30	16	24
	Percent of Total	42.9%	22.9%	34.3%

TABLE B.7 T-tests showing grouping of FR coverall materials by statistically significant comparison of bench-scale areal shrinkage to PyroMan™ areal shrinkage

PyroMan™ Exposure Duration	Bench-scale Test	Bench-Scale Overestimates	Bench-Scale Underestimates	Bench-Scale Accurately Estimates
3-seconds	ASTM F2894 Oven Test	D, E, F, G, H, J	A	B, C, I
	Cylindrical TPP- 3-seconds contact	A, B, C, D, E, F, G, H, I, J		
	Cylindrical TPP- 3-seconds spaced	A, B, C, D, E, F, G, H, I, J		
	TPP- 3-seconds Contact	A, B, C, D, E, G, H, I, J		F
	TPP- 3-seconds spaced	A, B, C, D, G, H, I, J		E, F
	TPP- continuous exposure contact	B, C, D, E, F, G, H, I, J		A
	TPP- continuous exposure spaced	B, C, D, E, F, G, H, I, J		A
	Total	61	1	8
	Percent of Total	87.1%	1.4%	11.4%
4-seconds	ASTM F2894 Oven Test	D, E, F, H, J	A, B, C	G, I
	Cylindrical TPP- 4-seconds contact	A, B, C, D, E, F, G, H, I, J		
	Cylindrical TPP- 4-seconds spaced	A, B, C, D, E, F, G, H, I, J		
	TPP- 4-seconds Contact	A, B, C, D, E, G, H, I, J		F
	TPP- 4-seconds spaced	A, B, C, D, E, G, H, I, J		F
	TPP- continuous exposure contact	B, C, D, E, F, G, H, I, J	A	
	TPP- continuous exposure spaced	C, D, E, F, G, H, I, J	A, B	
	Total	30	6	4
	Percent of Total	75.0%	15.0%	10.0%

TABLE B.8 Correlations Between Bench-Scale Tests of Dimensional Shrinkage and PyroMan™ Dimensional Shrinkage for FR Coveralls

PyroMan™ Exposure Duration	Bench-Scale Test	Pearson Correlation Coefficient (r)	P-value
3-seconds	ASTM F2894 Oven Test	0.796	0.0059*
	Cylindrical TPP- 3-seconds Spaced	0.914	0.0002*
	Cylindrical TPP- 3-seconds Contact	0.903	0.0003*
	TPP- 3-seconds Spaced	0.583	0.0769
	TPP- 3-seconds Contact	0.481	0.1588
	TPP- Continuous Exposure Spaced	0.67	0.0339*
	TPP- Continuous Exposure Contact	0.825	0.0033*
4-seconds	ASTM F2894 Oven Test	0.604	0.0643
	Cylindrical TPP- 4-seconds Spaced	0.65	0.0418*
	Cylindrical TPP- 4-seconds Contact	0.733	0.0158*
	TPP- 4-seconds Spaced	0.652	0.041*
	TPP- 4-seconds Contact	0.469	0.1719
	TPP- Continuous Exposure Spaced	0.645	0.044*
	TPP- Continuous Exposure Contact	0.724	0.0179*

*Indicates statistical significance

TABLE B.9 Correlations Between Bench-Scale Tests of Areal Shrinkage and PyroMan™ Areal Shrinkage for FR Coveralls

PyroMan™ Exposure Duration	Bench-Scale Test	Pearson Correlation Coefficient (r)	P-value
3-seconds	ASTM F2894 Oven	0.698	0.0247*
	Cylindrical TPP- 3-seconds Spaced	0.939	<.0001*
	Cylindrical TPP- 3-seconds Contact	0.858	0.0015*
	TPP- 3-seconds Spaced	0.585	0.0757
	TPP- 3-seconds Contact	0.528	0.1162
	TPP- Continuous Exposure Spaced	0.603	0.0651
	TPP- Continuous Exposure Contact	0.752	0.0122*
4-seconds	ASTM F2894 Oven	0.531	0.1143
	Cylindrical TPP- 4-seconds Spaced	0.864	0.0013*
	Cylindrical TPP- 4-seconds Contact	0.786	0.007*
	TPP- 4-seconds Spaced	0.767	0.0096*
	TPP- 4-seconds Contact	0.548	0.1007
	TPP- Continuous Exposure Spaced	0.497	0.1441
	TPP- Continuous Exposure Contact	0.704	0.0231*

*Indicates statistical significance

TABLE B.10 Correlations between Bench-Scale Tests of Areal Shrinkage and PyroMan™ Volumetric Shrinkage for FR Coveralls

PyroMan™ Exposure Duration	Bench-Scale Test	Pearson Correlation Coefficient (r)	P-value
3-seconds	ASTM F2894 Oven	0.715	0.0201*
	Cylindrical TPP- 3-seconds Spaced	0.909	0.0003*
	Cylindrical TPP- 3-seconds Contact	0.852	0.0017*
	TPP- 3-seconds Spaced	0.574	0.0825
	TPP- 3-seconds Contact	0.463	0.178
	TPP- Continuous Exposure Spaced	0.549	0.1002
	TPP- Continuous Exposure Contact	0.6995	0.0243*
4-seconds	ASTM F2894 Oven	0.515	0.1274
	Cylindrical TPP- 4-seconds Spaced	0.891	0.0005*
	Cylindrical TPP- 4-seconds Contact	0.819	0.0038*
	TPP- 4-seconds Spaced	0.813	0.0042*
	TPP- 4-seconds Contact	0.597	0.0683
	TPP- Continuous Exposure Spaced	0.458	0.1834
	TPP- Continuous Exposure Contact	0.723	0.0183*

*Indicates statistical significance

TABLE B.11 Correlations between Dimensional Shrinkage and % Total Body Burn on PyroMan™ for FR Coveralls

PyroMan™ Exposure Duration	Bench-Scale Test	Pearson Correlation Coefficient (r)	P-value
3-seconds	ASTM F2894 Oven	0.318	0.3704
	Cylindrical TPP- 3-seconds Spaced	0.709	0.0218*
	Cylindrical TPP- 3-seconds Contact	0.606	0.0633
	TPP- 3-seconds Spaced	0.636	0.0479*
	TPP- 3-seconds Contact	0.595	0.0698
	TPP- Continuous Exposure Spaced	0.067	0.8531
	TPP- Continuous Exposure Contact	0.38	0.2789
	PyroMan™ Marker Measurements	0.619	0.0003*
4-seconds	ASTM F2894 Oven	0.327	0.3565
	Cylindrical TPP- 4-seconds Spaced	0.366	0.2983
	Cylindrical TPP- 4-seconds Contact	0.313	0.3788
	TPP- 4-seconds Spaced	0.268	0.4537
	TPP- 4-seconds Contact	0.291	0.4147
	TPP- Continuous Exposure Spaced	0.221	0.5392
	TPP- Continuous Exposure Contact	0.219	0.5431
	PyroMan™ Marker Measurements	0.332	0.0784

*Indicates statistical significance

TABLE B.12 Correlations between Areal Shrinkage and % Total Body Burn on PyroMan™ for FR Coveralls (with PyroMan™ Volumetric Shrinkage)

PyroMan™ Exposure Duration	Bench-Scale Test	Pearson Correlation Coefficient (r)	P-value
3-seconds	ASTM F2894 Oven	0.308	0.3863
	Cylindrical TPP- 3-seconds Spaced	0.704	0.0232*
	Cylindrical TPP- 3-seconds Contact	0.5995	0.067
	TPP- 3-seconds Spaced	0.639	0.0467*
	TPP- 3-seconds Contact	0.598	0.0681
	TPP- Continuous Exposure Spaced	0.08	0.827
	TPP- Continuous Exposure Contact	0.38	0.2789
	PyroMan™- Area Scans	0.525	0.0029*
	PyroMan™- Volume Scans	0.528	0.0027*
4-seconds	ASTM F2894 Oven	0.336	0.3427
	Cylindrical TPP- 4-seconds Spaced	0.274	0.4428
	Cylindrical TPP- 4-seconds Contact	0.314	0.3767
	TPP- 4-seconds Spaced	0.264	0.4618
	TPP- 4-seconds Contact	0.292	0.4123
	TPP- Continuous Exposure Spaced	0.23	0.5232
	TPP- Continuous Exposure Contact	0.218	0.5453
	PyroMan™- Area Scans	0.076	0.6982
	PyroMan™- Volume Scans	0.046	0.8079

*Indicates statistical significance

TABLE B.13 T-tests showing grouping of FR Rainwear Materials by Statistically significant comparison of bench-scale dimensional shrinkage to PyroMan™ dimensional shrinkage

PyroMan™ Exposure Duration	Bench-scale Test	Bench-Scale Overestimates	Bench-Scale Underestimates	Bench-Scale Accurately Estimates
3-seconds	ASTM F2894 Oven	D, E, F, M, N, O	L	K
	Cylindrical TPP-3-seconds contact	D, E, F, K, N, O		L, M
	Cylindrical TPP-3-seconds spaced	D, F, K, N, O	L	E, M
	TPP- 3-seconds Contact	K, N, O	D, E, F, L, M	
	TPP- 3-seconds spaced	K, N, O	D, E, F, L	M
	TPP- continuous exposure contact	K, N, O		D, E, F, L, M
	TPP- continuous exposure spaced	F, N, O	L, M	D, E, K
	Total	29	13	14
	Percent of Total	51.8%	23.2%	25.0%
4-seconds	ASTM F2894 Oven	D, E, F, M, O	K, L	N
	Cylindrical TPP-4-seconds contact	D, E, F, N, O	L	K, M
	Cylindrical TPP-4-seconds spaced	D, E, F, O	L	K, M, N
	TPP- 4-seconds Contact	N, O	E, F, L, M	D, K
	TPP- 4-seconds spaced	D, N, O	E, F, L, M	K
	TPP- continuous exposure contact	D, N, O	E, L, M	F, K
	TPP- continuous exposure spaced	N, O	K, L, M	D, E, F
	Total	24	18	14
	Percent of Total	42.9%	32.1%	25.0%

TABLE B.14 T-tests showing grouping of FR Rainwear materials by statistically significant comparison of bench-scale areal shrinkage to PyroMan™ areal shrinkage

PyroMan™ Exposure Duration	Bench-scale Test	Bench-Scale Overestimates	Bench-Scale Underestimates	Bench-Scale Accurately Estimates
3-seconds	ASTM F2894 Oven	D, E, F, K, L, M, N, O		
	Cylindrical TPP- 3-seconds contact	D, E, F, K, M, N, O		L
	Cylindrical TPP- 3-seconds spaced	D, E, F, K, M, N, O		L
	TPP- 3-seconds Contact	D, K, N, O		E, F, L, M
	TPP- 3-seconds spaced	D, E, K, N, O		F, L, M
	TPP- continuous exposure contact	D, E, F, K, L, M, N, O		
	TPP- continuous exposure spaced	D, E, F, N, O	L	K, M
	Total	44	1	11
	Percent of Total	78.6%	1.8%	19.6%
4-seconds	ASTM F2894 Oven	D, E, F, K, L, M, O		N
	Cylindrical TPP- 4-seconds contact	D, E, F, M, N, O	L	K
	Cylindrical TPP- 4-seconds spaced	D, E, F, M, O	L	K, N
	TPP- 4-seconds Contact	D, E, K, N, O	L, M	F
	TPP- 4-seconds spaced	D, E, N, O	L	F, K, M
	TPP- continuous exposure contact	D, E, F, K, N, O		L, M
	TPP- continuous exposure spaced	D, E, F, N, O	L	K, M
	Total	38	6	12
	Percent of Total	67.9%	10.7%	21.4%

TABLE B.15 Correlations between Bench-Scale Tests of Dimensional Shrinkage and PyroMan™ Dimensional Shrinkage for FR Rainwear

PyroMan™ Exposure Duration	Bench-Scale Test	Pearson Correlation Coefficient (r)	P-value
3-seconds	ASTM F2894 Oven	0.963	0.0001*
	Cylindrical TPP- 3-seconds Spaced	0.937	0.0006*
	Cylindrical TPP- 3-seconds Contact	0.911	0.0017*
	TPP- 3-seconds Spaced	0.645	0.0842
	TPP- 3-seconds Contact	0.869	0.0051*
	TPP- Continuous Exposure Spaced	0.63	0.094
	TPP- Continuous Exposure Contact	0.877	0.0042*
4-seconds	ASTM F2894 Oven	0.473	0.237
	Cylindrical TPP- 4-seconds Spaced	0.427	0.2908
	Cylindrical TPP- 4-seconds Contact	0.355	0.3869
	TPP- 4-seconds Spaced	0.35	0.3948
	TPP- 4-seconds Contact	0.224	0.5941
	TPP- Continuous Exposure Spaced	0.184	0.6632
	TPP- Continuous Exposure Contact	0.52	0.1861

*Indicates statistical significance

TABLE B.16 Correlations between Bench-Scale Tests of Areal Shrinkage and PyroMan™ Areal Shrinkage for FR Rainwear

PyroMan™ Exposure Duration	Bench-Scale Test	Pearson Correlation Coefficient (r)	P-value
3-seconds	ASTM F2894 Oven	0.899	0.0024*
	Cylindrical TPP- 3-seconds Spaced	0.891	0.003*
	Cylindrical TPP- 3-seconds Contact	0.877	0.0042*
	TPP- 3-seconds Spaced	0.606	0.111
	TPP- 3-seconds Contact	0.836	0.0097*
	TPP- Continuous Exposure Spaced	0.576	0.1353
	TPP- Continuous Exposure Contact	0.874	0.0045*
4-seconds	ASTM F2894 Oven	0.527	0.18
	Cylindrical TPP- 4-seconds Spaced	0.517	0.1899
	Cylindrical TPP- 4-seconds Contact	0.458	0.2542
	TPP- 4-seconds Spaced	0.45	0.2638
	TPP- 4-seconds Contact	0.345	0.4031
	TPP- Continuous Exposure Spaced	0.206	0.6247
	TPP- Continuous Exposure Contact	0.619	0.1019

*Indicates statistical significance

TABLE B.17 Correlations between Bench-Scale Tests of Areal Shrinkage and PyroMan™™ Volumetric Shrinkage for FR Rainwear

PyroMan™™ Exposure Duration	Bench-Scale Test	Pearson Correlation Coefficient (r)	P-value
3-seconds	ASTM F2894 Oven	0.865	0.0056*
	Cylindrical TPP- 3-seconds Spaced	0.857	0.0065*
	Cylindrical TPP- 3-seconds Contact	0.864	0.0056*
	TPP- 3-seconds Spaced	0.627	0.0959
	TPP- 3-seconds Contact	0.777	0.0232*
	TPP- Continuous Exposure Spaced	0.557	0.1514
	TPP- Continuous Exposure Contact	0.86	0.0062*
4-seconds	ASTM F2894 Oven	0.518	0.1881
	Cylindrical TPP- 4-seconds Spaced	0.538	0.1693
	Cylindrical TPP- 4-seconds Contact	0.485	0.2229
	TPP- 4-seconds Spaced	0.518	0.1884
	TPP- 4-seconds Contact	0.416	0.3058
	TPP- Continuous Exposure Spaced	0.221	0.5997
	TPP- Continuous Exposure Contact	0.63	0.0941

*Indicates statistical significance

TABLE B.18 Correlations Between Dimensional Shrinkage and % Total Body Burn on PyroMan™ for FR Rainwear

PyroMan™ Exposure Duration	Bench-Scale Test	Pearson Correlation Coefficient (r)	P-value
3-seconds	ASTM F2894 Oven	0.471	0.2384
	Cylindrical TPP- 3-seconds Spaced	0.513	0.1933
	Cylindrical TPP- 3-seconds Contact	0.685	0.0611
	TPP- 3-seconds Spaced	0.768	0.026*
	TPP- 3-seconds Contact	0.445	0.2694
	TPP- Continuous Exposure Spaced	0.519	0.187
	TPP- Continuous Exposure Contact	0.742	0.0349*
	PyroMan™ Marker Measurements	0.547	0.0057*
4-seconds	ASTM F2894 Oven	0.504	0.2025
	Cylindrical TPP- 4-seconds Spaced	0.692	0.0573
	Cylindrical TPP- 4-seconds Contact	0.698	0.054
	TPP- 4-seconds Spaced	0.811	0.0146*
	TPP- 4-seconds Contact	0.787	0.0205*
	TPP- Continuous Exposure Spaced	0.618	0.1024
	TPP- Continuous Exposure Contact	0.802	0.0166*
	PyroMan™ Marker Measurements	0.526	0.0083*

*Indicates statistical significance

TABLE B.19 Correlations between Areal Shrinkage and % Total Body Burn on PyroMan™ for FR Rainwear (with PyroMan™ Volumetric Shrinkage)

PyroMan™ Exposure Duration	Bench-Scale Test	Pearson Correlation Coefficient (r)	P-value
3-seconds	ASTM F2894 Oven	0.462	0.2487
	Cylindrical TPP- 3-seconds Spaced	0.505	0.2021
	Cylindrical TPP- 3-seconds Contact	0.684	0.0612
	TPP- 3-seconds Spaced	0.767	0.0263*
	TPP- 3-seconds Contact	0.443	0.2715
	TPP- Continuous Exposure Spaced	0.531	0.1761
	TPP- Continuous Exposure Contact	0.741	0.0356*
	PyroMan™- Area Scans	0.578	0.0031*
	PyroMan™- Volume Scans	0.667	0.0004*
4-seconds	ASTM F2894 Oven	0.496	0.2117
	Cylindrical TPP- 4-seconds Spaced	0.613	0.1064
	Cylindrical TPP- 4-seconds Contact	0.683	0.0618
	TPP- 4-seconds Spaced	0.812	0.0144*
	TPP- 4-seconds Contact	0.786	0.0208*
	TPP- Continuous Exposure Spaced	0.636	0.097
	TPP- Continuous Exposure Contact	0.801	0.0168*
	PyroMan™- Area Scans	0.565	0.0040*
	PyroMan™- Volume Scans	0.662	0.0004*

*Indicates statistical significance